FINAL REPORT

PERFORMANCE AND ANALYSIS OF INCINERATOR BOTTOM ASH AS STRUCTURAL FILL

David Lentz, Graduate Assistant
Kenneth R. Demars, Associate Professor
Richard P. Long, Professor
Norman W. Garrick, Associate Professor

September 1994

JHR 94-232 Proj. 92-6

This research was sponsored by the Joint Highway Research Advisory Council (JHRAC) of the University of Connecticut, the Connecticut Resources Recovery Authority, and the Connecticut Department of Transportation and was carried out in the Civil Engineering Department of the University of Connecticut.

This work is the thesis by David Lentz submitted in partial fulfillment of the Master of Science degree.

Technical Report Documentation Page

1. Report No. JHR 94-232	2. Government Accession No.	3. Recipient's Catalog No.
4. Title and Subtitle Performance and Analysis of Incinerator Bottom Ash as Structural Fill		5. Report Date September 1994
		6. Performing Organization Code
7. Author(s) David Lentz, Kenneth R. Demars, Richard P. Long, and Norman W. Garrick		8. Performing Organization Report No. JHR 94-232
9. Performing Organization Name and Address University of Connecticut Department of Civil Engineering 191 Auditorium Road, Box U-37 TI Storrs, CT 06269		10. Work Unit No. (TRAIS)
		11. Contract or Grant No.
12. Sponsoring Agency Name and Address Connecticut Department of Transportation 280 West Street Rocky Hill, CT 06067-0207		13. Type of Report and Period Covered Final Report
		14. Sponsoring Agency Code

15. Supplementary Notes

This project was co-sponsored by the Connecticut Resources Recovery Authority.

16. Abstract

Bottom ash from a municipal solid waste mass burn incinerator was used to construct a structural roadway fill. Three 30 meter long by 3 meter high test sections were constructed: one of bottom ash, another of gravel and a third having a mix of these two materials. The test sections are part of an access road within a landfill. Instrumentation was installed during construction to monitor the performance of each fill section including settlement plates, slope stakes and lysimeters for leachate sampling. Samples of each material were obtained during road construction for laboratory testing of physical and chemical properties. The laboratory and field results show that bottom ash has very good structural properties for use as roadway fill, but the ferrous metals should be separated before use. The ash leachate contains high levels of soluble salts. Based on limited TCLP testing, the bottom ash is categorized as non-hazardous under EPA guidelines although lead is problematic.

17. Key Words bottom ash, incinerator, structural fill, physical properties, leachate, chemical properties	18. Distribution Statement No Restrictions

19. Security Classif. (of this report)	20. Security Classif. (of this page)	21. No. of Pages	22. Price
Unclassified	Unclassified	96	

Form DOT F 1700.7 (8-72) Reproduction of completed page authorized

ACKNOWLEDGMENTS

This study was funded jointly by the Connecticut Resource Recovery Authority and the Connecticut Department of Transportation. Their support is greatly appreciated.

Special thanks go to Dr. Jack Stephens for his knowledge, experience and constructive comments and to Chris Recchia of CRRA for his support and technical knowledge.

Jan Heitert and Liz Fumal of the Environmental Research Institute performed most of the chemical analyses. Laboratory specific gravity analyses were performed by Bill Winters of the United States Geological Survey, Woods Hole, MA and are also greatly appreciated. Thanks are extended to grad and undergrad students Ram Maddali, Leslie Sweeney, Doug Franklin, and Mike Sollmi for their valuable assistance in laboratory and field investigations. The staff of the University of Connecticut Macintosh Computer Laboratory provided assistance in producing this document. Cheri Rivard provided editorial and technical assistance.

SI* (MODERN METRIC) CONVERSION FACTORS

APPROXIMATE CONVERSIONS TO SI UNITS

Symbol	When You Know	Multiply By	To Find	Symbol
	LENGTH			
in	inches	25.4	millimetres	mm
ft	feet	0.305	metres	m
yd	yards	0.914	metres	m
mi	miles	1.61	kilometres	km
	AREA			
in^2	square inches	645.2	millimetres squared	mm^2
ft^2	square feet	0.093	metres squared	m^2
yd^2	square yards	0.836	metres squared	m^2
ac	acres	0.405	hectares	ha
mi^2	square miles	2.59	kilometres squared	km^2
	VOLUME			
fl oz	fluid ounces	29.57	mililitres	mL
gal	gallons	3.785	Litres	L
ft^3	cubic feet	0.028	metres cubed	m^3
yd^3	cubic yards	0.765	metres cubed	m^3

NOTE: Volumes greator than 1000 L shall be shown in m^3.

Symbol	When You Know	Multiply By	To Find	Symbol
	MASS			
oz	ounces	28.35	grams	g
lb	pounds	0.454	kilograms	kg
T	short tons (2000 lb)	0.907	megagrams	Mg
	TEMPERATURE (exact)			
°F	Fahrenheit temperature	5(F-32)/9	Celcius temperature	°C

*SI is the symbol for the International System of Measurement

APPROXIMATE CONVERSIONS TO SI UNITS

Symbol	When You Know	Multiply By	To Find	Symbol
	LENGTH			
mm	millimetres	0.039	inches	in
m	metres	3.28	feet	ft
m	metres	1.09	yards	yd
km	kilometres	0.621	miles	mi
	AREA			
mm^2	millimetres squared	0.0016	square inches	in^2
m^2	metres squared	10.764	square feet	ft^2
ha	hectares	2.47	acres	ac
km^2	kilometres squared	0.386	square miles	mi^2
	VOLUME			
mL	millilitres	0.034	fluid ounces	fl oz
L	litres	0.264	gallons	gal
m^3	metres cubed	35.315	cubic feet	ft^3
m^3	metres cubed	1.308	cubic yards	yd^3
	MASS			
g	grams	0.035	ounces	oz
kg	kilograms	2.205	pounds	lb
Mg	megagrams	1.102	short tons (2000 lb)	T
	TEMPERATURE (exact)			
°C	Celcius temperature	1.8C + 32	Fahrenheit temperature	°F

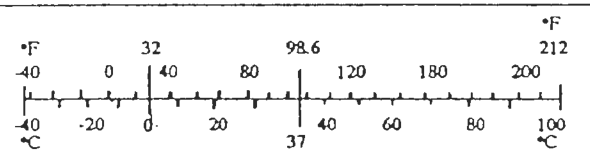

TABLE OF CONTENTS

LIST OF FIGURES

LIST OF TABLES

NOTATION

AS	Mixed 50% bottom ash/50% gravel subsection
ASTM	American Society for Testing and Materials
BA	Bottom ash subsection
CRRA	Connecticut Resource Recovery Authority
EPA	United States Environmental Protection Agency
EP Toxicity	Extraction Procedure Toxicity Test
ERI	Environmental Research Institute
FHWA	Federal Highway Administration
GS	Global sump
HDPE	High density polyethylene
ICP	Inductively Coupled Plasma
LS	Local sump
MSW	Municipal solid waste
No.	U.S. Standard sieve number
PVC	Polyvinyl chloride
RCP	Reinforced concrete pipe
RDF	Refuse derived fuel
S	Gravel or soil subsection
SP	Settlement platform
TCLP	Toxicity Characteristic Leaching Procedure
U	Unconfined compression test
WTE	Waste-to-energy

1.0 INTRODUCTION

1.1 Statement of Problem

Solid waste disposal in the United States has become progressively problematic as available landfill space steadily decreases. Many landfills across the United States are at or approaching maximum capacity. In an effort to reduce the volume of waste being deposited in landfills, many states have developed plans to incinerate municipal solid waste (MSW). According to the United States Department of Energy, approximately 16% of the country's MSW is presently burned at facilities where the heat of combustion is used to generate electricity (Shepard, et al., 1993). Incinerators which use solid waste to generate electric power are referred to as waste-to-energy or WTE facilities. Two types of WTE facilities are refuse-derived fuel (RDF) and mass-burn. RDF facilities prepare MSW for incineration by removing noncombustibles such as metals and glass. Mass burn facilities incinerate MSW in its "as received" state. The future holds promise for the WTE industry, as the quantity of MSW incinerated is predicted to double to 32% by the year 2000 (Styron, 1992).

The primary advantages that incineration offers as a waste disposal solution are the 70% mass reduction and 85% volume reduction resulting from combustion. Although the volume and mass reductions are substantial, the ash byproducts must be landfilled. Connecticut incinerator facilities currently combust about 1.5 million metric tons of MSW yearly (State of Connecticut Adopted Waste Management Plan, 1991). The resulting 450,000 tons of ash is comprised of two primary components, fly ash and bottom ash. Fly ash represents 10% of the waste stream, while the remaining 90% consists of bottom ash. The ash is delivered to landfills in a combined state, where the fly ash and bottom ash are mixed.

As an alternative to landfilling, incinerator ash may be substituted for conventional aggregate in construction applications. Bottom ash may be used specifically in place of naturally occurring gravel in a structural fill application. To determine the suitability of bottom ash as construction aggregate, an investigation of its physical characteristics, chemical composition, and engineering properties must be performed.

1.2 Review of Literature

Past investigations involving incinerator ash have focused on four primary topics:

- Physical properties and engineering behavior
- Chemical composition and contaminant mobility
- Modifying physical/chemical properties
- Practical applications

This literature review will address each of the four primary topics independently using articles from journals, federal publications, and proceedings from the various International Conferences on Municipal Solid Waste Combustor Ash Utilization.

1.2.1 Physical Properties and Engineering Behavior - Investigations into the physical properties and engineering behavior of incinerator residues have shown that properties inherent to ash from a particular incinerator remain relatively consistent and predictable over time (Chesner, 1990, Aziz and Ramaswamy, 1992, and others). Studies have also shown that ashes from different incinerators possess similar physical and engineering characteristics. Commonly examined parameters have been gradation, maximum dry density, specific gravity, angle of internal friction, permeability, and loss on ignition. An example of the consistency in properties between ash originating from different sources is shown in Figure 1.1. The figure shows the gradation of incinerator residue produced at four different incinerators. Studies by Schoenberger and Fungaroli

(1971) and Chesner (1989) were performed on bottom ash from incinerators in the United States. Studies by Kalajian, et al. (1990) and Aziz and Ramaswamy (1992) were performed on bottom ash from incinerators in Singapore. The figure shows that gradations

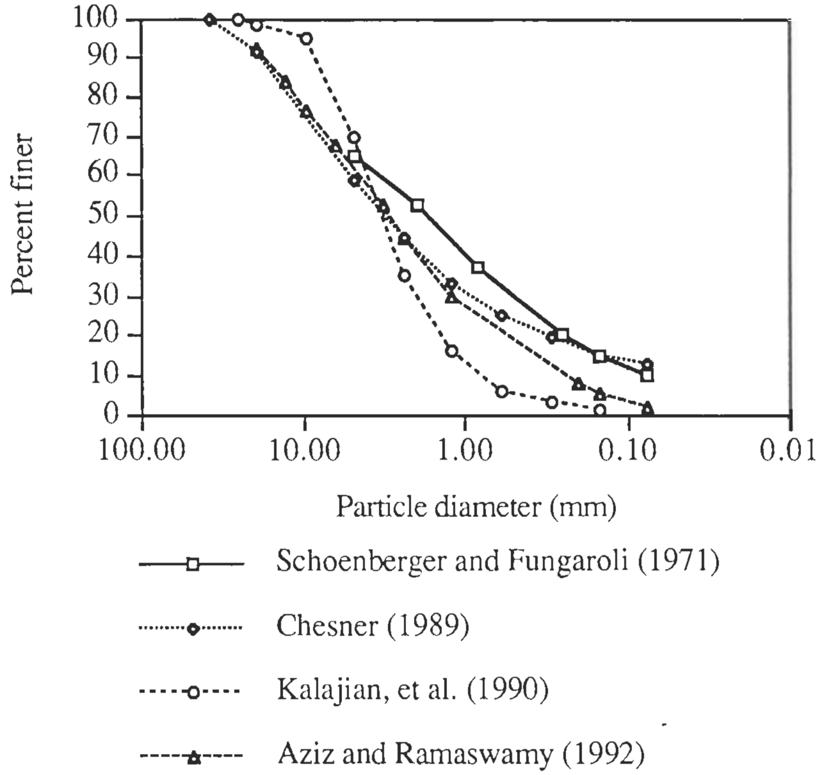

Figure 1.1 Bottom ash gradation from four incinerator residue studies

for the four materials fall into a relatively narrow band over the entire range of particle sizes. The materials are all well-graded and possess particles from gravel size to silt and possibly clay sizes. Chesner (1990) described the bottom ash as a "silty, sandy-gravely mixture".

Early investigations of incinerator residue by Schoenberger and Fungaroli (1971) indicated that bottom ash possesses substantial strength characteristics. The angle of internal friction was found to be 45°. The material was lighter than most naturally occurring aggregates with respect to in-place density, which was roughly 15.7 kN/m^3. A later study by Chesner in 1989 also compared the physical properties of incinerator ash to those of natural aggregates. Chesner found that bottom ash exhibited physical properties which made it a viable substitute for natural aggregates. Chesner determined the maximum dry density of bottom ash to be slightly less than that of typical natural aggregates. For five incinerators sampled in the study, the dry densities ranged from 12.3 to 17.3 kN/m^3 with an average of 14.5 kN/m^3. The average optimum moisture content of the samples was 14.8%, which is slightly higher than most naturally occurring granular materials. Chesner found that the organic matter content varied considerably between incinerators. Loss on ignition measurements ranged from 3.7 to 19.8%, where the mean was 5.5%. Bagchi and Sopcich (1989) also examined the organic content of ash and found that it averaged 7.9% by loss on ignition. The specific gravity of the material examined in their study was 1.52.

In a 1990 report on incinerator ash, Chesner reports that the permeability of bottom ash samples ranged from 10^{-3} to 10^{-5} cm/s. Tay and Goh (1991) report permeability values similar to those of Chesner. The ash from Singapore had a permeability of 3.3×10^{-3} cm/s at a density of 15.1 kN/m^3. Tay and Goh determined that the angle of internal friction was 46.5°. The specific gravity was 2.67 and the loss on ignition was 2.7%. Another examination of bottom ash by Aziz and Ramaswamy in 1992 found that the specific gravity ranged from 2.27 to 2.60. The bulk density of the material ranged from 10.9 to 12.1 kN/m^3. Aziz and Ramaswamy state that low densities resulted from the composition of solid waste in Singapore. The refuse contained large quantities of paper, cardboard, vegetable matter, fruits, and garden wastes. Although the unburned MSW contained a large fraction of organic vegetative matter, the loss on ignition of the ash was only 1 to 3%. The study also reported that the weight fraction of ferrous metal ranged from 10 to 20%.

1.2.2 Chemical Composition and Contaminant Mobility in Leachate - Investigations involving the chemical makeup and behavior of incinerator residues have focused on chemical composition and mobility of compounds in leachate. The chemical composition of solid ash samples is first analyzed in the laboratory. Knowing the chemical constituents of the ash, experimenters (Sundstrom, 1991, Theis and Gardner, 1992, and others) have then examined the potential for those compounds to migrate from the ash into leachate. The literature shows that leaching has been the subject of the majority of investigations regarding mechanisms of contaminant transport in incinerator ash. This Review of Literature will examine the subjects of chemical composition and contaminant mobility in leachate independently.

Chemical Composition - Experiments by Roffman (1989) showed that combined ash samples from five different incinerators contained high chloride and sulfate concentrations. Roffman reports that the total quantity of soluble solids leached from ash samples ranged from 6440 to 65,800 parts per million (ppm). The investigation also examined metals listed in the primary and secondary drinking water standards. The ash contained measurable levels of barium, cadmium, chromium, copper, lead, manganese, mercury, and zinc. Chesner (1990) found similar trace elements in combined and bottom ash samples, noting that lead, cadmium, zinc, copper, and mercury were of primary concern from an environmental perspective. Chesner determined that the concentrations of various metals differed according to source. Cadmium and zinc concentrations were higher in fly ash than in bottom ash. Copper was present at higher concentrations in bottom ash than in fly ash. Lead was present at significant levels in both the bottom and fly ash.

Experiments by Franklin (1990) determined the source of three environmentally hazardous metals found in incinerator residue. Franklin examined unburned MSW to determine the components contributing lead, cadmium, and mercury. Lead-acid storage batteries and consumer electronics contributed over 90% of the lead found in the combusted ash. Household batteries and plastics combined to contribute 80% of the available cadmium. Common sources of mercury were household batteries, electric lighting, thermometers, and thermostats.

Hooper (1991) analyzed ash from three Florida incinerators and found high levels of aluminum, calcium, copper, iron, sodium, lead, and zinc. Goodwin (1992) analyzed ash collected from incinerator residue monofills. Tests showed that the material contained arsenic, cadmium, chromium, lead, and selenium.

Leaching Characteristics - Studies on contaminant mobility have focused on the leachability of environmentally hazardous compounds (such as those listed previously). Experiments on contaminant mobility have involved chemical analyses of leachate using United States Environmental Protection Agency (EPA) standardized leaching tests, column leaching tests, and leachate extracted from landfills. The purpose of leachate chemical analyses is to determine the contaminants which will leach and to determine the concentration of those dissolved contaminants. The EPA has used two test methods to determine whether waste material is hazardous or nonhazardous. The Extraction Procedure (EP) Toxicity test (replaced by the EPA in 1986), and the currently used Toxicity Characteristic Leaching Procedure (TCLP) have been cited in the literature for the evaluation of incinerator residues. Column leaching tests, in which ash is placed in a containment vessel and water is passed through it have been used by experimenters attempting to simulate field leaching conditions. Leachate sampled from field fill sections has been analyzed by experimenters to determine actual field contaminant levels and to compare field contaminant concentrations with those found in laboratory leaching experiments.

Schoenberger and Fungaroli (1971) analyzed leachate extracted from an incinerator ash fill site. The results showed the leachate contained significant concentrations of iron, zinc, lead, copper, and chromium. Total dissolved solid concentrations of 8000 mg/l were very high according to the authors. The dominant cation and anion was sodium and chloride respectively. Roffman (1989) performed TCLP tests on incinerator ash. Analyses indicated that lead, cadmium, and sodium were present. Lead was found at 26.4 mg/l, cadmium at 1.6 mg/l, and sodium at up to 1640 mg/l. Roffman also found barium, chromium, copper, iron, manganese, mercury, and zinc present in the TCLP extract.

Bagchi and Sopcich (1989) tested bottom ash in water leaching tests and using the EP Toxicity test to determine whether their ash samples were categorized as hazardous waste. The water leaching tests showed significant levels of soluble salts (e.g. sodium and chloride), as well as trace elements such as arsenic, barium, cadmium, chromium, lead, selenium, and silver. EP Toxicity test results showed the bottom ash samples to be nonhazardous.

A study of ash sampled at a Long Island, NY incinerator by Chesner (1990) found significant salt concentrations. Chesner found that the majority of chlorides and sulfates contacting water would dissolve and leach. The study also pointed to lead and cadmium as having high leachability potential. Chesner found that the potential for lead and cadmium leaching may be pH dependent. Leachability was inhibited when the pH of the ash ranged from 6.0 to 10.0.

Experiments by Roffman in 1990 examined leachate extracted from a fill area containing incinerator ash. Roffman measured dissolved solids and chloride concentrations and compared those concentrations to the characteristics of sea water. The total dissolved solids in ash leachate ranged from 32,900 to 45,700 mg/l compared to 35,000 mg/l in sea water. Chloride levels in ash leachate ranged from 19,500 to 29,100 mg/l compared to 19,000 mg/l in sea water.

Sundstrom, et al. (1991) performed column leaching tests on bottom ash. The tests, which used water as a leachant showed high trace element concentrations during initial dowsings with water. The concentrations decreased rapidly as the first quantities of water had passed through the sample material.

Theis and Gardner (1992) examined the rate at which trace elements and soluble salts dissolve into leachate. They found that soluble salts such as sodium, potassium, and chloride dissolved as a function of leachant contact time. For slow flow rates, where contact time was prolonged, soluble salts dissolved in greater quantities. The study also concluded that the dissolution of trace elements was not a function of flow rate. Instead, the release of trace elements was found to be dependent on pH and the solubility of solid phases of the trace element at a given pH.

1.2.3 Amending Physical or Chemical Properties to Improve Performance - A number of experimenters have devised methods for improving the performance of incinerator ash. Work has centered on altering the leaching characteristics since the physical and engineering properties have been generally regarded as acceptable. Williams (1989) presented a patented method by which ferrous and non-ferrous metals were removed from incinerator ash to improve its composition and homogeneity. The ash was processed to achieve a more uniform gradation, while extracting 80-95% of the ferrous and non-ferrous metals.

Work on chemical fixation was performed by Plumley and Boley (1990). Their patented process utilized combined bottom and fly ash mixed with lime, water, and unspecified chemical compounds. The mixture was pelletized and dusted with an embedding material. The finished aggregate was lightweight and chemically stable. The authors contended that the product consistently passed EPA toxicity tests. Forrester (1991) presented a patented fixation process in which lead, cadmium, copper, and zinc were stabilized. The method involved adding forms of phosphate and alkali to control pH in the incinerator residue. Complex metal molecules exhibiting low solubility resulted from the fixation process. Tests showed that the amended material was nonhazardous according to TCLP toxicity limits.

Another fixation method was developed by Styron and Shannonhouse (1992) using silicates. The addition of silicates creates insoluble compounds which become bonded to the aggregate matrix. The process also included pelletization. Casey (1993) used cement mixed with ash to create a "volumetrically stable compound." Contaminants were immobilized in the material, which was referred to as Permabase. Casey found that the processed aggregate was suitable for fill material, particularly beneath load bearing surfaces such as roads. Chemical analyses showed that Permabase was nonhazardous according to TCLP toxicity limits.

1.2.4 Practical Applications - There have been numerous practical applications using incinerator ash dating back to the World War II era, when incinerator residue was used for subgrade material beneath the streets of Brooklyn, NY (Federal Highway Administration, 1977). The Federal Highway Administration (FHWA) has investigated ash for use as construction or structural fill material. A 1977 report states that incinerator ash is suitable fill material if it is "well burned." Well burned incinerator residue comprises 10% the volume and 20-30% the weight of the original unburned MSW. The FHWA suggested that improved physical characteristics were developed by aging the ash prior to implementation. Chesner (1990) presented guidelines for use of combustor ash in various applications. The report cited three primary applications for the material. Ash may be used as aggregate substitutes in bituminous concrete, Portland cement concrete, and as an aggregate for fill material. Studies involving these three types of applications are described sequentially in this Review of Literature.

Bituminous Concrete - A project by Demars, et al. (1993) incorporated bottom ash as aggregate in pavements for a roadway test section. The roadway was utilized by heavily loaded haul trucks delivering waste to a landfill. Performance characteristics were found to rival those of pavements consisting of conventional aggregates. Hooper (1993) used a similar procedure to pave a roadway in Tampa, FL. The ash was treated using a patented fixation process prior to use as aggregate. Hooper contended that the wearing and skid resistance characteristics as well as the engineering characteristics of the pavement equaled or exceeded those of conventional pavements.

Portland Cement Concrete - Experiments using bottom ash in various types of concrete structures were performed by Roethel and Breslin (1990). Ash was substituted for natural aggregate in the manufacture of concrete blocks, cement masonry blocks, and shoreline protection blocks. The study concluded that material strengths were adequate for each particular use and that the concrete retained its integrity over the long term. Kalajian, et al. (1990) studied the use of ash as aggregate in the manufacture of concrete block for artificial reef construction. Results showed the ash was a viable substitute for natural aggregates. Two additional studies examined the use of ash as aggregate in concrete masonry blocks. Black (1991) and Berg and Neal (1992) both concluded that incinerator ash may be used as aggregate for manufacturing masonry blocks.

Fill Material - Applications using ash as a load bearing structural fill material are few in number. A Swedish study by Hartlen and Fallman (1990) utilized bottom ash for structural fill at an incinerator complex. The experimenters constructed a test road 500 m long and 9 m wide. The bottom ash fill proved to be a viable aggregate substitute in road construction due to its granular nature and high bearing capacity. Tay and Goh (1991) speculated, based on laboratory test results that bottom ash would be an acceptable fill material. They cite the low unit weight, high bearing capacity, and high permeability as reasons for its use.

1.3 Objectives of study

The objectives of this study are to evaluate the potential for using mass-burn incinerator bottom ash as a structural aggregate. Numerous past investigations have examined the use of bottom ash as aggregate, but limited work has been performed on large scale structural fill demonstration projects. Specific concerns in the performance evaluation are the physical and chemical behavior of bottom ash in a field application. The study will also correlate results from laboratory tests on bottom ash with physical and chemical observations from the test embankment. The study consists of field and laboratory testing programs.

1.3.1 Field Testing Program- The primary goal in constructing the test embankment is to determine the suitability of incinerator bottom ash as construction material. The research study examines a wide range of parameters vital to the use of aggregates as fill material. Two primary topics of interest are physical and chemical performance. Physical performance characteristics include long-term settlement and horizontal displacements, lateral stability, susceptibility to frost heave, and the potential for particle degradation resulting from repetitive heavy loading conditions. Lateral and vertical deformations are measured periodically by a survey crew. The embankment undergoes periodic visual inspections to ascertain its qualitative performance.

The environmental monitoring program focuses on the quality of leachate generated by the embankment. Leachate is extracted periodically from collection systems within the embankment and analyzed for selected trace elements. Chemical analyses are performed on bottom ash samples to determine the total quantity of selected trace elements present. Results of leachate analyses and total chemical analyses are compared to determine which if any of the selected trace elements are mobile in leachate. Chemical analyses are performed to determine whether the bottom ash is classified as hazardous material according to United States EPA standards.

1.3.2 Laboratory Testing Program - The purpose of the laboratory testing program is to evaluate the physical properties and engineering behavior of bottom ash and to compare those results with observations from the field test section. In order to compare the qualities of bottom ash with those of naturally occurring aggregate, standardized testing procedures are performed using samples of bottom ash, gravel, and mixed bottom ash/gravel . Physical characteristics of concern are gradation, composition, maximum dry density, specific gravity, permeability, internal strength, and organic content.

The laboratory testing program examines the chemical characteristics of leachate generated in controlled laboratory conditions. Trace element and anion concentrations are analyzed in leachate produced from several laboratory leaching apparatus. Results from leachate produced in the laboratory are compared to results from leachate collected from the field. Differences and similarities in long-term contaminant concentrations are examined to determine the accuracy of laboratory testing relative to field conditions.

2.0 EMBANKMENT CONSTRUCTION AND MATERIALS

2.1 Test Site

The test embankment is located at the Shelton Landfill in Shelton, CT. The landfill is owned by the Connecticut Resource Recovery Authority (CRRA) and operated under contract with the Archer Company. The landfill currently receives approximately 1650 metric tons of combined incinerator ash daily. The ash originates at the Bridgeport Recycling Trash-to-Energy facility in Bridgeport, CT which is a mass-burn facility. The waste deposited at the landfill is combined ash, consisting of 90% bottom ash and 10% fly ash by weight. The landfill facility began accepting incinerator ash only recently. Before the Bridgeport incinerator began operations the landfill was a depository for unburned MSW. The landfill facility received MSW until 1988. A cross section of the landfill would show two primary features. The base of the site consists of unburned MSW in thicknesses ranging from 15 to 20 meters below the centerline of the roadway test section. Incinerator ash deposited since 1988 overlies the unburned MSW. The landfill is covered by a one-meter thick low permeability soil cover material in all areas where dumping is not presently occurring.

2.2 Construction Site Conditions

The Shelton Landfill and surrounding area are shown in Figure 2.1. The landfill lies on the west bank of the Housatonic River and abuts the Shelton-Stratford town line. Access to dumping areas at the landfill is provided by an access road which intersects Connecticut Route 110 in the western corner of the landfill. The access road stretches from Rt. 110 to the apex of the landfill. The road extends from Rt. 110 to the east-southeast toward the Housatonic River for 300 meters where it turns to the northwest for approximately 350 meters in parallel with the river. The last section of road leads a distance of 100 meters in a northwesterly direction toward the top of the landfill. The test embankment is located on the east slope of the landfill and is part of the roadway lying in parallel with the river. The exact location of the test section is shown in Figure 2.1.

The access road was reconstructed in 1992 when the original roadway had deteriorated to a condition where travel upon it was difficult. The original construction plans called for the use of conventional granular aggregates in fill sections. The proposed reconstruction provided an opportunity to demonstrate the usefulness of incinerator bottom ash as structural fill material. In addition to using incinerator ash as fill material, bottom ash was used as aggregate in the bituminous concrete with which the road was paved. Details on the study of incinerator bottom ash as a bituminous aggregate are reported in Demars, et al. (1993).

The primary problem with the original access road was excessive differential settlement caused by the decomposition of the underlying unburned MSW fill. The MSW fill acted as the foundation for the original roadway. Along the roadway centerline, the MSW has a minimum depth of 15 meters. Subsidence resulting from the continual MSW

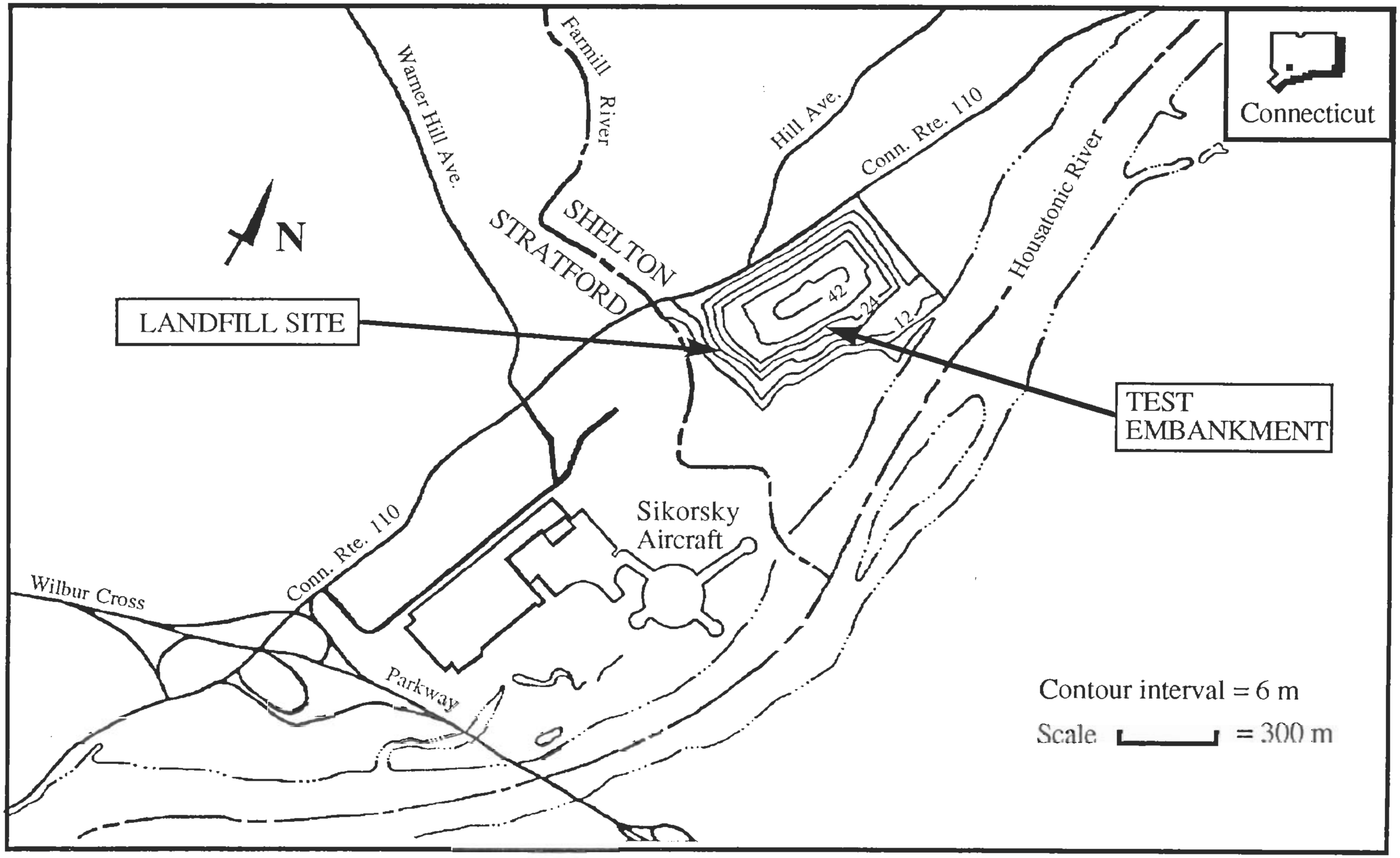

Figure 2.1 - Sitemap of Shelton Landfill and surrounding area

decay caused the roadway to have significant dips and grade changes. Localized vertical settlements in excess of 1.5 meters over a horizontal distance of 20 meters were present. One of the primary concerns during the design of the new access road was the susceptibility of the test embankment to the compression of the MSW foundation. The construction of a new road presented a low cost solution for improving the deteriorating existing access road.

The Shelton Landfill presents an optimal site at which to conduct research using incinerator bottom ash. The two main issues involving bottom ash usage in a roadway demonstration project are environmental effects and the possibility of embankment failure. The primary environmental concern is introducing contaminants into the local ground water supply. The landfill already contained unburned MSW and combined ash, meaning that the addition of a relatively small test embankment to the landfill would not introduce new contaminants to the local ground water supply. The surface of the test embankment would be covered with bituminous asphalt, thus preventing movement of bottom ash particles by surface transport mechanisms.

Potential problems associated with excessive settlements in the test section are not of major concern because the roadway test section is not used as a public thoroughfare. Traffic usage is limited to haul trucks carrying incinerator ash to the top of the landfill. If settlement problems arise over time, temporary fill can be placed in areas of subsidence. If settlements are small, problems may be ignored since truck traffic using the road travels at speeds less than 30 km/hr.

2.3 Test Embankment Construction Materials

2.3.1 Bottom Ash - Bottom ash used in the embankment originates from the Bridgeport Recycling Trash-to-Energy facility located in Bridgeport, CT. Wheelabrator Environmental Systems Inc. designed, constructed, and operates the mass-burn facility. The plant began operations in 1988 after a two year construction period. The $300-million facility generates 67 megawatts of power. United Illuminating Company purchases electricity generated by the plant, providing power produced by non-recyclable waste to approximately 40,000 Connecticut households.

Municipal solid waste processing at the Bridgeport Recycling Trash-to-Energy facility is summarized by Gibbs and Hepp (1990). MSW arriving at the facility is tipped into a refuse pit. The refuse pit is large enough to stockpile waste to facilitate 24 hour/day 7 day/week plant operation. The plant combustion capacity is 2040 metric tons/day. The average throughput is 1630 metric tons/day. The MSW, with an estimated energy content of 12140 kJ/kg is fed into any of three hoppers above the refuse pit via overhead crane. Hoppers provide fuel for each of three separate process lines operating at the facility. The downward feeding hoppers supply plug flow to the furnace. MSW flow rates into the furnace are controlled by a hydraulic ram located in the lower part of the hopper. A reciprocating grate conveys waste through the furnace. During the 30-45 minute residence time within the furnace, the waste is dried and heated to ignition temperature. Temperatures within the furnace exceed 1370° C. To create the optimum combustion environment, air is injected above and below the reciprocating grate. In an effort to curb odor and dust generation, the facility inducts air for combustion from above the refuse pit area. Waste entering the furnace is usually completely burned. MSW soaked with fluids such as water or oil may not burn completely. In addition to fluid soaked MSW, densely packed combustible materials such as paper products or thick pieces of wood may not be entirely combusted.

The burning process produces two primary byproducts. Bottom ash is that material remaining on the reciprocating grate after passing through the furnace. Fly ash is that material which escapes the furnace as part of the flue gas. Flue gas is produced by the burning refuse in the furnace. The flue gas rises vertically out of the furnace where it enters the boiler. Here, heat is exchanged from the hot flue gas to form super heated steam. The high pressure steam cycle used at the facility is 260 MPa/400° C. The super heated steam drives the power generating turbines. Flue gas is processed to remove fly ash particles before stack emission. The ash particles removed during processing comprise the fly ash portion of the waste stream. Fly ash particles are wetted after removal from the flue gas to control dust. The wetted material is then mixed with bottom ash for disposal at the Shelton Landfill.

After traveling through the furnace on the reciprocating grate, bottom ash is expelled into a quench tank where it is soaked in water for approximately one hour. Bottom ash moves through the quench tank via a reciprocating ram. After leaving the quench tank, the bottom ash is at approximately 18% moisture content by weight. During normal plant operations, bottom ash travels from a discharge area where it is transferred by belt conveyor for mixing with the fly ash. Since the test embankment was to be constructed using bottom ash only, ash used for the demonstration project was removed from the process line before fly ash was added. The final processing step is the grizzly conveyor, a grate which separates particles larger than 254 mm. Historically, particles larger than 254 mm have been ferrous or other types of metal. Material retained on the grizzly grate is sent for metals recycling at another facility. Ash is stored on site before delivery to the landfill.

Bottom ash delivered to the landfill for construction had not passed through the grizzly grate at the incinerator. As a result, the largest particles were still present in the ash. To prepare the bottom ash for construction use, it was passing through a 100 mm vibratory screen. The screening was performed at the landfill using a bucket loader to manipulate the material. After screening, the bottom ash was stockpiled for 48 hours or more to permit moisture content reduction by gravity drainage.

2.3.2 Gravel - Gravel used in the embankment construction originated from the J.J. Brennan gravel pit in Shelton, CT. Gravel produced by the pit included excavated soft rock from on-site deposits as well as unprocessed material purchased from various other aggregate vendors. All material excavated on site and purchased by Brennan was processed in a crusher and passed through a 38.1 mm screen. As a result of the crushing process, the gravel used for construction was angular upon visual inspection. Identifiable mineral constituents were dominated by schist in addition to some quartz. The mineral composition of the gravel varied because Brennan incorporated material from several sources. The Unified Soil Classification designates the material (as determined by field inspection) as a well graded silty sandy gravel or WMSG.

2.3.3 50% Bottom Ash/50% Gravel - A mix of bottom ash and gravel was used to construct one of the three subsections in the test section. The material will be referred to as mixed material throughout this paper. Equal quantities of gravel and screened bottom ash were mixed at the landfill using a bucket loader. The two materials were measured in one bucket quantities. Mixing was performed using the bucket loader. The operator of the loader mixed the material until it was adequately blended as based on visual inspection.

2.4 Test Embankment Design/Layout/Typical Cross Sections

The primary objective in the embankment design is to determine the physical and environmental performance of incinerator bottom ash as fill material. Performance data from the bottom ash subsection is to be compared with performance data from the gravel control subsection and the mixed material subsection. To achieve the objectives, the embankment must be of adequate thickness to provide dependable settlement measurements and must be outfitted with deformation monitoring equipment. To provide environmental impact data, the embankment must be isolated from the natural ground water in the landfill and must be constructed with a leachate collection/extraction system. Each subsection is isolated from adjoining subsections to separate leachate between subsections.

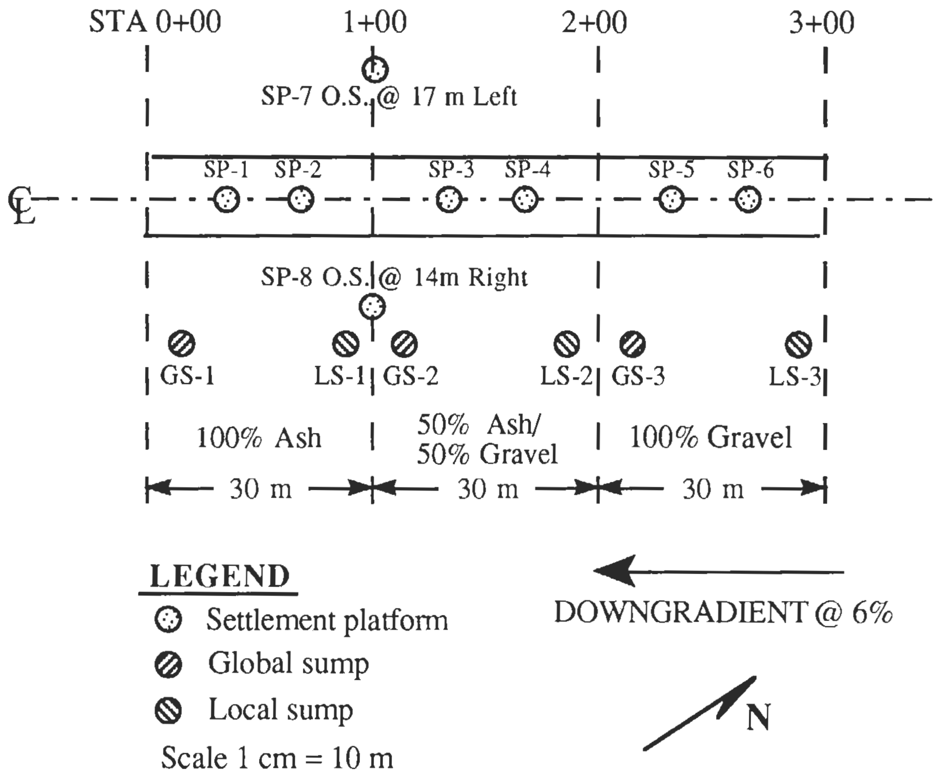

Figure 2.2 Plan view of roadway test section showing instrumentation

A plan view of the roadway test area in shown in Figure 2.2. The total length of the embankment is 91 m. Each of the three subsections is 30.5 m long, 3 m thick, and 8 m wide at ground level. The embankment was constructed using dimensions in the English measurement system. Although this paper uses SI units, references to stations on the test embankment will be in English units. The figure shows the arrangement of the three construction materials. The bottom ash section is located in the first or southwest section from station 0+00 to 1+00. The last section is the control section composed of gravel, extending from station 2+00 to 3+00. The mixed material is located between the bottom ash and gravel sections. Figure 2.2 also shows the locations of instrumentation installed to monitor the behavior of the embankment. Settlement platforms are positioned at the quarter points of each subsection. Two slope pins are off set to the left and right of the roadway centerline. A local and global sump is positioned downgradient of each subsection to permit separate leachate collection from each of the three fill materials.

A typical cross section of the embankment is shown in Figure 2.3. The fill section is located on a bench excavated into the side of the existing landfill. Unburned MSW was exposed along the full extent of the test section during the bench excavation. The interface between the unburned MSW and the bottom of the test section is shown in Figure 2.3. The first layer of material above the unburned MSW is sand. The lower sand cushion is positioned over the MSW to a thickness of 0.15 m to permit free flow for ground water traveling beneath the embankment. The surface of the bench had been sloped to the southeast (see Figure 2.2) to allow for ground water flow in the lower sand cushion and to conduct water away from the embankment. A high density polyethylene (HDPE) geomembrane was placed over the sand cushion with its upgradient or northwest edge raised 0.6 m. The purpose of the geomembrane is to isolate the test section from the ground water in the landfill and to contain leachate generated within each subsection. The upgradient edge of the geomembrane is raised to prevent leachate from entering the fill section from the northwest or upgradient direction in Figure 2.3. The upper sand cushion in Figure 2.3 was placed over the geomembrane to a depth of 0.15 m in order to permit free flow for leachate infiltrating to the bottom of the fill material as well as to prevent punctures

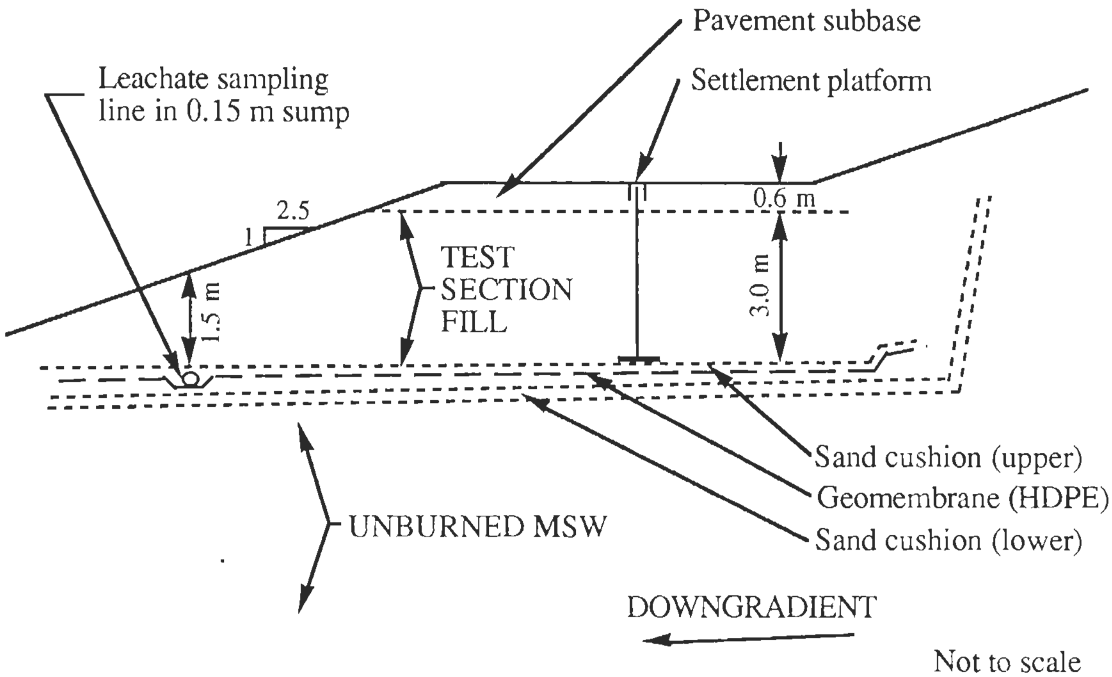

Figure 2.3 Typical embankment cross section showing instrumentation

in the geomembrane by the overlying fill. Figure 2.3 shows a leachate sampling line located along the downgradient edge of the fill section. The sampling line consists of a perforated polyvinyl chloride (PVC) pipe positioned in a 0.15 m depression to intercept leachate flowing through the upper sand cushion. Leachate entering the sampling line flows to a collection point located at the low point of the subsection. The figure also shows the position of the settlement platforms. Each platform rests on the upper sand cushion and extends vertically to within 0.25 m of the pavement surface. A conventional subbase aggregate lies on top of the 3.0 m thick test section. The pavement subbase is composed of conventional aggregate to insure that the pavement performance is not influenced by a subbase of unknown quality.

2.5 Instrumentation

Instrumentation within the embankment facilitates physical and chemical measurements. Settlement platforms positioned along the roadway centerline measure deformations occurring in each of the embankment subsections as well as deformations in the underlying fill. A schematic of the platform assembly is shown is Figure 2.4. The settlement platform consists of a 0.6 m x 0.6 m x 0.012m plywood platform with a rigidly attached 38 mm diameter steel riser pipe. The pipe ends are threaded to permit the

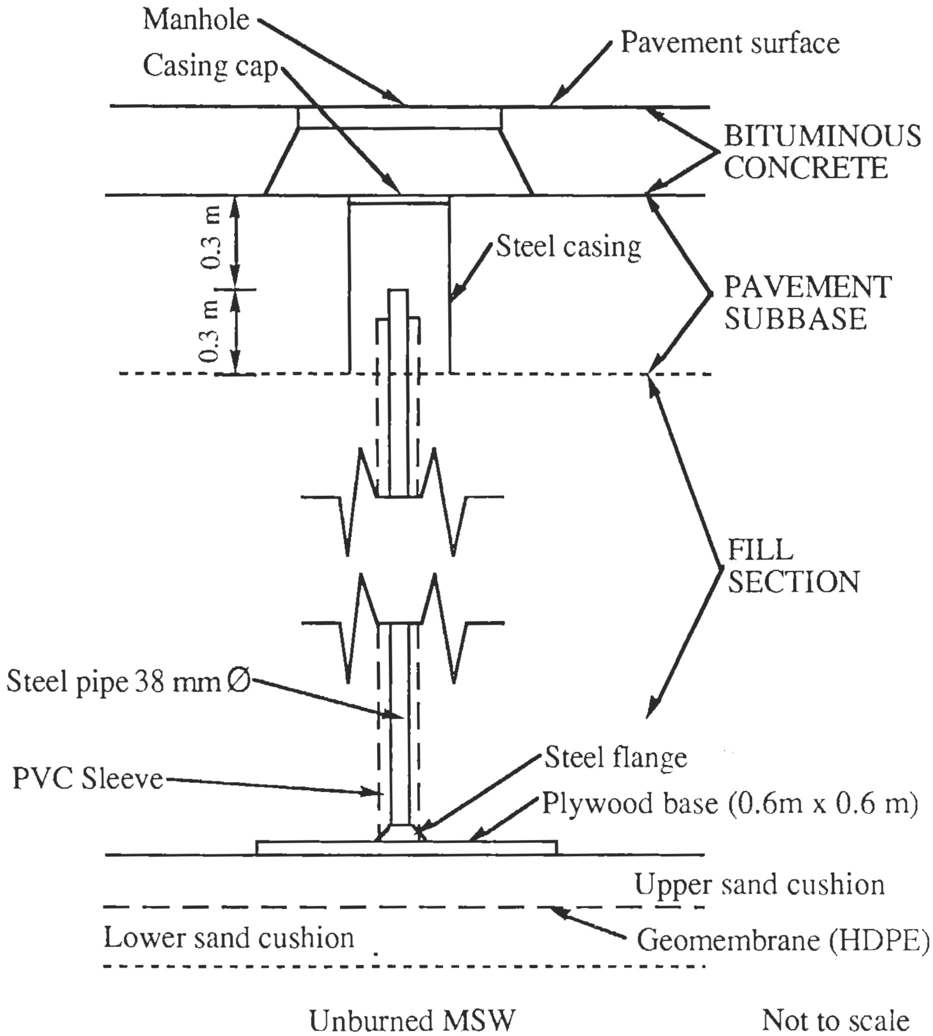

Figure 2.4 Settlement platform assembly installed on roadway centerline

attachment of extensions as the fill elevation rose during embankment construction. A 0.15 m diameter PVC outer sleeve surrounds the riser pipe for damage protection and to permit unrestricted movement of the surrounding fill material. The outer sleeve is not fixed to the settlement platform. The riser pipe is accessible through a steel casing. The casing allows access for survey measurements on the top of the riser pipe. The top of the casing is at the same elevation as the top of the pavement subbase. A manhole surrounds the casing to facilitate access through the pavement. The settlement platforms are designed to measure deformations occurring within the embankment as well as those occurring in the underlying MSW. Survey measurements are taken at the top of the platform riser pipe and on the casing cap. The compression of the underlying MSW are indicated by changes in elevation of the riser pipe. The difference in elevation between the platform riser pipe and the casing cap indicates compression occurring within the embankment.

The local and global sumps provide leachate samples. A schematic of the local and global sumps is shown in Figure 2.5. One global sump collects leachate from each of the embankment subsections. Global sumps are positioned at the lowest vertical elevation within each subsection as shown in the plan view in Figure 2.2. Figure 2.3 shows one element of the global leachate collection system. The leachate sampling line located along the downgradient edge of the bench cut in Figure 2.3 drains to a sump at the low point of each subsection. Leachate flowing along the length of the subsection through the upper sand cushion is collected in a depression oriented in the cross section of the roadway and situated at the low point of the subsection. The depression in the sand cushion reaches a depth of 0.3 m. The leachate sampling line and the 0.3 m depression intersect at the southern corner of each subsection. Both the perforated collection line and the depression channel water to a sump, shown in Figure 2.5. The sump was constructed by making a depression in the sand cushion and placing the geomembrane in the depression. Sampling tubes were placed in the depression which was filled with 12 mm stone. The depression was covered with a geotextile to prevent particles from migrating from the embankment into the sump. Gravity drainage of the sumps was permitted by installing long sampling tubes. The tube ends could be placed below the elevation of the sump, causing gravity drainage to occur and allowing water to drain freely. The roadway was constructed at a 6% grade from station 0+00 to 3+00. Therefore, barriers were constructed to prevent leachate migration into adjacent subsections. The barriers were constructed at the interface between subsections and consisted of a berm with a geomembrane cover.

The local sumps were designed to function as lysimeters. A typical local sump is shown in Figure 2.5. They were constructed similar to the global sumps. The difference

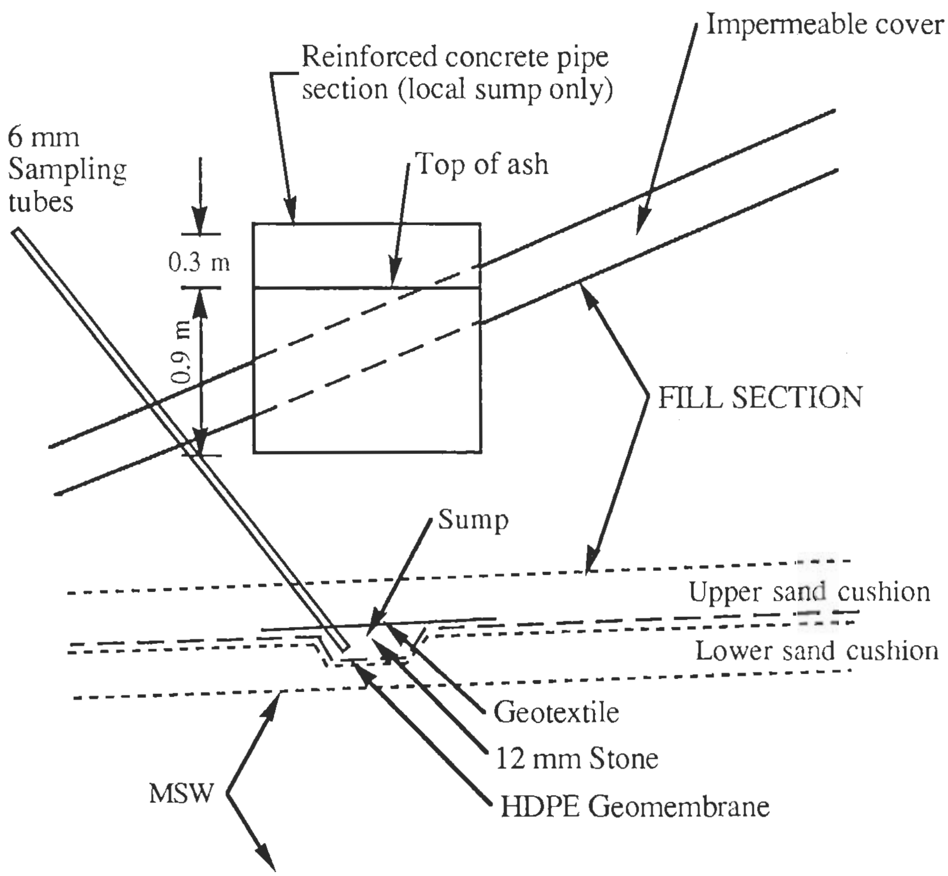

Figure 2.5 Cross section of leachate collection system for global / local sumps

was that pore water accumulating in local sumps originated from a section of reinforced concrete pipe (RCP) placed on end above the sump. The top of the 1.2 m diameter by 1.2 m long RCP section was placed above ground level to permit dowsing of the underlying fill with measured quantities of water. Leachate was also generated by rain falling into the pipe section. Leachate entering the pipe section infiltrated the underlying fill and accumulated in the sump where it was vacuum extracted through two 6 mm sampling tubes.

2.6 Embankment Construction

The construction process began with the excavation of a bench into the existing landfill. The excavation occurred on the southeastern (Figure 2.2) side of the existing access road. The position of the bench cut provided continuous access to the top of the landfill on the existing roadway while creating an expansion of the filling volume for the landfill. The lower sand blanket was placed on the exposed MSW and compacted with a vibratory roller. Depressions were excavated for the six sumps, three leachate sampling lines, and three intercepts for leachate traveling the length of the road. Berms were constructed on the upgradient edge of the bench cut and at the interface between subsections, thus creating cells to accommodate separate leachate collection from each subsection. A 30.5 m section of HDPE geomembrane was rolled out onto the lower sand layer on each of the three subsections. Leachate sampling tubes were installed into the sumps which were filled with 12 mm stone and covered with geotextile before the upper sand layer was spread and compacted. When the upper sand layer was in place, the settlement platforms were placed at the quarter points of each subsection. Surveyors measured the horizontal and vertical position of each platform before filling operations began. Two slope pins were placed at 17 m left and 14 m right along the roadway and their positions were measured. The outer PVC sleeves were placed around the riser pipes on the settlement platforms in preparation for placement of the embankment fill. The first subsection to be filled was the 100% bottom ash section. Material was delivered by haul trucks and spread in 0.3 m lifts using a bulldozer. In an effort to prevent punctures in the geomembrane, haul trucks were not permitted to travel onto the fill area until two lifts were placed. A bulldozer was used to do all of the material manipulations for the first two lifts. Each lift was compacted with a vibratory roller. Field density tests were conducted using the balloon density method and nuclear density measuring device. Field densities were acceptable for 90% or greater of the modified Proctor density. Filling continued for all of the subsections until the thickness of the embankment reached 3.0 m. During filling, extensions were placed on the riser pipes and outer sleeves as needed. As the fill depth approached 3.0 m, steel casings were installed around the tops of the riser pipes to provide access for survey measurements. A conventional aggregate subbase was placed along the entire embankment. Manhole covers were positioned over the steel casings to provide access to the casing and to separate the casing from overlying subbase material. The roadway was paved with bituminous concrete.

2.7 Sampling Methods

2.7.1 Aggregate Sampling - During embankment construction bottom ash, gravel, and mixed material were sampled regularly. As each of the ten 0.3 m thick lifts were placed on the fill section, a sample of material was taken. Several locations on each lift were selected for sampling. Material was excavated at randomly selected locations using a hand shovel. Ten samples of each construction material were taken for a total of 30 samples. Sample size was approximately 11 liters (3 gal). Individual samples were labeled according to type of material and lift of origin. The following letters were used to denote the type of material: bottom ash - BA, gravel - S, and mixed material - AS. The lift of origin was denoted with a number from one to ten, where lift number 1 denotes the first lift constructed. This paper will use the same system of sample identification.

During the course of the laboratory test program many of the bottom ash samples which had been stockpiled during construction were utilized in experiments and subsequently discarded. As a result, additional bottom ash was collected. For this method of sample collection, material was excavated from the local sump in the bottom ash subsection of the embankment (LS - 1). The material was excavated by hand shovel and included portions of the first three lifts placed during construction. Approximately 130 liters (35 gal) were taken. Two additional 130 liter buckets of material were later taken for large scale laboratory leaching studies. These two samples were excavated in similar fashion to the first 130 liter sample but at a different location. The samples were excavated from the side of the embankment approximately 2 meters from LS-1. Material was excavated from the third through the sixth lifts.

2.7.2 Field Leachate Sampling - As part of the field testing program leachate samples were periodically extracted from the global and local sumps. Leachate was extracted using the leachate sampling tubes shown in Figure 2.5. The sampling tube ends were extended below the elevation of the sump and a vacuum was applied until gravity flow was maintained. The sumps were permitted to drain for a short time before a 1 liter sample was collected for laboratory analysis. At the conclusion of sampling, the sumps were permitted to drain completely. When the sumps were fully drained, the tube ends were placed at an elevation above the sump to prevent further gravity drainage and to allow the sump to refill.

3.0 LABORATORY TESTING PROGRAM

The purpose of the laboratory testing program is to determine the physical and chemical characteristics of bottom ash, gravel, and mixed material samples collected in the field during embankment construction. In addition to the three primary construction materials, two other materials were used during laboratory tests to investigate the effects of blending on the physical characteristics of bottom ash. Commercially manufactured kaolinite produced by Babcock and Wilcox and coal fly ash produced at the AES Thames electric power plant were used for blending with bottom ash.

Laboratory tests were performed in accordance with American Society for Testing and Materials (ASTM) specifications whenever possible. Due to the nature of bottom ash, special handling procedures were developed to best evaluate the physical characteristics of the material. Some of the specially developed procedures deviate from ASTM specifications. Table 3.1 shows the tests performed in laboratory analyses along with the associated ASTM standard. In cases where testing procedures deviate from ASTM specifications, this chapter details the exact procedure used.

Physical Characteristic	Text Section	ASTM Standard
Particle size distribution	3.1.1	D422 / D1140
Ferrous metals content	3.1.2	No standard test
Compaction - dynamic	3.1.3	D698 / D1557
Specific gravity - gas method	3.1.4	ASTM aproved
Specific gravity - wet method	3.1.4	D854
Direct shear	3.1.5	D3080
Permeability - constant head	3.1.6	D2434
Shrink/swell properties	3.1.7	No standard test
Unconfined compression	3.1.8	D2166
Loss on ignition	3.1.9	D2974

Table 3.1 Physical characteristics with associated ASTM standard

3.1 Physical Testing Procedures

3.1.1 Particle Size Analysis - Particle size analyses were performed in accordance with ASTM D422. After drying at 70° C, the material was tested for gradation in a two-step process due to limitations on sample size requirements. The first step involved sieving the entire contents of each 11 liter bucket sample through 1 1/2 in (38.1 mm) and 3/4 in (19.1 mm) sieves. Material retained on each sieve was weighed to determine the percent retained. A smaller subsample of material passing the 3/4 in (19.1 mm) sieve was placed into a nest of six sieves which included Nos. 4, 10, 20, 40, 100, and 200. After shaking, material retained on sieve Nos. 4, 10, and 20 was weighed. Sieve Nos. 40, 100, and 200 were further processed by washing to improve accuracy. The washed sieves were oven dried before weighing.

3.1.2 Ferrous Metals Content - The weight-based fraction of ferrous metals was determined using magnetic separation. Because magnetic separation is not standardized by ASTM, a protocol was developed for use with bottom ash. Two types of tests were performed. The bulk ferrous fraction method was used to determined the total ferrous metals fraction of a bottom ash sample taken directly from the field. Using a sample size of approximately 2.5 kg, ferrous particles were magnetically removed from nonferrous constituents. The total weight of ferrous material divided by the original sample weight yielded the ferrous fraction.

The graded ferrous fraction method was used to determine the quantity of ferrous material retained on U.S. Standard sieve Nos. 4, 10, 20, 40, 100, and 200. Material tested passed either the 3/4 in (19.1 mm) or No. 4 sieve. Sample size was in accordance with ASTM D1140. After the sample had been shaken in the sieve nest, ferrous particles were magnetically separated from nonferrous constituents retained on each sieve size. The weight of ferrous material retained on each sieve divided by the total sample weight yielded the ferrous fraction for each sieve size. The summation of the ferrous material weight for all of the sieves divided by the total sample weight yielded the total ferrous metal content for the sample.

3.1.3 Maximum Dry Density - Compaction testing was performed in accordance with ASTM D698 and D1557. The purpose of compaction testing was to determine how variations in test parameters affected maximum dry density and optimum moisture content. The test methods used for compaction of the bottom ash were varied, causing some of the compaction experiments to deviate from ASTM specifications. ASTM guidelines were followed as closely as possible for those tests which deviated from specifications. The following elements of ASTM specifications for compaction testing remained unchanged during testing: mold dimensions, hammer weights and dimensions, sample preparation procedures, and moisture content determination. Elements of ASTM standards which varied were: mold size required for maximum particle diameter, number of layers of material in the mold, number of hammer drops, and compaction energy input. Section 4.2 details the procedures used for individual test results.

3.1.4 Specific Gravity - Two types of specific gravity tests were performed on materials used in the embankment. The gas pycnometer test method was used to determine the specific gravity for bottom ash and the wet pycnometer test was used for the specific gravity for gravel. The helium (gas) pycnometer method was recently accepted by ASTM and uses the pressure-volume relationship (Boyle's Law) to determine sample volume. Bottom ash passing the No. 4 sieve was used for testing. Gravel samples were tested by the conventional wet pycnometer using ASTM D854. Gravel samples passed the No. 4 sieve. Direct testing was not performed to determined the specific gravity of the mixed material because it is a combination of two materials with known specific gravities. ASTM D854 details a method for determining the specific gravity for two materials. The equation given in Section 1.1 of the specifications is

$$G_{avg} = \frac{1}{\dfrac{R_1}{100G_1} + \dfrac{P_1}{100G_2}} \qquad \textbf{Eq. 3.1}$$

where G_{avg} = weighted average specific gravity, R_1 = percent fraction of bottom ash, P_1 = percent fraction of gravel, G_1 = specific gravity of bottom ash, and G_2 = specific gravity of gravel.

3.1.5 Direct Shear - Direct shear tests were performed according to ASTM D3080. Samples were tested using a Wykeham Farrance direct shear apparatus with a fixed lower shear box. The shear box featured a permeable top and bottom stone with a circular sample area of 28.6 cm^2. The top shear box was vertically separated approximately 0.5 mm from the bottom shear box prior to testing to reduce frictional effects. Vertical displacement and load ring data were recorded at predetermined horizontal displacements. Horizontal and vertical displacements were measured to the nearest 0.00025 mm. Tests were conducted using normal stresses of 77.8 kPa, 155.5 kPa, 311.1 kPa, and 622.1 kPa. Samples were sheared at a strain rate of 0.42 mm/min.

Tests were performed on wet and dry samples. Samples of bottom ash were tested wet. The bottom ash permeability was determined to be sufficiently high to prevent pore pressures from developing during shearing. Material passing the No. 4 sieve was compacted to within 90-95% of the maximum dry density at optimum moisture. To eliminate unnatural reinforcement of the shear plane by a single particle, abnormally long particles such as small nails and heavy gauge metal wire were manually removed prior to compaction. Material was compacted in five layers using a Harvard miniature spring loaded tamper. The interface between compacted layers was always located above or below the shear plane in order to avoid the creation of a weak failure surface in the plane of shearing. Sample thickness and weight were determined after compaction. After testing samples were oven dried to determine moisture content .

Gravel and mixed material were tested dry to avoid pore pressure effects. The permeability of both materials was sufficiently low to cause pore pressure to develop. Test material passed the No. 4 sieve. Abnormally long particles were removed from these materials. Samples were compacted in the shear box using one minute of vibration. The goal of the vibratory procedure was to achieve a dry density as close as possible to the maximum dry density. Samples were weighed and the thickness measured prior to testing.

3.1.6 Permeability - Constant head permeability tests were performed in accordance with ASTM D2434. Samples were tested in a flexiwall permeameter using water as the confining fluid. Samples were subjected to backpressures of 345 kPa and gradients between 5 and 15. All material tested passed the 3/4 in (19.1 mm) sieve. Samples were compacted in a 7.3 cm diameter Shelby tube using 5 layers with 16 modified Proctor hammer blows per layer. Compaction energy input was comparable to a modified Proctor test based on energy per unit volume. Test material at optimum moisture was compacted to within 90% of the maximum dry density. Two types of samples were prepared. Unblended samples of bottom ash, gravel, and mixed material were sieved, wetted and compacted into the Shelby tube. Blended samples consisting of bottom ash with varying amounts of kaolinite and/or coal fly ash were also prepared and compacted into the mold.

3.1.7 Shrink/Swell - The expansion and contraction characteristics of bottom ash and bottom ash/kaolinite blends were investigated using samples prepared in a Harvard miniature mold. Samples were compacted using a Harvard miniature tamper. Material was compacted at optimum moisture in five lifts with 25 blows per layer. After extrusion from the mold the diametric and longitudinal dimensions of each sample were measured. The diameter at the top, middle, and bottom of the sample was measured. The sample length was measured at two opposite positions on the cylindrical sample. Dimensions were measured to the nearest 0.01 mm using Vernier calipers. After oven drying at 110 °C, the dimensions were remeasured at the same locations. The difference between the wet and dry dimensions divided by the original wet dimension yielded the strain resulting from drying. The expansion and contraction characteristics of selected permeameter samples were also investigated. After permeability testing, samples were removed from the triaxial chamber. The strain resulting from drying was determined using procedures similar to those used for the Harvard miniature samples.

3.1.8 Unconfined Compression - Unconfined compression (U) tests were performed in accordance with ASTM D2166. Test material passed the No. 4 sieve. Specimens were compacted in a Harvard miniature mold. Material was compacted using a Harvard miniature tamper in 5 layers with 25 blows per layer. Samples were compacted to within 90% of the maximum dry density. Strain rates of about 2%/min were used. The maximum load applied to each sample was recorded during testing. Sample deformation data was not recorded. The compressive strength was determined by dividing the maximum applied load by the cross sectional area of the sample. Each sample was weighed and oven dried to determine moisture content and dry density.

3.1.9 Loss on Ignition - Loss on ignition testing was performed using ASTM D2974. The testing procedure utilized material passing the 3/4 in (19.1 mm) sieve. Procedures followed ASTM specifications with one exception. Initial tests indicated that particles were exploding upon heating to 440 °C. To prevent exploding particles from escaping from the sample, each porcelain bowl used for testing was covered with perforated aluminum foil. The foil cover permitted air flow to the sample while preventing the loss of mass from explosion.

3.2 Chemical Testing Procedures

Chemical analyses were performed on solid and aqueous samples by the Environmental Research Institute (ERI) at the University of Connecticut. ERI utilized a combination of Environmental Protection Agency (EPA) standardized test methods and analytical methods developed by ERI to perform various chemical analyses. Section 3.2 provides a brief description of protocols used by ERI and the purpose of each test procedure.

3.2.1 Metals Analysis on Leachate - Leachate samples extracted from field sumps and laboratory leaching apparatus were analyzed for the presence of selected metals and their corresponding concentrations. The concentration of arsenic, barium, cadmium, calcium, chloride, chromium, lead, manganese, potassium, selenium, silver, and sodium were determined. ERI used EPA Method 3010: Acid Digestion of Aqueous Samples and Extracts for Total Metals for Analysis by Flame Atomic Absorption Spectroscopy or Inductively Coupled Plasma Spectroscopy to prepare the leachate samples for metals analysis by Inductively Coupled Plasma (ICP) spectroscopy. Method 3010 is published by the EPA in *Test Methods for Evaluating Solid Waste Physical/Chemical Methods Third Edition*. Sample preparation using Method 3010 began by digesting the leachate sample in nitric acid. The combined leachate and nitric acid were heated without boiling to promote digestion and evaporation. After the initial heating cycle, additional nitric acid was added and the sample was reheated. This process was repeated until digestion was complete. Hydrochloric acid was added to the sample. The digestate was filtered and diluted. The sample was analyzed for metals composition by ICP spectroscopy.

3.2.2 Toxicity Characteristic Leaching Procedure (TCLP) - The TCLP test is designed to assimilate the mobility of compounds present in single or multiphase materials. The procedure is detailed in the *Federal Register*, Friday June 29, 1990, pp. 26985-26998. The TCLP prep was used to prepare solid samples for analysis by ICP spectroscopy. Samples submitted to ERI for TCLP analysis originated from the bottom ash and gravel subsections of the test embankment. The bottom ash and gravel samples were analyzed for metals leachability, conductivity and chloride concentration. All material used for TCLP testing passed a 9.5 mm sieve. The TCLP prep entailed agitating the solid sample in extraction fluid containing dilute glacial acetic acid for 18 hours. The extracting fluid was agitated by rotary agitation which allowed compounds to leach from the test material and dissolve in the extraction fluid. After agitation, solids were filter separated from the extraction fluid. The TCLP extract was next treated as an aqueous sample and prepared for metals analysis by ICP spectroscopy using Method 3010 detailed in Section 3.2.1.

3.2.3 Total Chemical Analysis - Pulverized dry solid samples of bottom ash and gravel were analyzed for metals concentration using the Hydrofluoric Microwave Digestion

Procedure. The test was performed to determine the total contaminant concentrations in the sample material. The procedure was developed by ERI and is not standardized by EPA. Solids used for testing were pulverized using dynamic impact energy. The crushed material passed the No. 100 sieve. Sample preparation for ICP spectroscopy analysis began by completely digesting the pulverized solids. Digestion began by adding 10 ml concentrated hydrofluoric acid to a 0.07 g sample. The sample was heated for 3 minutes and permitted to cool without venting. After venting, 10 ml concentrated nitric acid and 5 ml concentrated hydrochloric acid were added. The mixture was reheated for 3 minutes and permitted to cool without venting. The digestate was vented and filtered using acid washed filter paper. The sample was diluted to 100 ml and analyzed by ICP spectroscopy.

3.2.4 Column/Lysimeter Leaching - Laboratory tests to determine the rate of attenuation for dissolved contaminants in leachate were performed using small and large scale testing apparatus. Small scale tests were performed in a column leaching apparatus. Large scale tests were performed using a lysimeter. Column tests were performed using a cylindrical plexi-glass tube 7 cm in diameter. The vertically oriented column was covered on the bottom with a geotextile to prevent particle migration. The geotextile was held in place at the column base with a steel collar. The top of the column was open to facilitate the addition of water for dowsing. Approximately 200-300 g of test material passing the No. 4 sieve was vibratorily compacted in the column. The material in the column was repeatedly dowsed with a volume of distilled water equal to the volume of the voids contained within the sample. Samples were dowsed with a total of approximately 20 pore volumes of water. After leachate was collected from the sample material, it was weighed, brought to 25 °C, and the conductivity was measured using a Barnstead Conductivity Bridge.

Large scale leaching studies were performed using a lysimeter containing approximately 0.12 m^3 of bottom ash. A schematic of the lysimeter is shown in Figure 3.1. Bottom ash was held in a 130 liter PVC container. The top of the container was open to permit dowsing of the bottom ash samples with water. The base of the vessel contained a drainage layer composed of compacted masonry sand. Leachate was extracted from the drainage layer using a leachate collection pipe. The perforated PVC collection pipe was 3 cm in diameter and 25 cm long with capped ends. The pipe was wrapped in Polyfelt TS 500 geotextile to provide separation from the masonry sand. Leachate was vacuum extracted from tubes installed in the leachate collection pipe.

To construct the lysimeter, bottom ash was placed on top of the drainage layer in 15 cm lifts. Compaction was performed with a combination of vibratory and dynamic impact energy. The drainage layer was separated from the bottom ash by Polyfelt TS 500 geotextile. The weight of bottom ash compacted into the vessel was recorded during placement.

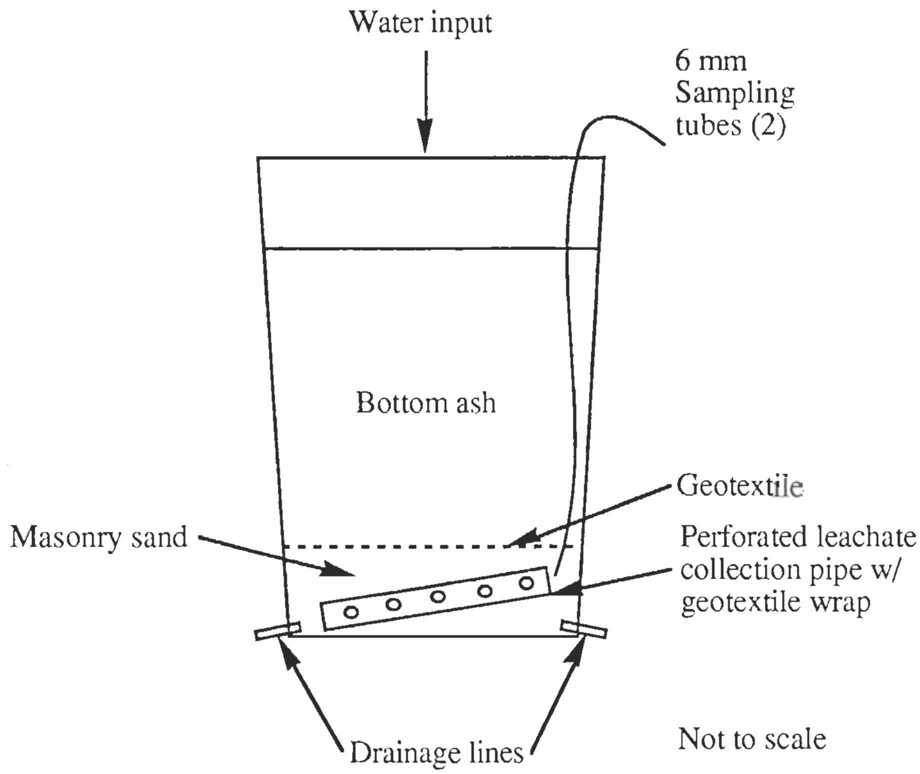

Figure 3.1 Laboratory lysimeter apparatus

The lysimeter was dowsed with a volume of water equal to one-half the volume of the voids contained within the bottom ash. Tap water was used for dowsing. Samples were extracted from the leachate collection pipe when approximately one half of the original quantity of water used for dowsing had drained from the lines at the bottom of the containment vessel. The drainage lines were closed while a 1 liter sample was extracted from the leachate collection pipe. After sample extraction, the drainage lines were opened and the remaining leachate was permitted to escape. The lysimeter was redowsed when water from the previous cycle had completely drained from the lysimeter. A total of 20 pore volumes of water were passed through the test material. Each 1 liter leachate sample was tested for conductivity and alternating samples were tested for total dissolved solids. To determine the total dissolved solids, leachate was heated at 108 °C until completely evaporated. The concentration of residue per volume was determined using the weight of solids remaining after evaporation. Samples extracted from pore volumes 1, 3, 10, and 20 were submitted for metals analysis at ERI. The leachate was analyzed using Method 3010 and ICP spectroscopy, as outlined in Section 3.2.1. The samples were analyzed for the concentration of arsenic, barium, calcium, cadmium, chromium, potassium, manganese, sodium, lead, selenium, sulfates, electrical conductivity, total dissolved solids, and pH.

4.0 PHYSICAL TEST RESULTS

4.1 Particle Size Distribution

4.1.1 Bottom Ash - The average particle size distribution for ten samples of bottom ash is shown in Figure 4.1. Of the three curves shown in Figure 4.1, the middle curve represents the average gradation for the ten samples. The upper and lower curves represent the range of percent passing values amongst the samples. Data points in the figure represent the following U.S. Standard sieve sizes (from left to right in figure): 1 1/2 in (38.1 mm), 3/4 in (19.1 mm), and Nos. 4 (4.75 mm), 10 (2.00 mm), 20 (0.840 mm), 40 (0.42 mm), 100 (0.150 mm), and 200 (0.075 mm). The narrow range between the upper and lower curves along the full extent of the gradation curve indicates that bottom ash

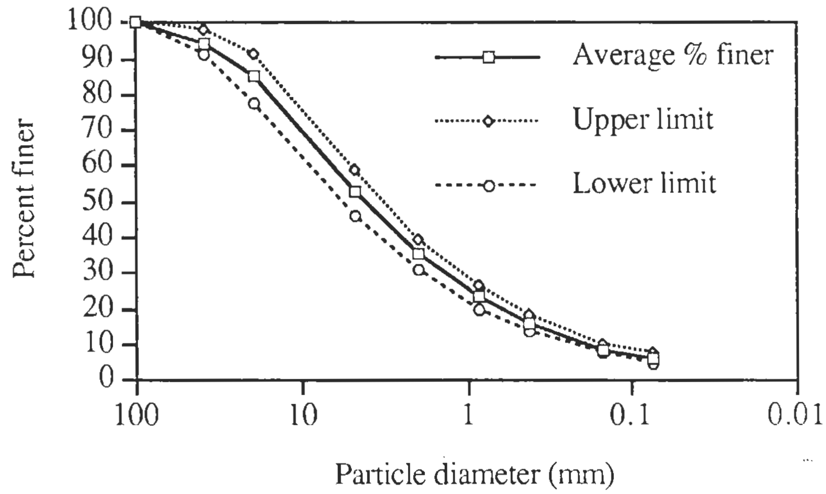

Figure 4.1 Gradation data for bottom ash

maintains a consistent gradation. Although Figure 4.1 represents data for approximately three days of ash production from the incinerator, the gradation is consistent and predictable. The smooth and symmetrical shape of the gradation curve indicates that bottom ash is a well graded material (Dunn, et al., 1983). The median particle size D_{50}, is 4.2 mm. The uniformity coefficient C_u, the ratio of D_{60} to D_{10} is 29.5. Well graded soil exhibits a uniformity coefficient greater than 15. The coefficient of curvature C_c (the ratio of D_{30}^2 to the product of D_{60} and D_{10}) is 1.3. For well graded soil, the coefficient of curvature ranges between 1 and 3 (Dunn, et al., 1983). In terms of fine grained fraction, an average of 7.4% of the bottom ash passes the No. 200 sieve. This indicates that the silt sized fraction of particles is small. The bottom ash may be considered a granular material due to the absence of a significant quantity of fine grained particles.

The data shown in Figure 4.1 is a summary for all of the bottom ash samples taken during embankment construction. Specific gradation data for each of the samples taken during construction is listed in Appendix A1. The data in Appendix A shows the relative quantities of gravel (percent retained on No. 4), coarse sand (percent passing No. 4 and retained on No. 40), fine sand and silt (percent passing No. 40 and retained on No. 200), and clay (percent passing No. 200) sized particles.

Composition - In preparing the bottom ash for construction, it was sieved through a 100 mm screen at the landfill. Particles retained on the screen were visually examined for size and composition. The particles ranged in size from 100 mm to 600 mm. The majority of particles separated were metallic and tended to be ferrous in composition. A large number of the screened particles were easily identifiable. Recognizable particles commonly appearing on the screen were automotive parts, scrap metal, construction debris, partially burned wood, and oil soaked cloth and paper. A notable aspect of the screening process was that many elongated particles with width dimensions less than four inches and length dimensions exceeding four inches passed through the screen. Some commonly occurring oblong materials passing the screening process were metal rods, automotive suspension components, and metal wire and cable. Gradation analyses were not performed on particles separated during screening.

Similar to trends observed during field screening, laboratory sieving revealed higher fractions of metallic particles retained on the larger sieve sizes based on visual observation. Due to the simplicity of magnetic separation, experiments were performed to determine the weight-based percentage of ferrous material retained on each sieve. Figures 4.2a and 4.2b show the distribution of ferrous and nonferrous constituents retained on sieve Nos. 4, 10, 20, 40, 100, 200, and the pan for two test specimens prepared using different procedures. Figure 4.2a represents data for material passing the 3/4 in (19.1 mm) sieve and will be referred to as Sample A. Figure 4.2b represents data for material passing the No. 4 sieve and will be referred to as Sample B.

Figure 4.2a reveals that the No. 4 sieve retains both the largest quantity of material and the largest quantity of ferrous material. The No. 200 sieve retains the least amount of both ferrous and nonferrous material. Generally, the fraction of ferrous material retained decreases as the sieve opening size decreases. The total amount of ferrous material contained in the Sample A is 19.3%.

The data in Figure 4.2b for Sample B shows a similar trend in ferrous metal distribution to that of Sample A. The exception is data for the No. 20 sieve. This data represents an anomaly in the predicted distribution of ferrous metals. This anomaly can be explained by the large quantity both ferrous and nonferrous materials retained on the No. 20 sieve. The quantity of ferrous material retained on a sieve is proportional to the quantity of nonferrous material retained on the sieve. Figure 4.2b shows that less ferrous material is retained on the smaller sieve sizes than the larger size sizes. The total amount of ferrous material contained in Sample B is 17.2% compared to 19.3% ferrous metal in Sample A. The total quantity of ferrous material contained in Sample B is less than the total quantity of ferrous material contained in Sample A as a result of removing particles larger than the No. 4 sieve and smaller than the 3/4 in (38.1 mm) sieve.

A second type of ferrous metals testing was performed on bottom ash. The method utilized bottom ash samples which were not specially sieved prior to analysis. Using samples collected in the field having passed the 100 mm screen, the total ferrous fraction was found to range from 10.8% to 18.0%. The average ferrous metal content is 15.5% for the 5 samples tested. A visual examination of the magnetically separated particles yields a similar trend in ferrous particle size distribution to that of the sieved samples shown in Figure 4.2. The fraction of ferrous particles is higher for the larger particles sizes.

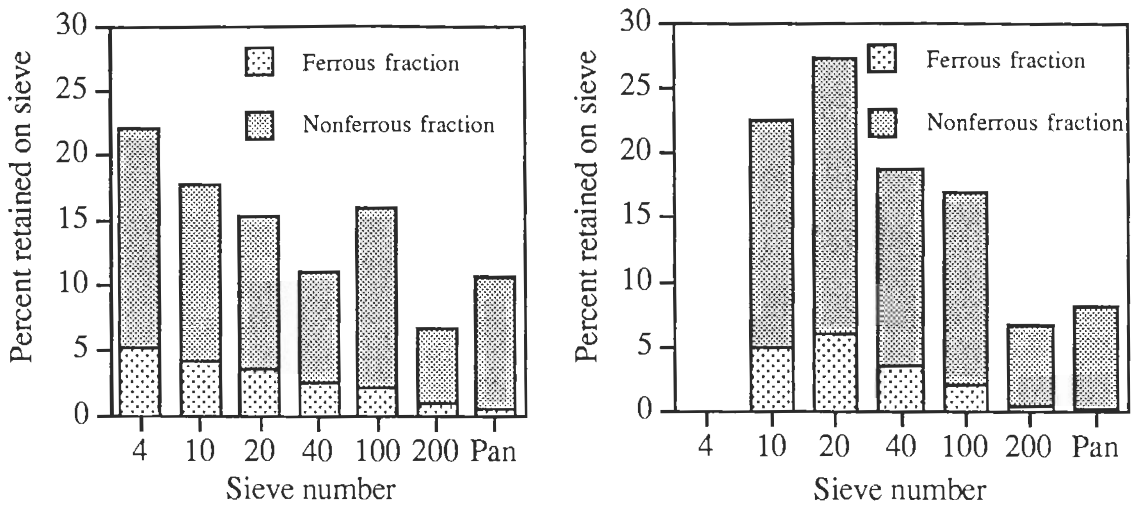

(a) (b)

Figure 4.2 Size distribution of ferrous and nonferrous bottom ash particles

4.1.2 Gravel Section - The particle size distribution for six samples of silty sandy gravel is shown in Figure 4.3. Of the three curves shown, the middle curve represents the average gradation for the six samples. The upper and lower curves represent the range of percent passing values amongst the six samples. Similar to bottom ash, the gravel is well graded. The gradation curve is smooth and symmetric, indicating well graded material (Dunn, et al, 1983). The median particle size, D_{50} is 3.90 mm. The uniformity coefficient C_u, is 77.8. The coefficient of curvature C_c is 1.04. Both the uniformity coefficient and coefficient of curvature values indicate that the gravel is well graded. The uniformity coefficient is considerably larger than 1.0, which is the value for a uniform material. The coefficient of curvature falls between 1 and 3, which is the range for a well graded soil (Dunn, et al., 1983). An average of 9.4% passes the No. 200 sieve indicating the absence of a large quantity of silt and clay size particles.

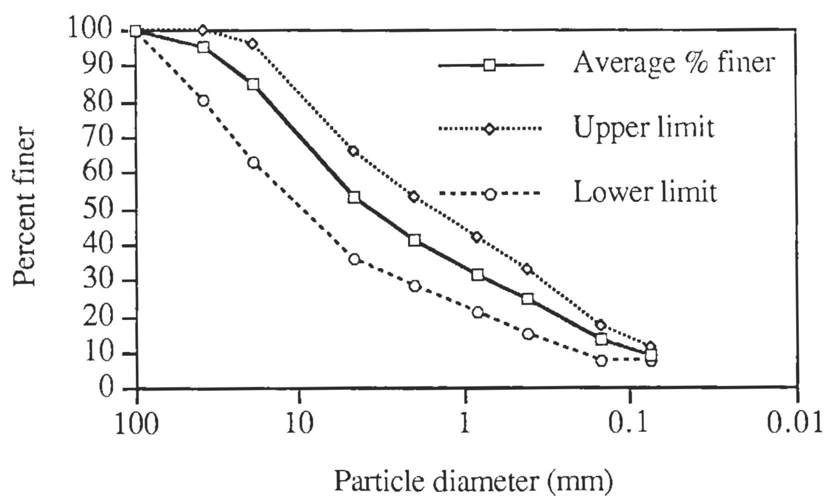

Figure 4.3 Gradation data for gravel

The effects of preconstruction processing are visible upon examination of individual gravel particles. As a result of having been crushed, particles larger than 1 mm appear angular to the unaided eye. Fine sand and silt sized particles appear angular under magnification. Figure 4.3 shows a large range between the upper and lower limits of gradation for the six samples tested. The range for the gravel is considerably greater than the range shown for bottom ash in Figure 4.1. Variability in gradation results from changes in the quality of rock being excavated from the gravel pit where the material was produced. Fluctuations in the hardness and durability of the excavated rock caused variations in the degree to which the gravel was crushed during processing.

A summary of gradation data for each of the gravel samples taken during construction is shown in Appendix A2. The breakdown of particle sizes is identical to data in Appendix A1.

4.1.3 Mixed Section - The particle size distribution for seven samples of mixed material is shown in Figure 4.4. The center curve in the figure represents the average gradation for all samples tested. The upper and lower curves represent the range of gradation for the seven samples. The mixed material is the combination of two well graded granular materials, as shown in Figures 4.1 and 4.3. The particle size distribution in

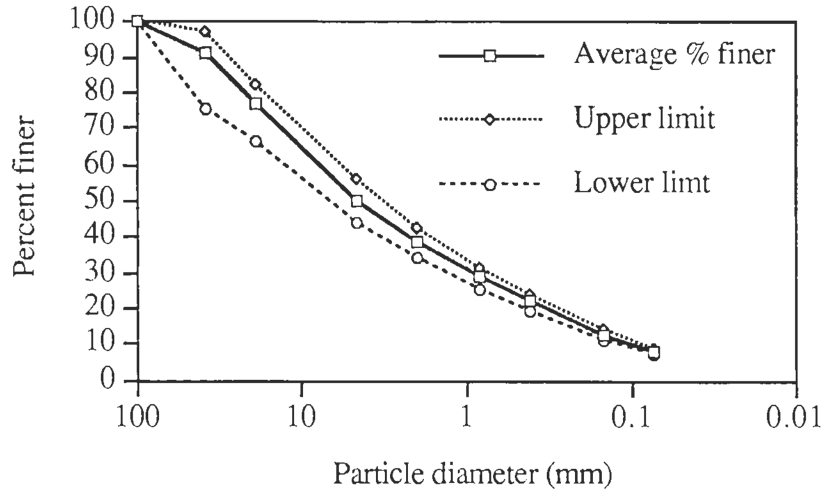

Figure 4.4 Gradation data for mixed material

Figure 4.4 shows that the mixed material has qualities similar to those of the bottom ash and gravel. The mixed material is well graded, as shown by the smooth symmetrical gradation curve (Dunn, et al., 1983). The median particle size, D_{50} is 4.60 mm, the uniformity coefficient, C_u is 81.1 and the coefficient of curvature, C_c is 1.43. Both the uniformity coefficient and the coefficient of curvature values indicate that the mixed material is well graded (Dunn, et al., 1983). An average of 8.0% passes the No. 200 sieve, indicating the absence of a significant quantity of silt and clay size particles. The mixed material is granular.

4.2 Maximum Dry Density

4.2.1 Bottom Ash - Compaction testing was performed using a variety of test methods. Test results show variable maximum dry density and optimum moisture content values for bottom ash samples. Variations in maximum dry density are significantly affected by variations in the metal content of the samples. Variability is less affected by other inconsistencies in ash composition. Samples with greater quantities of metal exhibit higher maximum dry densities because the specific gravity of steel (7.86 g/ml) is approximately 2.9 times greater than the specific gravity of natural minerals. As a result of the large difference in specific gravities, small volumes of metal are required to cause relatively large changes in dry density.

The effect of metal content on dry density is shown in Figure 4.5. This figure shows data for two Proctor tests (ASTM D1557). Separate bottom ash samples were used for each test. The material used to produce the upper curve passed the 3/4 in (19.1 mm) sieve and has a maximum dry density of 18.99 kN/m^3. The material used to produce the lower curve passed the No. 4 sieve and has a maximum dry density of 17.52 kN/m^3. Removing particles larger than 4.75 mm may cause a reduction in the maximum dry density. The reduction results from the absence of metallic particles larger than 4.75

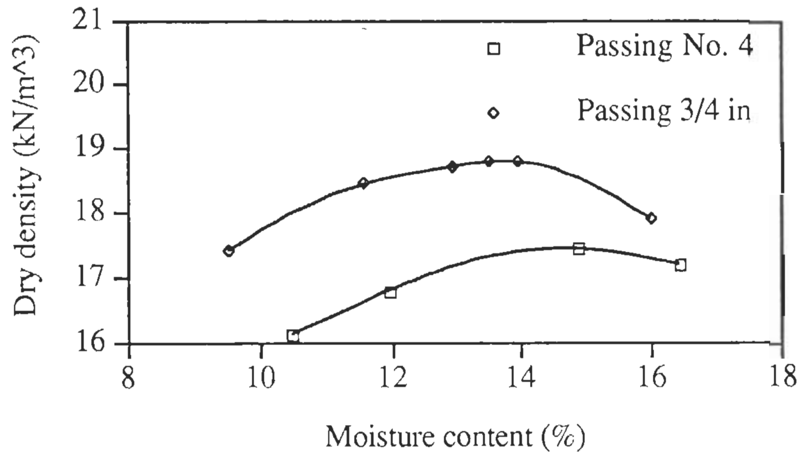

Figure 4.5 Effect of particle removal on moisture-density relationship

mm. With reference to Section 4.1.1, the fraction of metallic particles increases as a function of the particle size. Since the largest particles in the sample used to produce the lower curve were removed, a large fraction of the metal in the test material was removed as a result. The loss in mass is evident as a decrease in maximum dry density. Removing particles larger than 4.75 mm also increases the optimum moisture content. The sample passing the No. 4 sieve has a finer gradation than the sample passing the 3/4 in (19.1 mm) sieve. The volume of the voids increases as a result of the particles removal, resulting in a larger quantity of water contained within the sample at optimum moisture.

Consistent maximum dry density values were achieved when a specific sample was compacted repeatedly. Variable maximum dry density values occur when several bottom ash samples are compacted using identical test methods for each sample. Figure 4.6 shows data for two compaction tests using the same sample but implementing different procedures for each test. The upper curve in Figure 4.6 represents data for material passing

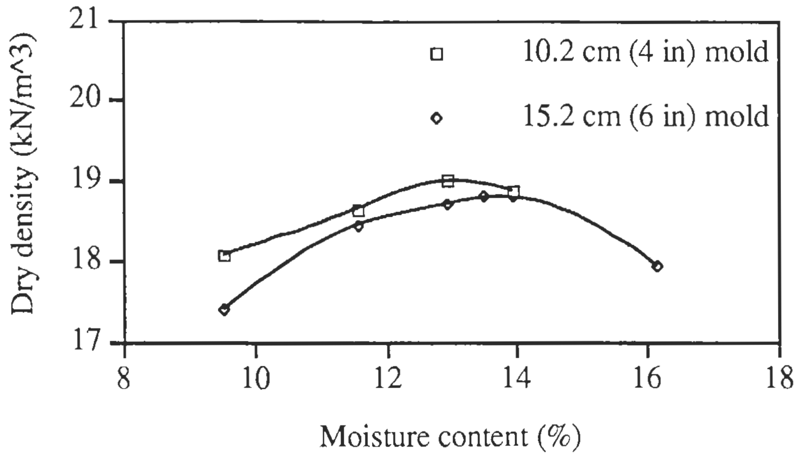

Figure 4.6 Effect of mold size on moisture-density relationship

3/4 in (38.1 mm) using a small Proctor mold, 4.54 kg hammer, and 5 layers with 25 blows per layer. The lower curve represents data for the same bottom ash sample source, but tested in a large Proctor mold, using a 4.54 kg hammer, and 5 layers with 56 blows per layer. The variation in maximum dry density is small. The small mold sample produced a maximum dry density of 18.99 kN/m^3, while the large mold sample produced a maximum dry density of 18.82 kN/m^3. Variations in maximum dry density result from inconsistencies in ash composition amongst several samples and are not a result of inconsistencies in behavior for a specific sample. An example of variable maximum dry density data between samples is shown in Figure 4.7. The figure presents compaction data from three different samples of bottom ash. Each sample was passing 3/4 in (38.1 mm), and was tested in a small Proctor mold using a 4.54 kg hammer, 5 layers, and 25 blows per layer. The range between maximum dry density for the three samples is from 17.9

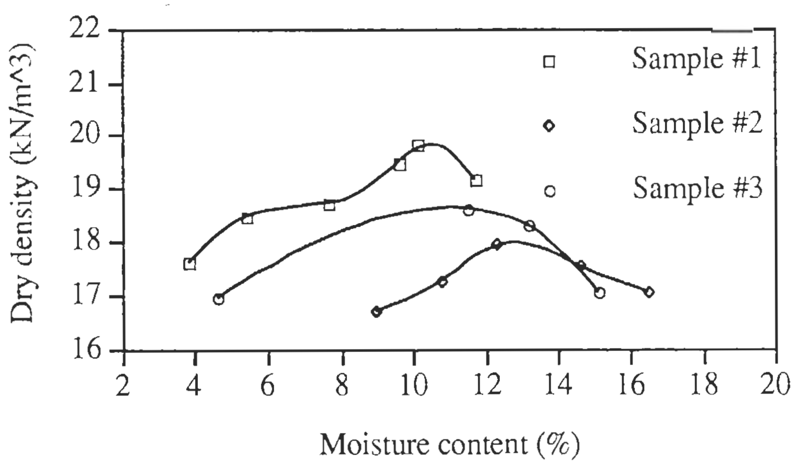

Figure 4.7 Compaction curves for three bottom ash samples

kN/m^3 to 19.8 kN/m^3. The optimum moisture content ranges from 10.2% to 12.3%. The maximum dry density varies to a higher degree than the moisture content. The effect of the metal content on dry density can be shown by a phase relationship, where increasing the volume of ferrous metal within a sample of dry solids causes an increase in the dry density. Experiments were performed to show the effect of metal content on dry density. Two dry samples of bottom ash were vibratorily compacted into a 15.2 cm diameter Proctor mold.

The dry density and the ferrous metal content were determined for the samples. The ferrous metal content of the samples is 9.20% (Sample A) and 17.82% (Sample B) with dry densities of 9.12 kN/m^3 and 9.41 kN/m^3 respectively. The dry density of Sample B is higher than that of Sample A because of the larger quantity of metal in Sample B. The ferrous metals were magnetically removed from Sample B and were replaced with bottom ash. Upon compaction, the dry density of the sample devoid of metal is 8.36 kN/m^3. These experiments show that the dry density is directly proportional to the quantity of metal within the sample material. Variability in the maximum dry density of bottom ash samples is caused primarily by fluctuations in ferrous metal content between samples.

The quantity of dynamic compaction energy applied to bottom ash directly correlates to the maximum dry density of the sample. Figure 4.8 shows the relationship between dynamic energy input and maximum dry density for samples of bottom ash compacted in a Proctor mold. Each data point corresponds to a different compaction method or compaction energy. Variations in compaction methodology included changes in hammer weight, number of blows per layer, and number of layers. The figure shows that samples subjected to larger quantities of compaction energy have higher maximum dry densities. Exponential increases in compaction energy were necessary to provide approximately linear increases in dry density.

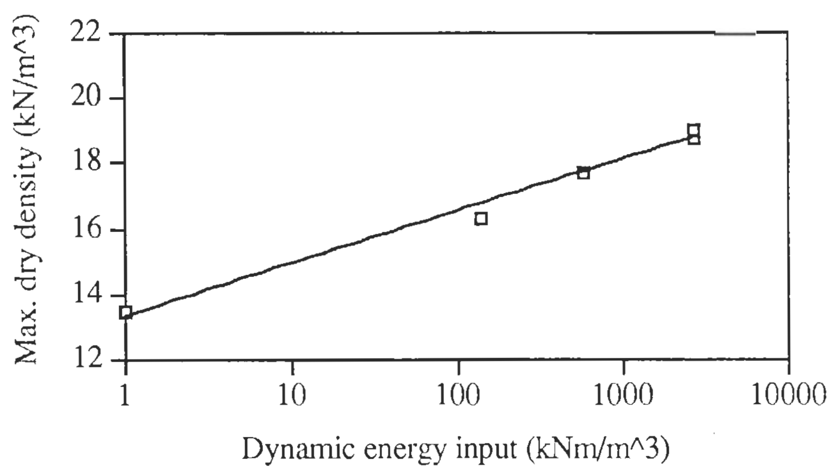

Figure 4.8 Compaction energy-dry density relationship for bottom ash

The effect of dynamic energy input on particle degradation is shown in Figure 4.9. The figure shows the particle size distribution for a noncompacted bottom ash sample and a compacted bottom ash sample. Compaction was performed in a small Proctor mold using a 4.54 kg hammer and 5 layers with 25 blows per layer. The figure represents the following sieve sizes from largest to smallest: 3/4 in (19.1 mm), and Nos. 4, 10, 20, 40, 100, and 200. Figure 4.9 shows that the curve representing compacted bottom ash shifts upward. The shift results from a greater number of particles passing each sieve size after compaction. The dynamic compaction energy supplied by the Proctor hammer causes particle fracture during impact. Particles having degraded during compaction pass through sieves upon which they had previously been retained. The magnitude of particle

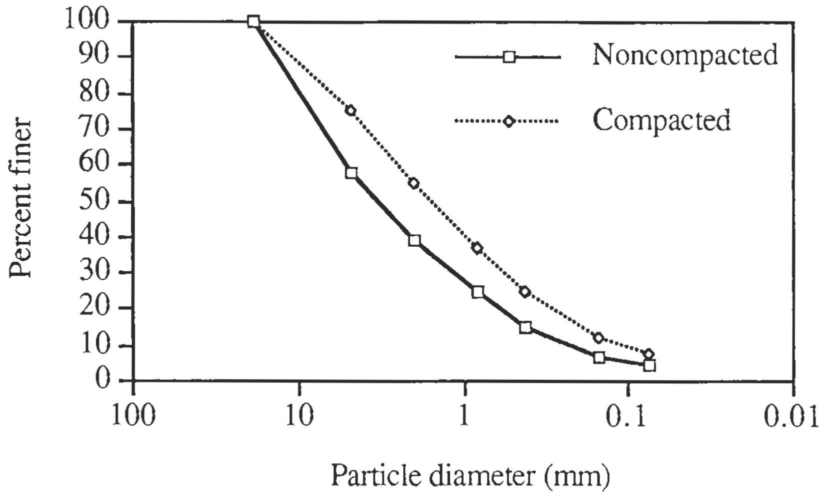

Figure 4.9 Effect of dynamic compaction energy on bottom ash gradation

breakage along the gradation curve is measured by the magnitude of the upward shift from the noncompacted gradation to the compacted gradation. Figure 4.9 shows that the magnitude of the shift decreases for decreasing sieve size. The magnitude of the shift on the No. 4 sieve is 17.6%, while the magnitude of the shift on the No. 200 is 2.5%. The decreasing trend is consistent on all sieve sizes from No. 4 to No. 200. This indicates that large particles are more likely to fracture than small particles during dynamic loading conditions.

4.2.2 Gravel - Two representative samples of silty sandy gravel were tested for maximum dry density. Both samples passed a 3/4 in (19.1 mm) sieve. The samples were compacted in different size Proctor molds. Figure 4.10 shows the results of the compaction tests on gravel. The upper curve, for which the gravel was compacted in a 10.2 cm (4 in) Proctor mold has a maximum dry density of 21.1 kN/m^3 at 7.4% moisture. The sample was compacted with a 4.54 kg hammer in 5 layers with 25 blows per layer. The lower curve, for which the gravel was compacted in a 15.2 cm (6 in) Proctor mold has a maximum dry density of 20.54 kN/m^3 at 7.2% moisture. The material was compacted with a 4.54 kg hammer in 5 layers with 56 blows per layer. The trend is similar to maximum dry density results for bottom ash in Figure 4.6 where the 10.2 cm (4 in) mold

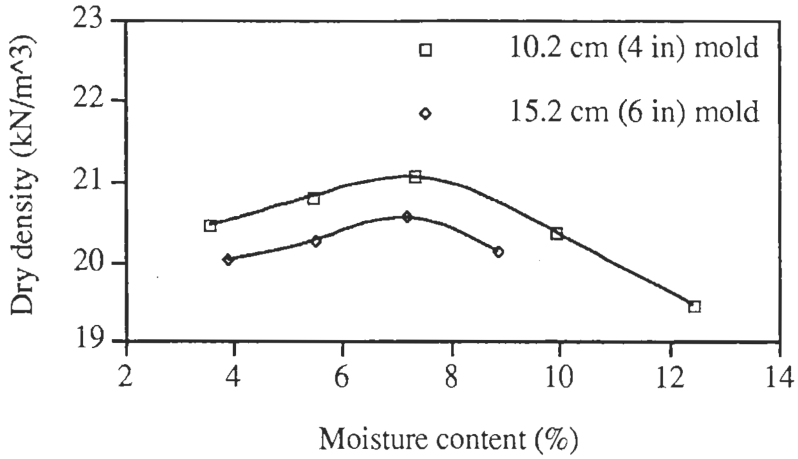

Figure 4.10 Moisture-density relationship for gravel

size produced a higher maximum dry density at a lower moisture content than the 15.2 cm (6 in) mold. The dynamic energy applied to the sample in the small mold was greater than that applied to the sample in the large mold by 13 kN-m/m^3. The difference in maximum dry densities may be due to the additional energy input into the small mold sample.

4.2.3 Mixed Material - Two representative samples of mixed material were tested for maximum dry density. Both samples were prepared for testing identically and passed the 3/4 in (19.1 mm) sieve. Each sample was compacted in a different size Proctor mold. The results of the compaction tests are shown in Figure 4.11. The sample compacted in the 10.2 cm (4 in) Proctor mold has a maximum dry density of 20.26 kN/m^3 at 9.1 % moisture. Compaction was performed with a 4.54 kg hammer in 5 layers with 25 blows per layer. The sample compacted in the 15.2 cm (6 in) mold has a maximum dry density of 19.81 kN/m^3 at 9.2% moisture. Compaction in the large mold was performed with a 4.54 kg hammer in 5 layers with 56 blows per layer. Similar to the bottom ash and gravel samples, material compacted in the small mold has a higher dry density than material compacted in the large Proctor mold. In comparing the maximum dry density of the mixed material with those of the bottom ash and gravel, the mixed material has a maximum dry density very close to the average for bottom ash and gravel. The average maximum dry density for the 10.2 cm mold samples of bottom ash and gravel is 20.05 kN/m^3, while the maximum dry density for the mixed material is 20.26 kN/m^3. The average maximum dry density for the 15.2 cm mold size samples of bottom ash and gravel is 19.67 kN/m^3, while the mixed material is 19.81 kN/m^3. Both of the dry densities for the mixed material were higher than the average of bottom ash and gravel indicating that the mix contained slightly more gravel than bottom ash. The imbalance of constituents results from the bottom ash and gravel having been mixed by unscientific means.

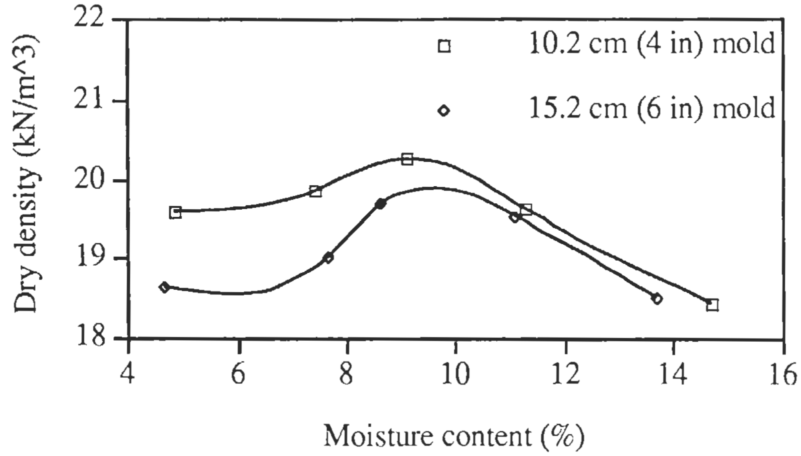

Figure 4.11 Moisture-density relationship for mixed material

4.3 Specific Gravity

Samples of bottom ash and gravel were tested for specific gravity. The gas pycnometer test method was used for bottom ash as a substitute for the ASTM standardized wet pycnometer method. The tests were performed by the United States Geological Survey, Woods Hole, MA. The gas pycnometer was chosen over the ASTM standardized test because of the shape and surficial features of bottom ash particles. The particle surfaces have highly irregular features including pits and small crevasses protruding into the particle. The gas pycnometer uses helium molecules to fill voids of the irregular surficial features. Helium molecules are smaller and considered more appropriate than water molecules to fill the smallest void spaces. Tests reveal that the specific gravity of the bottom ash samples passing No. 4 averages 2.70. Gravel samples passing the No. 4 sieve have a specific gravity of 2.73. The weighted average specific gravity of the mixed material is 2.71.

4.4 Friction Angle

Direct shear tests on bottom ash show that it possesses the behavioral characteristics of granular soil (Lambe and Whitman, 1969). Figure 4.12 shows shear stress-displacement and volume change-displacement data for direct shear tests on two samples of bottom ash. The figures show data for dense and loose samples. The dense sample was compacted at optimum moisture to a dry density of 17.21 kN/m^3. The loose sample was

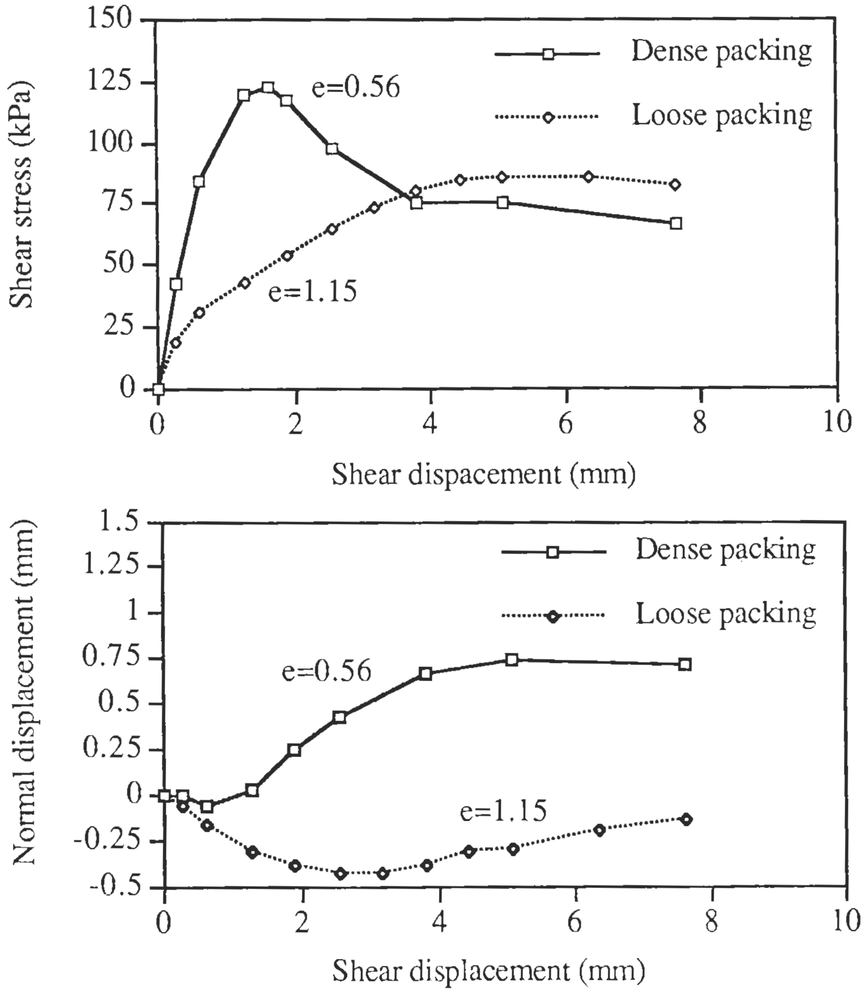

Figure 4.12 Typical results for direct shear test on bottom ash

compacted in a dry state to a dry density of 12.30 kN/m^3. The void ratios for the dense and loose samples were 0.56 and 1.15 respectively. The confining normal stress on both samples was 77.8 kPa. Figure 4.12a shows that the shear resistance of the dense sample peaks before reaching the ultimate or residual level of shear resistance. A peak followed by a decrease to a residual level of shear resistance is typical behavior for dense sand (Lambe and Whitman, 1969). The loose sample also behaves similarly to a granular soil. The frictional resistance of the loose sample steadily increases with corresponding increases in strain until the ultimate or residual stress is achieved. Theoretically, the residual level of shear resistance for the loose and dense samples should be about equal. Figure 4.12a shows that the residual values for the loose and dense samples are very close but not equal in magnitude because of composition differences.

The volumetric behavior of both bottom ash samples in Figure 4.12b is similar to the behavior of granular soil (Lambe and Whitman, 1969). The volume of the densely packed sample decreases initially followed by a volumetric increase to a level at which the sample undergoes zero change. The beginning of the zero volume change condition corresponds to the beginning of the residual shear resistance shown in Figure 4.12a. The loosely packed sample displays behavior different from the densely packed sample in

Figure 4.12b. The initial volume decrease is caused by the collapse of the loosely packed grain structure. After collapse, the sample undergoes zero volume change. Similar to the behavior of the densely packed sample, zero volume change indicates that the sample has entered a state of residual shear resistance.

Direct shear tests were performed at normal stresses of 77.8 kPa, 155.5 kPa, 311.1 kPa, and 622.1 kPa. The average peak and average residual friction angles for tests at each normal stress are shown in Figure 4.13. Six tests were performed at each stress level. All test samples were compacted to within 90% of the maximum dry density. The figure shows that the peak and residual friction angles decrease with increasing normal stress. The decrease results from particle behavior within the shear plane during deformation. The

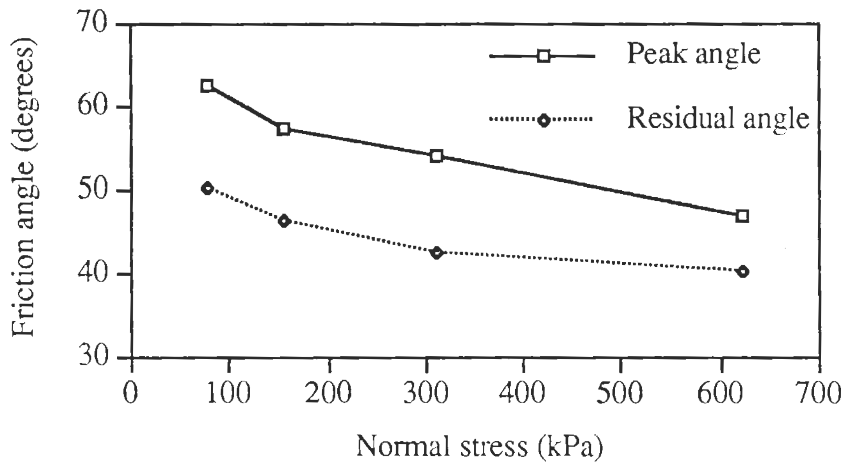

Figure 4.13 Average peak and residual friction angles for bottom ash at various normal stresses

two components of the friction angle, dilatancy and true friction are mobilized as a function of normal stress. At all levels of normal stress shown in Figure 4.13, the friction component of the friction angle remains relatively constant. The dilatancy component decreases as a function of increasing normal stress. At low stress levels dilatancy is large, contributing significantly to the friction angle. As normal stress increases, particles are unable to ride over one other during horizontal displacement resulting in less dilatancy. As the contribution of dilatancy decreases with increasing normal stress, the friction angle primarily becomes a function of true friction between particles. At high confining stresses, contact stresses between particles may cause particle crushing. The particle crushing decreases the shear resistance of the sample, causing the friction angle to decrease at high confining stress.

For the six direct shear tests performed at each normal stress, the peak and residual friction angles vary considerably. Figure 4.14 shows average peak friction angle and average residual friction angle data with upper and lower limits at 77.8 kPa, 155.5 kPa, 311.1 kPa, and 622.1 kPa. Each figure shows a significant range between the maximum and minimum friction angle for the six tests performed. The source of variability was

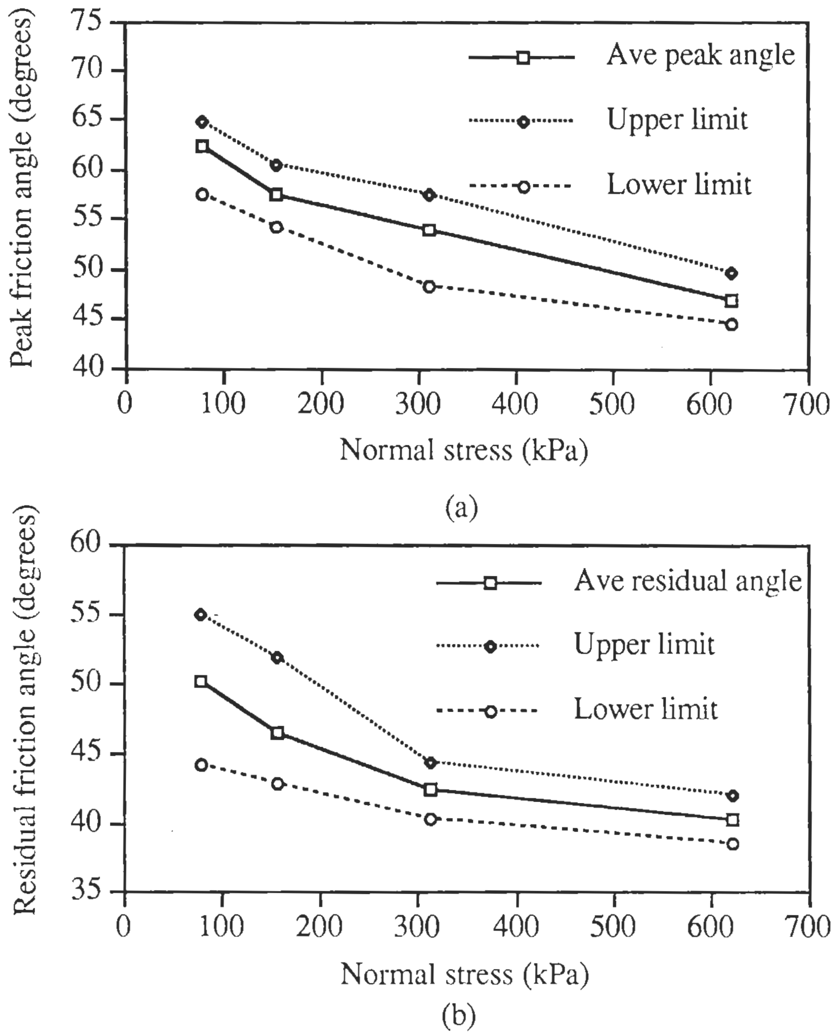

Figure 4.14 Peak and residual friction angle data for bottom ash at various normal stresses

revealed by an examination of the shear plane after testing. Due to inconsistencies in particle shape and composition, the shear plane became reinforced by one or several particles positioned perpendicular to the shearing plane. Although the largest oblong particles were removed prior to compaction, shards of glass and small elongated metallic particles remained in the bottom ash. When these particles reinforce the shear plane, the shear resistance increases dramatically. Incidence of high friction angles correlate directly to cases of visible shear plane reinforcement. For samples lacking reinforcing particles, friction angles tend to be toward the lower limit of the friction angle values shown in Figure 4.14.

4.5 Permeability

Thirteen samples were tested for permeability. Tests were performed on a variety of samples including each of the three embankment materials and blended samples incorporating varying fractions of bottom ash, kaolinite, and coal fly ash. Table 4.1 shows permeabilities for all samples tested. The columns show (from left to right) the number of each test specimen, the composition of the samples, and the corresponding permeability. The numbers for each test specimen will be used in this paper to identify the samples.

Numbers directly preceding the materials in the sample composition column represent the weight based percentage of that component.

Unblended bottom ash (sample numbers 1 and 2) has the highest permeability of all samples tested. The average permeability for two bottom ash samples is 1×10^{-4} cm/s. Although the gravel (3) used in the embankment is a granular soil, it exhibits relatively low permeability. The low gravel permeability results from the dense packing arrangement

Test No.	Sample Composition	Permeability (cm/s)
1	100 Bottom Ash	1.30 E-4
2	100 Bottom Ash	5.85 E-5
3	100 Gravel	3.96 E-6
4	50 Bottom Ash/50 Gravel	5.62 E-6
5	97 Bottom Ash/3 Kaolinite	8.70 E-6
6	94 Bottom Ash/6 Kaolinite	1.42 E-6
7	90 Bottom Ash/10 Kaolinite	3.33 E-7
8	100 Kaolinite	5.73 E-8
9	95 Bottom Ash/5 Coal Ash	7.48 E-6
10	92 Bottom Ash/5 Coal Ash/3 Kaolinite	3.57 E-6
11	89 Bottom Ash/5 Coal Ash/6 Kaolinite	1.25 E-6
12	85 Bottom Ash/5 Coal Ash/10 Kaolinite	7.78 E-7
13	100 Coal Ash	8.52 E-7

Table 4.1 Permeability data for all test samples

of the well graded particles. The mixed material (4) also possesses a relatively low permeability compared to that of bottom ash. The low permeability of the mixed material indicates that gravel particles occupy much of the interstitial space between bottom ash particles. The mixed material is densely packed which inhibits capillary flow.

In an effort to decrease the permeability of bottom ash to limit leachate mobility, varying quantities of fine grained materials were blended with bottom ash. The purpose of the blending is to block potential flow paths present in the bottom ash matrix with fine grained particles. The blends prepared include bottom ash/kaolinite and bottom ash/kaolinite/coal ash. Kaolinite, a coarse grained clay (predominant particle size from 20μ to 0.2μ), was selected for blending due to its low reactivity properties and absence of excessive expansion properties. Coal fly ash was used because it is a recyclable material with low reactivity and minimal expansive properties. Coal fly ash primarily consists of silt size particles (0.075 mm - 0.002 mm). Blends of bottom ash with 3%, 6%, and 10% kaolinite were tested. In Table 4.1, sample numbers (4) through (7) show that the permeability of the bottom ash/kaolinite decreases with the addition of clay. Blends incorporating coal ash (samples (9) through (12)) show a trend similar to that for bottom ash/kaolinite blends. Each sample contains 5% coal ash with 3%, 6%, or 10% clay. Table 4.1 shows that the permeability of samples (9) through (12) decrease as the clay content increases.

Permeability data is easily compared by examining the order of magnitude difference in permeability between any two samples. Table 4.2 displays the order of magnitude reduction in permeability for all blended permeameter samples. Permeability reduction is determined by comparing a given sample's permeability with the permeability of unblended bottom ash, which is the highest of the values. The figure shows kaolinite/bottom ash blends to the left and kaolinite/coal ash/bottom ash blends to the right. As a reference, the sample number from Table 4.1 is shown in parentheses. Table 4.2

% Kaolinite	Permeability Reduction (orders of magnitude)	% Kaolinite / 5% Coal Ash	Permeability Reduction (orders of magnitude)
0	N/A	(9) 0	1.02
(5) 3	1.08	(10) 3	1.16
(6) 6	1.66	(11) 6	1.75
(7) 10	2.08	(12) 10	2.01
(8) 100	3.06	N/A	-

Table 4.2 Order of magnitude reduction in permeability for blended samples

indicates that a two order of magnitude decrease in permeability occurs by adding 10% clay (sample 7) to bottom ash. The difference in permeability between 10% clay/90% bottom ash and a 100% clay sample (samples 7 and 10) is one order of magnitude. This indicates that ten percent clay fills the majority of the void space within the bottom ash. Only one additional order of magnitude decrease is achieved by adding more than ten percent clay which indicates that the most cost effective quantity of clay for blending is roughly ten percent.

The right side of Table 4.2 shows data for kaolinite/coal ash/bottom ash blends. The addition of 5% coal ash and 0% clay (sample 9) causes a one order of magnitude reduction in permeability. Coal ash blending produces an effect similar to that of clay blending. Adding clay along with coal ash results in further permeability reduction, depending upon the quantity of clay blended. Comparison of the results on the left and right sides of Table 4.2 shows that blends including coal ash with clay and bottom ash reduce permeability more effectively than blends with just clay and bottom ash. The presence of the silt size coal ash particles causes improved flow path blockage.

The permeabilities of all blended samples as a function of clay content are shown in Figure 4.15. The horizontal axis represents the kaolinite content of each sample. The two curves represent samples containing either 0% or 5% coal fly ash. The figure indicates that the blended bottom ash/kaolinite/coal ash is less permeable than blended bottom ash/kaolinite, but only for kaolinite contents of less than six percent. For kaolinite contents greater than six percent, the bottom ash/kaolinite blend is more effective at reducing permeability.

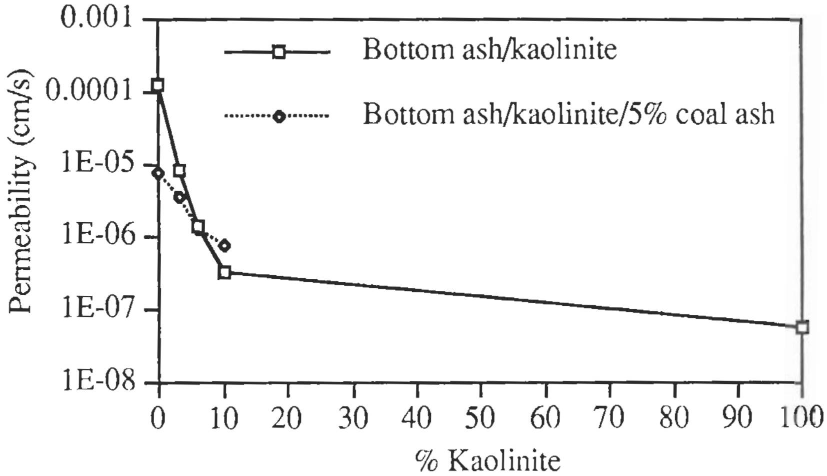

Figure 4.15 Permeability data for bottom ash/coal fly ash/clay blends

4.6 Shrink/Swell

The expansion and contraction properties of bottom ash and bottom ash/kaolinite blends were investigated to determine the possible effects of clay blending in field applications. Samples were prepared in Harvard miniature molds and subjected to only one cycle of oven drying. The results show that the samples do not expand or contract to an appreciable degree or in any recognizable pattern. Table 4.3 presents average strain data

Sample composition	Average diametric strain (%)	Average longitudinal strain (%)
100 Bottom Ash / 0 Kaolinite	0.29	-0.17
97 Bottom Ash / 3 Kaolinite	0.13	0.29
90 Bottom Ash / 10 Kaolinite	0.54	-0.22
70 Bottom Ash / 30 Kaolinite	-0.06	-0.26
0 Bottom Ash / 100 Kaolinite	-0.28	-0.09

Table 4.3 Shink/swell data for Harvard miniature samples

for samples with varying quantities of kaolinite. The weight based fraction of the sample components is indicated by numbers preceding each material in the Sample Composition column of Table 4.3. Diametric strain is the average strain occurring over the diameter of the cylindrical sample. The longitudinal strain is the strain occurring over the length of the sample. Samples of pure bottom ash and pure kaolinite as well as blends were tested. For all samples small strains occur after drying. This experiment confirms theoretical expectations regarding the behavior of bottom ash and kaolinite upon drying. Bottom ash samples are predicted not to shrink or swell because bottom ash is a granular material. However, multiple cycles of wetting and drying could oxidize the ferrous particles and lead to expansion. Samples of kaolinite exhibit minimal shrinkage and swelling because kaolinite is a nonexpansive clay mineral.

Three permeameter samples were tested for shrink/swell behavior following permeability testing. The 2.8 x 14.5 cm samples behave similarly to the Harvard miniature samples. Table 4.4 shows the average diametric and longitudinal strains occurring after drying. All of the strains are relatively small, indicating that expansion/contraction problems in field application should be negligible based on one drying cycle.

Permeameter sample composition	Average diametric strain (%)	Average longitudinal strain (%)
97 Bottom Ash / 3 Kaolinite	0.03	0.26
94 Bottom Ash / 6 Kaolinite	0.35	0.05
90 Bottom Ash / 10 Kaolinite	-0.32	-0.06

Table 4.4 Shrink/swell data for permeameter samples

4.7 Unconfined Compression

Samples of bottom ash and blended bottom ash/kaolinite were tested for compressive strength in the U test. Bottom ash was blended with kaolinite at 0%, 3%, 10%, 30%, and 100% based on weight. Figure 4.16 shows compressive strength as a function of clay content. Four samples of 100% bottom ash were tested. The unconfined compressive strength of 100% bottom ash is small compared to the strength gained from adding kaolinite. Since bottom ash is a granular material, the unconfined strength should be zero. Any measurable strength shown in U tests is attributable to pore pressure occurring during loading. The average strength for four samples of 100% bottom ash is 24.6 kPa. The absence of significant compressive strength for bottom ash is anticipated

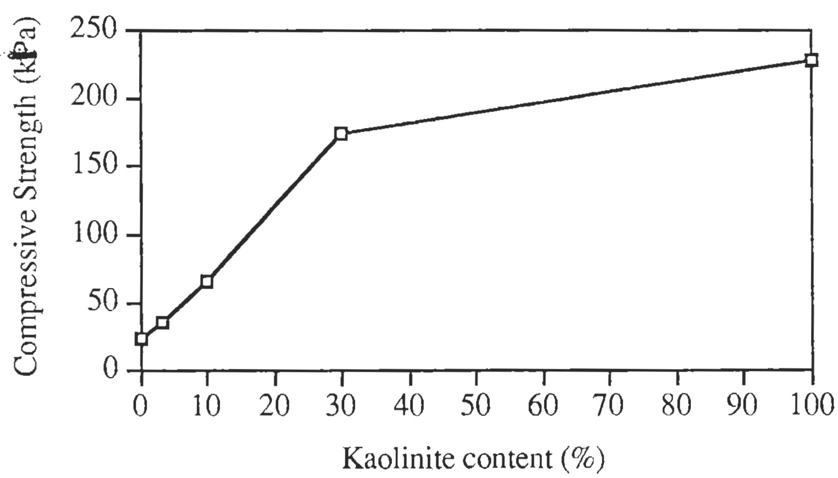

Figure 4.16 Compressive strength data for bottom ash/kaolinite blends

because bottom ash is cohesionless. The gain in strength from particle interlocking evident during direct shear testing does not apply in U tests. The absence of confining stress to the ash nullifies the potential for particles to interlock.

Failed samples did not show an identifiable inclined failure plane. During loading the samples first expanded at midheight. Vertical cracks formed and enlarged at approximately 5 mm intervals along the circumference of the enlarged midsection. The top and bottom of each sample maintained the original diameter. The failed samples were barrel shaped.

4.8 Loss on Ignition

Each material used in the embankment construction was tested for organic content. Nine samples of bottom ash were tested and the average loss on ignition is 2.28% with the range for the nine tests between 1.32% and 2.84%. Visible unburned matter in the bottom ash prior to testing included wood, oil soaked cloth and paper and fibrous strands. Material which did not burn during the incineration process may have been fluid saturated prior to incineration or may have been located in an area of the furnace where burning was unsatisfactory. Three samples of gravel were also tested and the average loss on ignition is 0.57% with the range between 0.44% and 0.81%. Possible sources of ignitable material in the gravel are wood and leaves which fell into the excavated material at the gravel pit or during construction but there is not visible sign of organics. Two samples of mixed material were tested. The average loss on ignition is 1.55% with the range between 1.25% and 1.81%. Sources of ignitable material include all of those listed for bottom ash and gravel.

5.0 CHEMICAL TEST RESULTS

5.1 Total Chemical Analysis

Total chemical analyses were performed on three samples. Two samples of bottom ash and one sample of gravel were analyzed using the Hydrofluoric Microwave Digestion Procedure and ICP spectroscopy. The purpose of the total chemical analysis is to determine the total quantity of selected contaminants present within a test material. Results of the total chemical analysis can be compared to contaminant concentrations from TCLP results and field leachate test data to determine the extent of leaching for selected contaminants. The total chemical analysis is also performed to determine which contaminants to test for in the TCLP analysis.

In preparing sample material for total chemical analysis testing, the aim was to create a representative composite test material. To do this, material from different lifts was combined in equally weighted quantities. Of the two bottom ash samples, one is a combination of material from lift numbers three and seven (sample numbers A-3 and A-7), while the other bottom ash sample consists of material from sample numbers A-6 and A-10. The gravel sample is a mixture of sample numbers S-3 and S-5. Table 5.1

Sample	Silver	Arsenic	Barium	Cadmium	Chromium	Lead	Selenium
A-3 / A-7	0.033	0.484	0.416	0.059	0.254	2.686	0.214
A-6 / A-10	0.034	0.409	0.350	0.048	0.273	1.834	0.226
S-3 / S-5	0.061	1.137	0.653	0.037	0.093	0.335	0.468

Concentrations in mg/g dry weight

Table 5.1 Total chemical analysis for bottom ash and gravel

shows the total chemical analysis test results. The table shows the concentration in milligrams per gram dry weight of silver, arsenic, barium, cadmium, chromium, lead, and selenium. The results in Table 5.1 indicate that each of the metals must also be analyzed by the TCLP test to determine their respective leachability in an aqueous environment. A notable aspect pertaining to the chemical composition of bottom ash is its variability. Individual samples of bottom ash yield varying concentrations of metals for the total chemical analysis. The chemical composition is dependent upon the composition of MSW processed at the incinerator. Waste containing high levels of specific metals (such as lead batteries) has the potential to cause an inordinate contaminant concentrations level of lead in the data. The results in Table 5.1 suggest that the concentrations shown are representative of bottom ash because of the consistency between different samples. Lead concentration varies greatest between samples A-3 / A-7 and A-6 / A-10. The other six metals fall into a relatively small range. The soil metal concentrations are unexpectedly high compared to the bottom ash.

5.2 Toxicity Characteristic Leaching Procedure (TCLP)

TCLP analyses were performed on six samples. Four tests were performed on bottom ash and two on gravel. The TCLP test is used to determine whether waste material is classified as hazardous or nonhazardous under EPA guidelines. The EPA characterizes waste as hazardous if it exhibits traits of ignitibility, corrosivity, reactivity, or toxicity (Grasso, 1993). The TCLP test was used to determine the toxicity of the material for this project. The total chemical analysis indicates that arsenic, barium, cadmium, chromium, lead, selenium, and silver are present in bottom ash. The TCLP test determines if the extract derived from the bottom ash contains contaminant levels exceeding EPA regulatory limits.

Table 5.2 shows the results for bottom ash and gravel samples as well as EPA toxicity limits for the TCLP test. Concentrations shown in Table 5.2 are in milligrams per liter. Composite samples A-3 / A-7, A-6 / A-10, and S-3 / S-5 were prepared by mixing material from two construction lifts, in similar fashion to the total chemical analysis samples. Samples A-2, A-7, and S-3 were composed of material from one construction lift. The results of the TCLP test show that bottom ash is within regulatory limits for all metals tested with the exception of lead. Of the four bottom ash samples tested, only sample A-6 / A-10 exceeds the EPA lead limit. The occurrence of random samples

Sample	Arsenic	Barium	Cadmium	Chromium	Lead	Selenium	Silver
A-3 / A-7	0.197	0.170	0.206	0.053	0.648	0.196	ND
A-6 / A-10	1.407	0.277	0.398	0.395	9.000	0.521	ND
A-2	ND	0.176	0.198	0.147	1.659	ND	ND
A-7	ND	0.174	0.201	0.150	0.929	ND	ND
S-3	ND	0.258	0.016	0.034	0.230	ND	ND
S-3 / S-5	0.087	0.296	0.012	ND	0.150	0.093	ND
TCLP Limit	5.0	100.0	1.0	5.0	5.0	1.0	5.0

Concentrations in mg/l

TCLP - Toxicity Characteristic Leaching Procedure

ND - Non-detected

Table 5.2 TCLP results for bottom ash and gravel

exceeding the TCLP limits does not necessarily classify material as hazardous. The frequency with which the material exceeds the limits for a specific constituent and the magnitude by which the regulatory levels are exceeded dictate the classification. For the case of lead in the bottom ash, more samples must be tested to determine the frequency of excessive lead. For metals other than lead, contaminant levels are below EPA limits. Arsenic and selenium are detectable in only two of four samples. Silver is not detected in any of the four samples. Barium levels are less than one percent of the 100 mg/l maximum. Cadmium and chromium are safely below their respective limits for each of the four samples. As expected for uncontaminated material, each soil sample is below TCLP limits.

5.3 Laboratory Leaching Tests

Although the test embankment was instrumented with leachate collection systems, the environment in which these systems operate is uncontrollable. Variables affecting the field embankment are the quantity of water supplied by natural rainfall, seasonal temperature fluctuations, and the possibility of contaminants entering the test embankment from the surrounding landfill. To eliminate uncertainties resulting from variables associated with the field based leachate collection systems, two types of laboratory leaching apparatus were fabricated in the laboratory. A small scale column leaching apparatus was used to measure changes in conductivity with the passing of multiple pore volumes of water through the sample material. On a larger scale than the column, a lysimeter was assembled to monitor the attenuation of dissolved metals, chlorides, salts, and conductivity in leachate. Specifications on each apparatus are described in Section 3.2.4.

A column leaching apparatus was used to examine the rate of conductivity attenuation in leachate generated from bottom ash, mixed material, and gravel. Samples of mixed material and gravel were tested for comparison with bottom ash results. The results of the column leaching tests predict the rate at which soluble compounds present in bottom ash attenuate. Using the laboratory data, estimates are made regarding the rate at which contaminant levels decrease and the volume of water required to leach a specified quantity of contaminant. Figure 5.1 shows a comparison of the results from column leaching tests on bottom ash, mixed material, and gravel. Each test material passed the No. 4 sieve. The test specimen was dowsed repeatedly with two pore volumes of distilled water at 20 °C. Approximately twenty pore volumes were passed through each sample. Figure 5.1 shows that the bottom ash has the highest initial conductivity, followed by the mixed material and then gravel. The high initial conductivity of the bottom ash and mixed material indicates the presence of large quantities of soluble salts. Leachate from the bottom ash sample has slightly higher conductivity than leachate from the mixed material. This is due to the presence of a larger quantity of soluble salts in the bottom ash sample than in the mixed material. For similar sample volumes, the pure bottom ash sample has twice the quantity of bottom ash than the mixed material. The larger quantity of bottom ash supplies the leachate with more soluble salts than the mixed material. The figure also shows that the gravel sample contains minimal quantities of salt, thus having a very low conductivity.

Figure 5.1 shows that the first five pore volumes cause the highest rate of conductivity attenuation for the bottom ash and mixed material. The majority of the most soluble compounds leach from the test material during the period of rapidly decreasing conductivity (pore volumes one through five). After the initial decrease in conductivity,

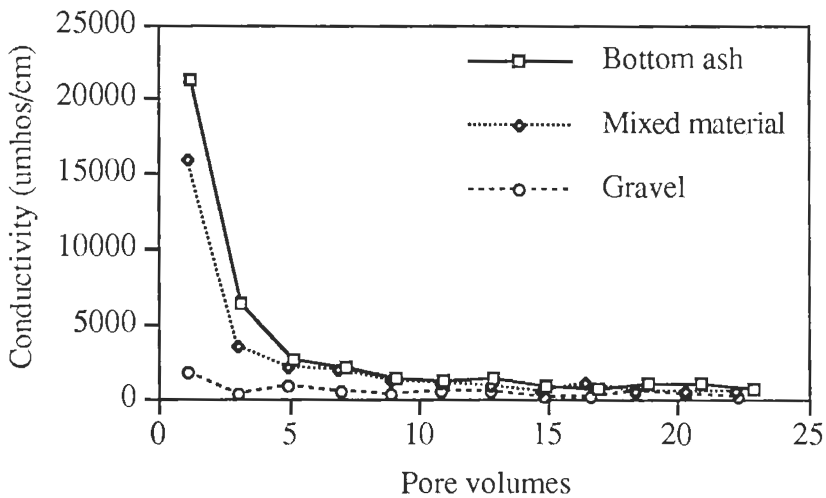

Figure 5.1 Conductivity attenuation in column leaching apparatus

the rate of attenuation stabilizes and the conductivity decreases very little with the addition of additional pore volumes. Gravel maintains a relatively constant conductivity for all of the pore volumes added to the test sample. The gravel contains an insignificant quantity of highly soluble salts.

The column leaching apparatus provides a small scale representation of conditions present in the field test embankment. Size limitations of the testing apparatus prevent testing samples with a gradation and composition representative of the field conditions. All particles larger than the No. 4 sieve are removed from the bottom ash for column testing. As part of the fraction larger than the No. 4 sieve, the majority of the metals are removed from the test material thus changing the composition. A large scale testing vessel, using unsieved bottom ash is required to more closely model field conditions.

A lysimeter was constructed using approximately 130 kg of bottom ash. Test material was not sieved after being excavated from the embankment, thus retaining the original gradation and composition. Bottom ash was compacted into the testing vessel to within 85% of the maximum dry density. The lysimeter was dowsed with tap water in one-half pore volume increments. The conductivity of the tap water is 115 umhos/cm, which is negligible compared to the conductivity of the leachate generated. Figure 5.2 shows the results for two lysimeter tests. The vertical scale represents the conductivity

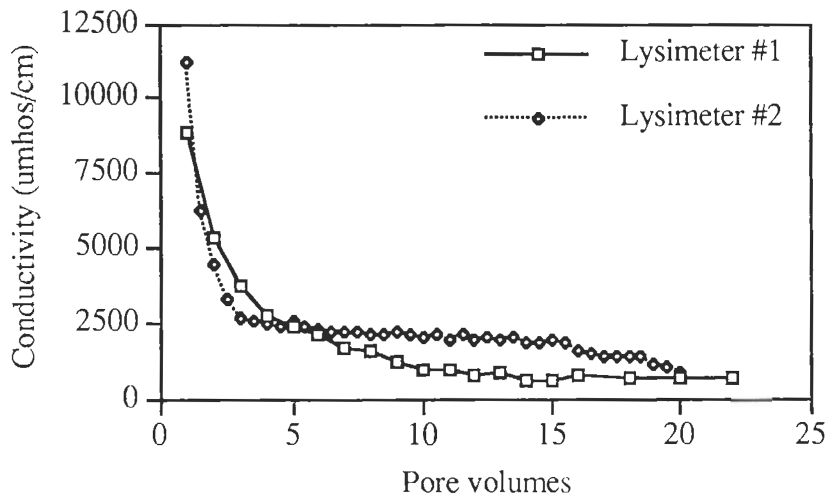

Figure 5.2 Conductivity attenuation in lysimeter leachate

of leachate extracted from the leachate collection pipe (see Figure 3.1). The horizontal scale in Figure 5.2 represents the number of pore volumes having passed through the test material. Compared to the column test results in Figure 5.1, the lysimeter test results exhibit very similar conductivity attenuation properties. Each test method yields a high initial conductivity which decreases rapidly during the first five pore volumes. Following the initial decrease, there is relatively little conductivity change during the addition of the next fifteen pore volumes. A notable difference between the results from the two types of testing apparatus is the difference in initial conductivity. Conductivity of leachate from the column tests is approximately two times that of the lysimeter leachate. The source of the difference may be associated with the gradation of the two test materials. Ash used in the column passed a No. 4 sieve, while ash used in the lysimeter passed the 100 mm screen during preparation for construction. The lysimeter ash is much coarser than the column ash, thus possessing a larger mean particle size. The specific surface of the column ash is greater than that of the lysimeter ash because the column material is finer. Since salts contained in ash are affixed to the surface of the particles, samples with larger specific surfaces possess a larger total surface area on which salt may crystallize. The difference in conductivity between the samples may result from a greater quantity of salt available in the column test material.

A comparison of the magnitude and attenuation characteristics for the two types of leaching apparatus is shown in Figure 5.3. The figure shows the results from the column containing bottom ash and from the two lysimeters. With the exception of the initial

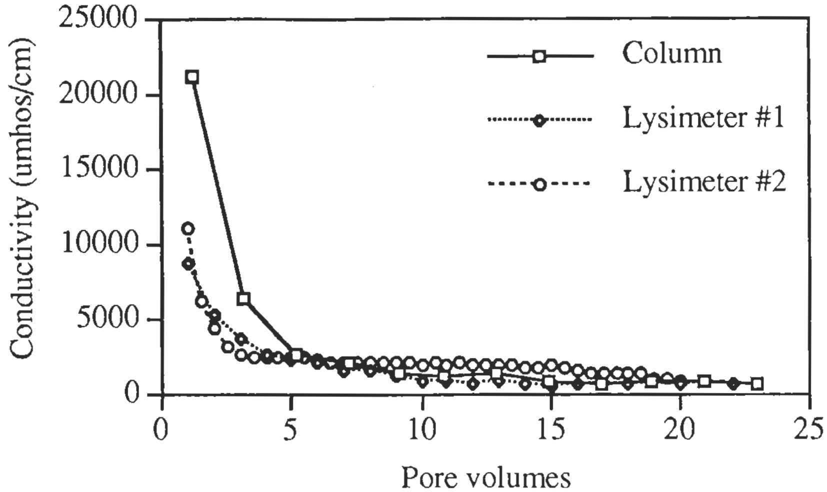

Figure 5.3 Comparison of conductivity from column and lysimeter leachate

conductivity values, the attenuation behavior is similar for small or large scale testing apparatus. The effect of removing particles larger than No. 4 does not significantly affect the outcome of conductivity measurements after the majority of the salt has been leached. All three tests yield similar conductivities after the passing of five pore volumes.

The conductivity levels for leachate extracted from bottom ash are primarily caused by the presence of dissolved salt compounds. Salts containing chloride anions in addition to either calcium, sodium, magnesium, or potassium cations are present at high concentrations in bottom ash leachate. To make an estimate at the concentration of dissolved salts within a leachate sample, the total dissolved solids on evaporation (Standard Methods, 1971) was determined. The total dissolved solids test does not determine the concentration of specific compounds, it indicates the presence of substances such as salts which have similar properties. Because conductivity is heightened by the presence of chloride ions in solution, the concentration of dissolved solids is directly proportional to the conductivity of the leachate. A comparison of the conductivity attenuation with total dissolved solids concentration shows that the highest conductivities occur when the total dissolved solids concentration is at a maximum. Figure 5.4 shows the total dissolved solids concentration of leachate extracted from lysimeter #2 versus pore volumes. The total dissolved solids concentration, measured in grams per liter, directly correlates with the level of conductivity shown in Figure 5.2. Similar to the attenuation of conductivity, the total dissolved solids concentration decreases rapidly during the first three pore volumes. Following the rapid initial decrease, the concentration decreases slowly and steadily during the following 17 pore volumes of leachate. To determine the composition of the total dissolved solids, a chemical analysis was performed by ERI.

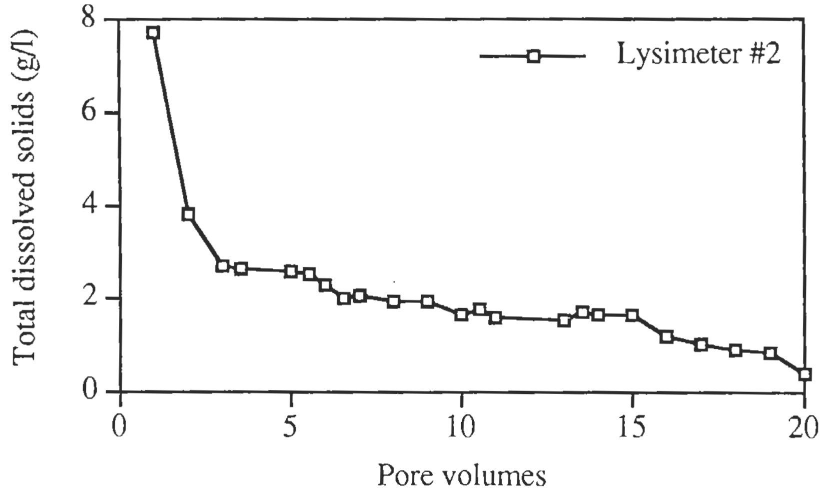

Figure 5.4 Concentration of dissolved solids in lysimeter leachate

5.4 Chemical Analysis of Lysimeter Leachate

Leachate extracted from Lysimeter #2 was analyzed to determine the concentration of metallic and nonmetallic elements. Samples extracted from pore volume numbers 1, 3, 10, and 20 were analyzed for the concentration of arsenic, barium, calcium, cadmium, chromium, potassium, manganese, sodium, lead, selenium, total dissolved solids, chloride, and sulfate in addition to the conductivity and pH levels. Results for all compounds tested are shown in Appendix C. The appendix shows the concentration of each compound versus the number of pore volumes passed through the lysimeter. The most notable aspect of the chemical analyses is the attenuation of salt compounds dissolved in the leachate. Figure 5.5 shows the relative concentrations of calcium, potassium, manganese, sodium, and chloride ions. Comparing the concentration levels reveals that the anion, chloride has the highest concentration of all the compounds. The most abundant cation is sodium, but only in leachate extracted from the first pore volume of water.

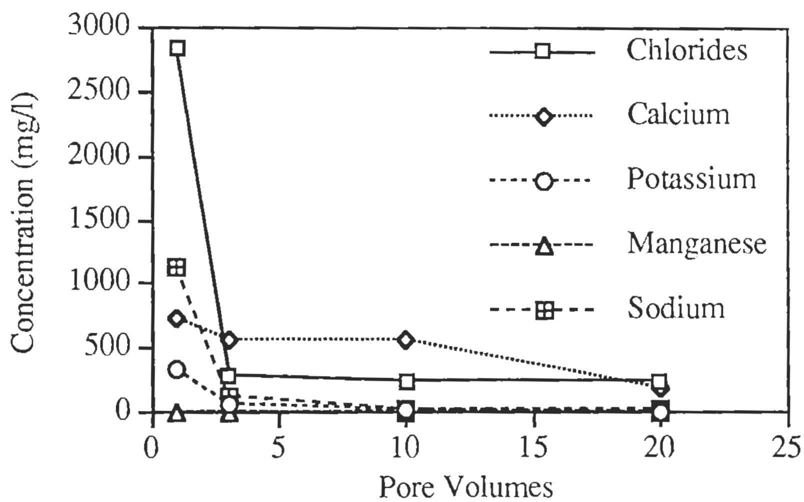

Figure 5.5 Cation and anion concentrations in lysimeter leachate

Following sodium are calcium, potassium, and manganese. Manganese is present in only trace quantities and may be considered inconsequential in comparison to the sodium, calcium, and potassium concentrations. Although the sodium concentration is the highest of the cations at one pore volume, its concentration decreases most rapidly. Calcium and potassium concentrations attenuate similarly, but at slower rates. The conclusion is that sodium is more soluble than calcium and potassium in the lysimeter environment. Additionally, chlorides are highly soluble and mobile, as shown by the decrease in concentration from 2843 mg/l at one pore volume to 290 mg/l at three pore volumes. The concentration decrease is nearly one order of magnitude during the passage of two pore volumes of water. The chemical analysis shows that salts are highly soluble and that large quantities of these compounds leach as the initial pore volumes of water pass through the bottom ash.

The leaching behavior of metallic compounds such as arsenic, barium, cadmium, chromium, lead, and selenium is not as predictable as the behavior of salt compounds. The behavior of lead and cadmium is shown in Figure 5.6. The figure shows the two typical types of leaching behavior observed as arsenic, barium, cadmium, chromium, lead, and selenium leach from the bottom ash. One behavior type is that the concentration increases

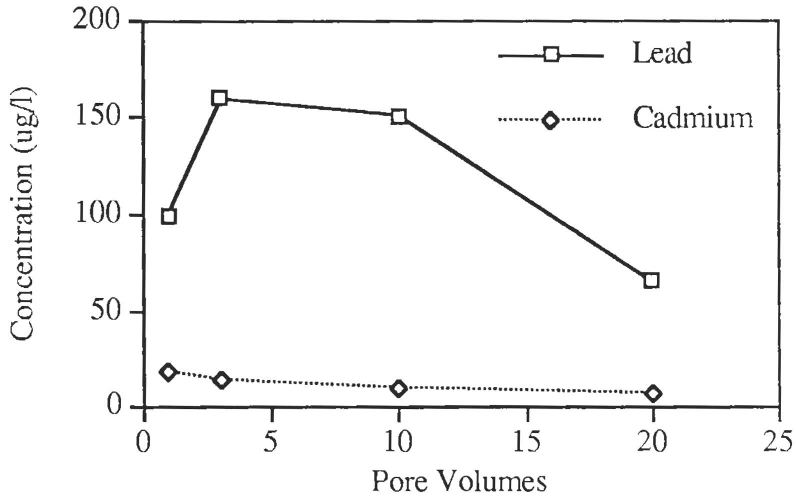

Figure 5.6 Typical contaminant behavior for Lysimeter #2 leachate

initially and then decreases, as shown by lead in Figure 5.6. The other behavior is similar to that of the salts, where the concentration decreases with each addition of pore water, as shown by cadmium. The leaching behavior may be associated with the pH of the pore water, where the solubility of certain elements increases as the pH becomes acidic (lower). Figure 5.7 shows the pH level in leachate passing through a column leaching apparatus. The figure shows that tap water initially at 7.3, the pH becomes increasingly basic (higher pH) as additional pore volumes are passed through the bottom ash. Although an insufficient number of tests were performed to establish a solid correlation between pH

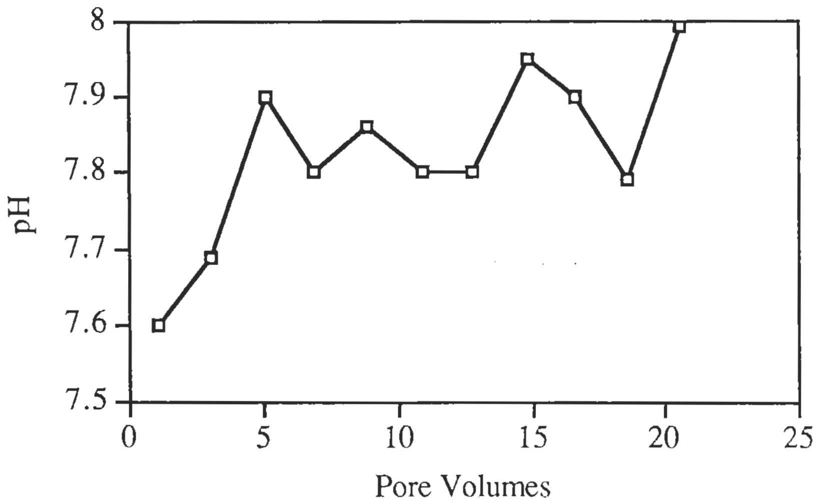

Figure 5.7 pH level in bottom ash leachate

level and metals leaching behavior, Figure 5.7 shows that the pH is not constant in bottom ash leachate. The variability of pH in leachate may affect the rate at which metals leach from ash by percolating pore water.

6.0 EMBANKMENT PERFORMANCE

6.1 Physical Performance

6.1.1 Field Densification - During embankment construction each lift was compacted using a vibratory roller. The density of the compacted fill materials was measured using the balloon density method (ASTM 2167) and the nuclear density method (ASTM 2922). Various lifts within the three embankment subsections were tested using the balloon method. One lift in each subsection was tested at several locations using the nuclear method. Field compaction data are shown in Table 6.1. The table shows moisture content

	Moisture Content (%)	Dry Unit Weight (kN/m^3)
Bottom Ash		
Balloon - 8 samples	15.2 (14.1-17.1)	17.0 (15.4-18.2)
Nuclear - 10 samples	9.1 (6.7-11.5)	18.3 (17.8-19.3)
Mixed Material		
Balloon - 8 samples	10.6 (8.6-12.8)	19.2 (17.8-19.9)
Nuclear - 5 samples	7.7 (6.6-8.7)	20.0 (19.7-20.3)
Gravel		
Balloon - 3 samples	6.8 (5.7-8.7)	19.2 (18.3-20.7)
Nuclear - 8 samples	6.2 (5.1-7.9)	19.4 (17.5-21.2)

( ) - Range

Table 6.1 Field density results for bottom ash, mixed material, and gravel

and dry unit weight values measured in each of the three embankment subsections. The table also lists the average test results for the indicated number of tests. The range of test values appears in parentheses. The balloon method produces higher moisture content and lower dry density results than the nuclear method for all three fill materials. Variations in results between the test methods results from differences between the manner by which each test method samples material. The volume of material excavated for the balloon test is smaller than the volume of material sampled for the nuclear test method. The larger testing volume yields more representative results for the nuclear method. Because the balloon method utilizes a smaller volume of test material, large particles are necessarily excluded from the sample because they cannot be excavated through the template. Referring to Section 4.1.1, the exclusion of larger particles sizes eliminates a considerable portion of the metallic particles. The exclusion of the metallic fraction of particles in bottom ash and mixed material testing causes lower dry densities results for the balloon method. Moisture content differences arise from the selectivity required to excavate a test hole for the balloon method. The balloon method can be used only where particles smaller than 5 cm are encountered during sample excavation. As a result of the particle size restrictions, the gradation of the bottom ash and mixed material test samples tends to be on the finer side of average. The finer gradation permits the test material to hold more moisture than the more representatively graded sample tested using the nuclear method. Table 6.1 also shows that the results become more consistent as the fraction of gravel in the test material increases. The presence of gravel creates a more homogeneous test material which increases the consistency of the test results.

In the interim between preconstruction sieving and final placement, the bottom ash was stockpiled for two days at the landfill. The ash arrived from the incinerator at approximately 18% moisture, greater than the optimum moisture content by roughly 3-4%. The material was stockpiled to permit gravity drainage of excess moisture. Although the bottom ash had partially drained, pumping action and bleeding were evident during compaction of the first two ash layers. After sitting for an additional day to allow drying and drainage, the material stiffened and densified much better when compacted. The compactive effort was checked using the nuclear density test method. The density was measured at the surface and at several depths with no pronounced difference in density with depth.

The effect of compaction equipment on hollow particles in the bottom ash was examined using aluminum cans and oil filters. A collapsible particle was buried approximately 15 cm below the surface. Compaction equipment was passed over the particle. Excavation revealed that many hollow metal particles had partially collapsed from the compaction energy, however considerable void spaces remained inside the particles. Voids remaining in hollow metallic particles may negatively effect the embankment. Corrosion rates are high in the embankment environment because of high chloride concentrations. Voids in the fill material may form as hollow metal particles deteriorate and collapse. The high corrosion rate was visibly noticeable upon inspection of ferrous particles.

6.1.2 Visual Observations Regarding Long-Term Performance - Twenty months after the end of construction the test road appears to be in excellent condition. The main physical performance concern, differential settlement, did not become problematic. On a visual basis, settlement effects are minimal. The roadway remains consistently at a 6% grade throughout its length. There is one visible dip in the pavement surface at the boundary between the bottom ash and mixed material subsections. The dip extends approximately 7 m along the east edge of the road and is approximately 5 cm deep at the low point. Two large cracks in the pavement surface developed at stations 1+00 and 3+30. The cracks are roughly 3 cm wide and 2 m long. They extend east-west across the roadway. Visual inspection of the cracks indicates that horizontal displacements in an east-west direction are occurring. The 2:1 slope to the southeast of the test road (see Figure 2.1) shows several rotational slope failures, but all are outside of the embankment fill area. These failures ranged in diameter from 3 m to 15 m. Although the failures did not occur within the test embankment, potential exists for further propagation of the problem.

Eleven months after the end of construction, bottom ash was excavated from the side of the embankment using a hand shovel (see Section 2.7.1). Two factors made the material difficult to excavate. The presence of springs, rods, wire, and other metallic objects provided reinforcement for the bottom ash particles. The reinforcement supplied strength to hold particles in position during shoveling. The bottom ash was also difficult to remove because the particles had become weakly cemented. The cemented strength was not of significant magnitude since agglomerations of particles were friable. The combination of the cementation and reinforcement necessitated a pick ax to dislodge the bottom ash particles. The particles were easily excavated by hand shovel once dislodged.

6.1.3 Settlement Measurements - The settlement platform assembly was designed to measure compression of both the embankment fill and the underlying unburned MSW. The magnitude of the embankment and underlying fill settlements are critical to the performance of the roadway. The primary concern is the occurrence of differential settlements large enough to impede traffic flow. Data for the embankment compression is shown in Figure 6.1. The figure shows settlement occurring in the bottom ash, mixed material, and gravel subsections. The data was measured in centimeters on settlement platform 2, settlement platform 4, and settlement platform 6 or SP-2, SP-4, and SP-6 respectively. The results shown in Figure 6.1 are a representative sample of data for embankment compression. Data for all six settlement platforms appears in Appendix D. For comparison purposes the appendix shows data for the two settlement platforms located

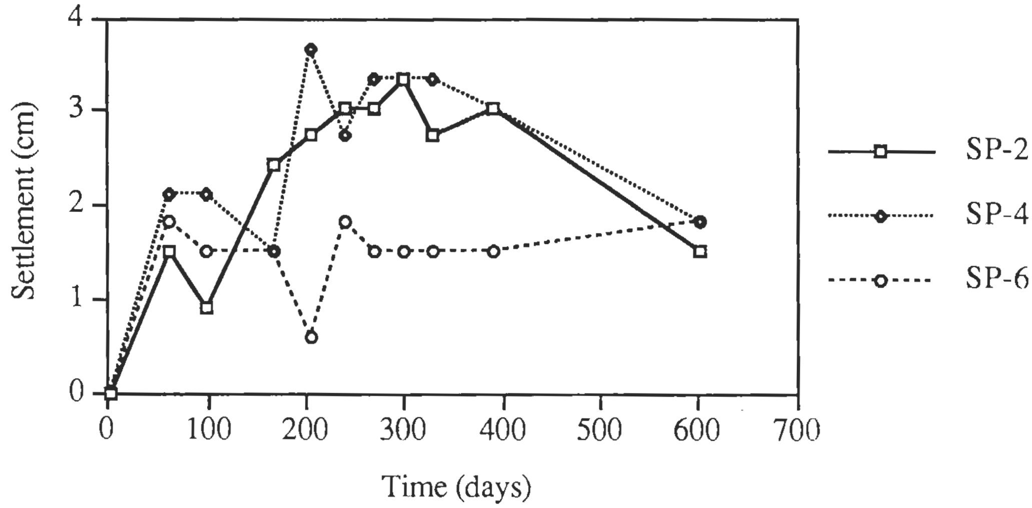

Figure 6.1 Compression of embankment subsections from end of construction

within each subsection on the same graph (e.g. data for SP-1 and SP-2 located in the bottom ash subsection are shown on the same graph). The data in Figure 6.1 shows that all three fill materials compress rapidly following the end of construction. The rate of compression then decreases and the subsections maintain a relatively constant thickness. The gravel equilibrates to constant thickness approximately 60 days after the end of construction while the bottom ash takes approximately 100 days and the mixed material 200 days to equilibrate. The bottom ash compresses approximately 3.2 cm 400 days after the end of construction, more than double that of the gravel control section, which compresses approximately 1.5 cm. The mixed material also compresses approximately 3.2 cm. At day 600, the bottom ash and mixed material subsection increase in thickness. The overall compression of the bottom ash section increased to 1.5 cm from 3.2 cm at 400 days. The mixed material subsection increased to 2.43 cm from 3.2 cm at 400 days. This may be due to the fact that the original survey crew was replaced by a new survey crew following the 400 day measurement. Changes in the exact positioning of the rod on the steel casing surrounding the riser pipe during the survey measurements may have altered the readings. Additionally, the replacement survey crew noted an elevation difference of +5.0 cm on the benchmark used by the original survey crew.

The difference in compression between the bottom ash and the gravel may result from two sources. Compression in the bottom ash can occur from the presence of large quantities of thin walled metal containers and hollow metallic particles. High chloride levels in leachate within the bottom ash subsection may have caused rapid deterioration of the particle's metallic walls. The deteriorated particles can create voids which collapse causing compression of the fill. The gravel may undergo less compression than the bottom ash because it consists of material which does not degrade in the presence of chlorides. Settlement in each of the fill materials may have also occurred as a result of particles rearranging in response to repeated heavy loadings. Another possible source of settlement for the bottom ash is post-construction dewatering. The bottom ash section was constructed at a moisture content above optimum. Loading and seepage may have caused water to migrate out of the fill resulting in consolidation.

The measured behavior of the fill material may be affected by factors other than particle degradation and dewatering. Following the end of construction the roadway remained unpaved for approximately 90 days. Although the final paving was incomplete, truck traffic used the road daily. The steel casing for each settlement platform (see Figure 2.4) was exposed at the top surface of the fill material. Traffic utilizing the access road traveled directly over the unprotected steel casings. The force of wheel loads may have driven the casings into the fill material. This factor is important in the fact that settlement measurements were taken from the top of the steel casing and the top of the riser pipe (see Figure 2.4). Downward displacement of the steel casings by wheel loads would result in increased embankment compression measurements.

Settlements within the embankment fill materials were small compared to those occurring in the underlying MSW. Figure 6.2 shows settlement versus time for the underlying unburned MSW. The figure shows data for SP-2, SP-4, and SP-6, located in the bottom ash, mixed material, and gravel subsections respectively. The data in Figure 6.2 is representative of settlements occurring at each of the platforms. Data for all

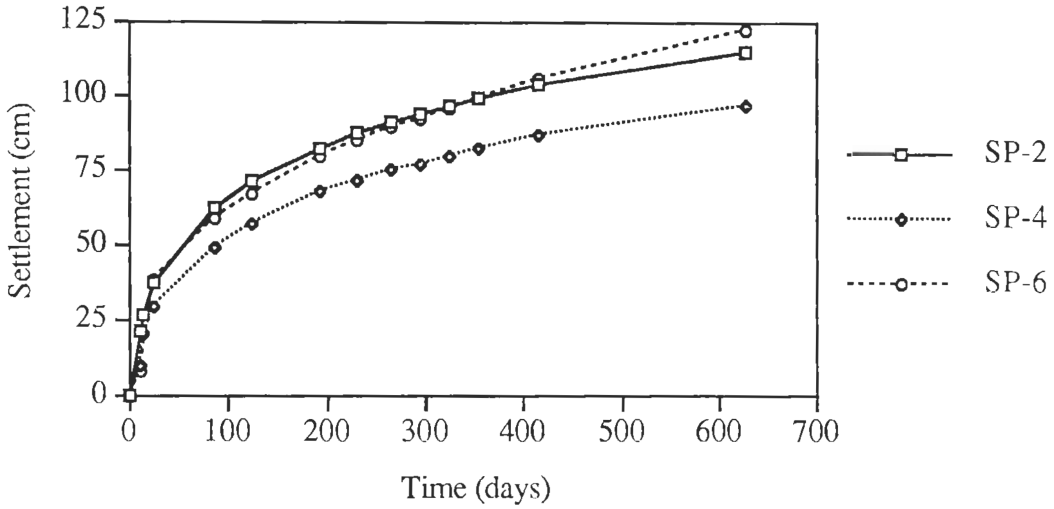

Figure 6.2 Compression of underlying MSW from beginning of construction

platforms appears in Appendix D. Appendix D contains data for the compression of the underlying MSW at each of the six settlement platforms. Data for the two settlement platforms located within each subsection appears on the same graph.

One of the primary concerns in the performance of the roadway is damage caused by excessive differential settlement in the underlying MSW. Figure 6.2 shows that differential settlement occurs between subsections. SP-2 and SP-6 each settle at a similar rate and magnitude. SP-4, located at the midpoint between SP-2 and SP-6 settles approximately 18 cm less than SP-2 and 25 cm less than SP-6. The total settlement of the platforms ranges from 96 cm at SP-4 to approximately 121.9 cm at SP-6. SP-2 settles 96 cm over the 626 days following the beginning of construction. Pavement cracks described previously may be the result of differential settling in the underlying MSW. The cracks are located at the boundaries of the subsections, indicating that the subsections are settling at different rates and that they are moving independently as blocks.

Vertical deformations occurring within the embankment and in the underlying MSW were measured at each settlement platform. The platforms were located at the quarter points of each subsection (see plan view of roadway in Figure 2.2). Lateral displacements were measured at half station intervals on the 2:1 slope to the southeast of the test section. Slope pins were placed at each half station starting at station 0+50 and ending at station 3+50. Seven slope pins were installed. All of the pins indicate that the embankment is shifting to the southeast in the direction of the Housatonic River. The total horizontal displacements from the beginning of construction until day 416 range from 10.9 cm to 19.2 cm. The displacement is the result of decomposing underlying MSW. The effect of the lateral shift to the embankment is minimal. Each of the slope pins indicates that the magnitude and direction of travel are relatively similar.

6.2 Chemical Performance

6.2.1 Leachate from Local and Global Sumps - Chemical analyses were performed on leachate withdrawn from the six sumps. The leachate was analyzed to determine the concentration of selected dissolved metals and chlorides. Results of chemical analyses do not show trends similar to those observed in column and laboratory lysimeter tests described in Section 5.3. Based on trends described in Section 5.3, contaminant concentrations decrease as multiple pore volumes of water percolate through a test material. Typical leachate data is shown in Figure 6.3. The figure shows the concentration of chlorides in leachate from the global and local sumps. Sampling commenced at the beginning of construction and continued on a monthly basis for approximately 200 days.

Figure 6.3 shows the concentration of chlorides in milligrams per liter on the vertical axis and the time after construction began on the horizontal axis. Figure 6.3a shows results for the three global sumps. The source of the leachate is indicated by GS-X, where 'X' represents the location within the embankment. The numbers 1, 2, and 3 represent the bottom ash, mixed material, and gravel subsections respectively. Figure 6.3b shows the results from the local sumps. The source lysimeter is indicated by LS-X, where the numbers 1, 2, and 3 represent the bottom ash, mixed material, and gravel sections respectively.

Each graph in Figure 6.3 shows irregular chloride concentrations over the entire sampling period. The attenuating contaminant concentrations observed in laboratory tests are not evident in field results. The results shown in Figure 6.3 are representative of the results for each of the contaminants analyzed. Concentrations of arsenic, barium, cadmium, chromium, lead, selenium, and silver show no recognizable attenuation over time. The metals concentrations are irregular and unpredictable. The results of field leachate chemical analyses are unsatisfactory due to problems associated with the embankment drainage control. For this reason leachate chemical results are shown in Appendix D. The appendix shows the concentration of arsenic, barium, cadmium, chromium, lead, selenium, and silver for the global and local sumps.

The behavior of contaminant concentrations in Figure 6.3 indicates that the embankment was subject to infiltrating ground water from an external source. Laboratory leaching results presented in Figure 5.1 show that the maximum contaminant concentrations occur when the smallest quantity of water has passed through the test material. Figure 6.3 shows that the initial contaminant levels are not the maximum. The contaminant concentrations in Figure 6.3 rise over time even though rainwater has passed

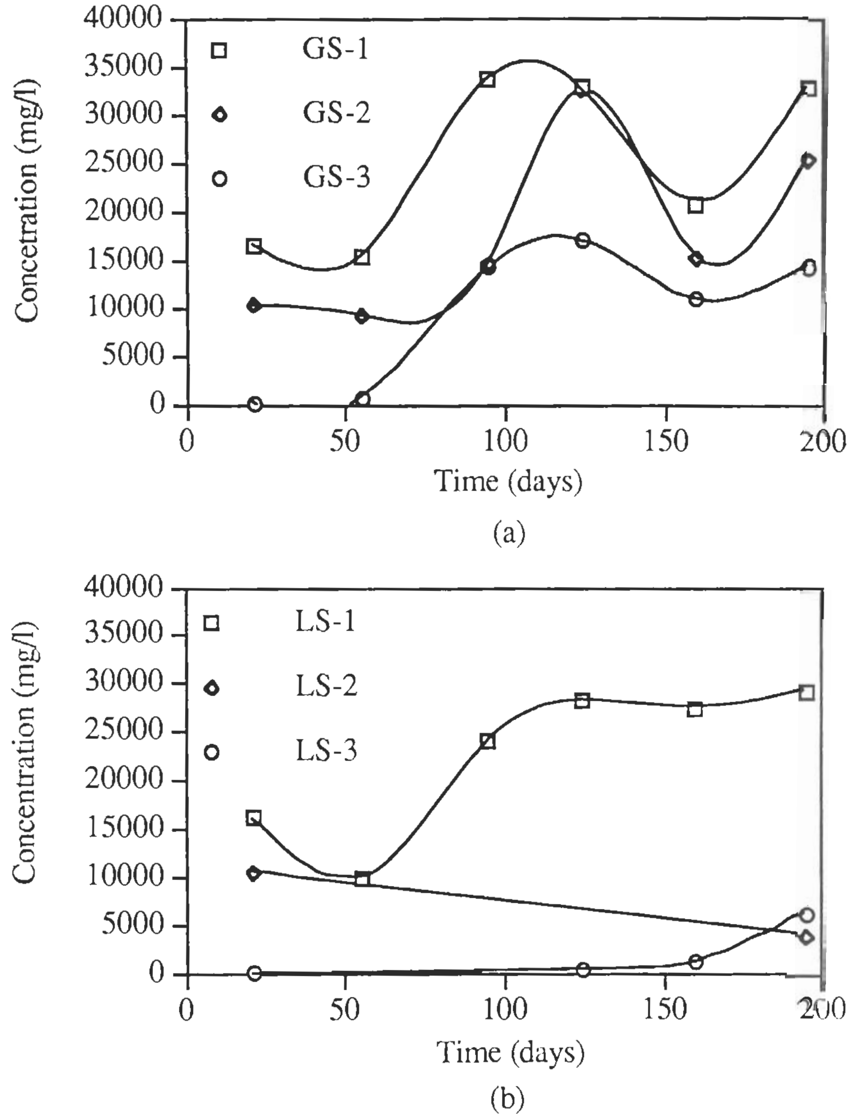

Figure 6.3 Concentration of chlorides in (a) global and (b) local sumps from beginning of construction

through the embankment. The elevated contaminant concentrations are the result of an external leachate source. Chlorides levels begin to rise in the bottom ash and gravel sections approximately 50 days after the beginning of construction. The delay occurred as ground water originating from the landfill traveled through the embankment fill toward the leachate collection sumps. Figure 2.3 shows a possible entry path for external leachate. The geomembrane intended for encapsulating the embankment extends horizontally only to the upgradient edge of the fill section. The absence of an impermeable vertical barrier along the upgradient edge of the fill allowed ground water to infiltrate the embankment.

6.2.2 Local Lysimeter Dowsing - The global and local sumps were designed for different purposes. Each global sump was designed to collect leachate from within an entire subsection. Water input was controlled by natural precipitation. The local sumps were designed to act as lysimeters by utilizing water input manually through the reinforced concrete pipe section shown in Figure 2.5. After manual dowsing, the sump collects water percolating from above. Leachate samples are collected and the sumps drained between each dowsing. Although the local sumps operate differently from the global sumps, each served to examine the attenuation of metals and chlorides dissolved in the leachate. The local leachate collection system is advantageous compared to the global system because controlled volumes of water may be added to the system.

From the beginning of construction until approximately day number 200, naturally occurring leachate was periodically extracted from the local sumps (see Section 6.2.1). Following day 200, the local sumps were drained and manually dowsed with predetermined quantities of tap water. On five consecutive days 680 liters of water were poured into each of the three concrete pipe sections. The previous day's leachate was vacuum extracted and each sump drained prior to the next dowsing. Figure 6.4 shows the chlorides concentration in leachate from the three sumps during dowsing. The vertical axis represents the chlorides concentration in milligrams per liter. The horizontal axis represents the quantity of water passed through the test material. Chemical analysis results for arsenic, barium, cadmium, chromium, lead, selenium, and silver appear in Appendix E. Each sump was dowsed with a fixed quantity of tap water. The variation in pore volumes passed for individual sumps results from variable test material thicknesses below each of

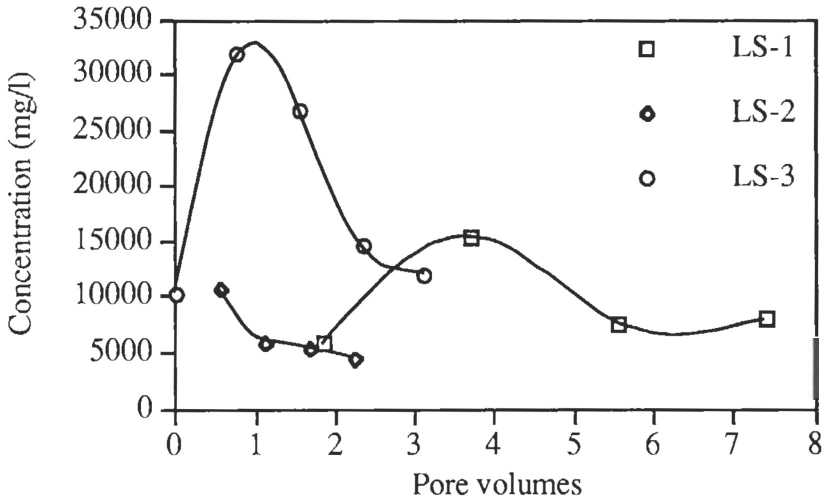

Figure 6.4 Chlorides concentration in local sumps during manual dowsings

the concrete pipe sections. The number of pore volumes passed is dependent on the total volume of soil in each local lysimeter.

The results of the manual dowsings generally do not resemble results observed in laboratory leaching studies. Local sump #2 (mixed material) shows results resembling those observed in laboratory leaching studies. The concentration of chlorides begins at approximately 10000 mg/l and decreases to one half the original value with the addition of one pore volume of water. The rate of attenuation decreases dramatically following the initial reduction. The bottom ash and gravel sections show results resembling the laboratory results. The chlorides concentration rises during the first two dowsings. After the initial increase, the concentrations decrease substantially and then begin to stabilize. The overall dependability of results from the local sumps is questionable. The local sumps were subject to the same contamination effects as the global sumps. Uncertainty regarding the extent of contamination makes the results inconclusive.

7.0 CONCLUSIONS AND RECOMMENDATIONS

7.1 Conclusions

This study has yielded valuable information regarding the physical and chemical properties of bottom ash from a mass burn incinerator. The following conclusions can be drawn regarding incinerator bottom ash:

1) Bottom ash is well graded and exhibits behavior similar to natural granular aggregates. The friction angle of the ash is approximately 45°. The permeability is roughly 10^{-4} cm/s for unblended bottom ash, but it may be lowered by over two and one half orders of magnitude by blending fine grained materials with the bottom ash. The loss on ignition averages 2.3%, indicating that the ash contains little organic matter.

2) The maximum dry density is slightly lower than naturally occurring gravel and varies according to the quantity of metal contained within a specific sample of ash. Removing ferrous metal lowers the maximum dry density while improving the homogeneity of the material. Compaction tests in a modified Proctor mold show that bottom ash particles are susceptible to degradation/breakage by dynamic compaction energy.

3) The chemical composition of dry bottom ash as determined by total chemical analysis testing includes arsenic, barium, cadmium, calcium, chloride, chromium, lead, manganese, potassium, selenium, silver, and sodium. However, TCLP test results show that bottom ash is categorized as nonhazardous under EPA guidelines for three of four samples tested in this study. The one sample exceeding TCLP regulatory limits contained slightly excessive lead.

4) Column and lysimeter leaching studies show that bottom ash contains a significant quantity of soluble salt. The primary anion present is chloride, while the primary cations present are sodium, calcium, and potassium. The quantity of salt present in leachate is determined by measuring the electrical conductivity. The conductivity is at a maximum in leachate taken from the first pore volume of water passing through a bottom ash sample. The conductivity decreases rapidly as pore volume numbers one through five pass through the test material. Following pore volume number five, the conductivity equilibrates and decreases very little up to twenty pore volumes. The concentration of total dissolved solids, which is a measure of the quantity of salt in solution, exhibits behavior similar to that of the conductivity. Leachate contains a large quantity of dissolved solids initially, but the concentration of the solids in solution decreases rapidly as pore volume numbers one through five pass through the test material.

5) Environmental contamination caused by compounds leaching out of a bottom ash embankment may be reduced by altering the percolation rate through the embankment. Percolation can be reduced by modifying the permeability of the bottom ash. Experiments show that adding ten percent by weight of kaolinite 1 lowers the permeability of bottom ash from 1×10^{-4} cm/s to 3.3×10^{-7} cm/s, a reduction of almost two and one half orders of magnitude. Tests show that silt sized particles such as coal fly ash also reduce the permeability of bottom ash. Further testing is necessary to determine the most effective types and quantities of material for blending.

6) Bottom ash behaves well as structural fill material. The short term performance of the test embankment is excellent. The bottom ash subsection of the test embankment shows very good strength and compressibility characteristics. The fill material has undergone relatively little compression during the first twenty months after the end of construction. Following an initial period of rapid settlement, both the bottom ash and reference gravel subsections stabilized and maintained a relatively constant thickness.

7.2 Recommendations

This research project has yielded valuable data concerning the use of bottom ash as structural fill material. Several physical, chemical and economic issues require further research if future applications are considered:

1) To achieve a more homogeneous bottom ash composition and to eliminate particles susceptible to rapid chemical degradation, the majority of the ferrous metals should be removed. Removing particles larger than 19.1 mm (3/4 in), eliminates a large portion of the metallic particles. This process may be performed using magnetic or gravimetric processes. The separation work may be done at the incinerator or on a construction site following delivery of the bottom ash from the incinerator. The literature shows that patented systems are currently available to perform this operation. Removing the ferrous fraction also presents the opportunity for metals recycling.

2) To avoid contaminating the ground water at a site, the bottom ash may be chemically modified. Modifying the chemistry of the bottom ash can render specific contaminants insoluble, thus inhibiting those compounds from dissolving in percolating ground water. Bottom ash can be modified using various patented fixation processes. The particles may also be physically encapsulated using Portland cement or asphalt materials. Bottom ash may also be washed to remove highly soluble components such as salts using commercially available systems.

3) A more comprehensive chemical testing program must be performed on bottom ash. The expanded chemical testing program should include additional total chemical analysis and TCLP tests. The number of compounds examined in total chemical analysis testing should be increased. The number of compounds analyzed in TCLP tests must increase in accordance with the results of the total chemical analyses. In addition to examining additional compounds, additional bottom ash samples must be tested to determine the frequency and magnitude with which bottom ash samples exceed TCLP contamination limits.

4) To gain additional experience with bottom ash as structural fill material, more demonstration projects should be performed within landfills. The ash may be used as fill material for constructing access roads on the landfill premises. The primary advantage of bottom ash use within landfills is the environmental considerations. Contamination pre-exists within the landfill. Using bottom ash will not contaminate the existing landfill environment or introduce additional contaminants to the site. Additionally, using bottom ash is less expensive than purchasing natural aggregate to construct access roads. Processing the ash after delivery from the incinerator involves removing particles larger than 25 mm. The necessary equipment is a front end bucket loader and a vibratory screening machine. The cost of each is relatively low and the equipment is readily available.

Bottom ash may also be used in landfills as low permeability daily cover material. Bottom ash mixed with roughly 10% clayey silt produces aggregate with a permeability of approximately 10^{-7} cm/s. Further testing must be performed to determine the most suitable types of blending material and the quantity of material required to achieve acceptable permeability levels. Using bottom ash for landfill cover requires relatively little processing and reduces the cost of purchasing large quantities of suitable natural aggregates.

REFERENCES

Aziz, M.A., and Ramaswamy, S.D. (1992). "Incinerator Residue for Roads." *Geotechnical Testing Journal*, 15(3), 300-304.

Bagchi, B., and Sopcich, D. (1989). "Characterization of MSW Incinerator Ash." *Journal of Environmental Engineering*, ASCE, 115(2), 447-452.

Berg E., and Neal, J.A. "Municipal Waste Combustor Ash in Concrete Block." *Proceedings of the Fifth International Conference on Combustor Ash Utilization*, Arlington, VA., November 17-18, 1992.

Black, G.A., and Cunningham, J.C. "Ash Block as a Prototype Ash Utilization Product." *Proceedings of the Fourth International Conference on Combustor Ash Utilization*, Arlington, VA., November 12-13, 1991.

Casey, W.W. "Permabase-Plus -A Solid Solution." *Proceedings of the Sixth International Conference on Combustor Ash Utilization*, Arlington, VA., November 16-17, 1993.

Chesner, W.H. "Aggregate-Related Characteristics of Municipal Solid Waste Combustion Residues." *Proceedings of the Second International Conference on Combustor Ash Utilization,* Arlington, VA, November 8-9, 1989.

Chesner, W.H. "Ash Management: A Brief Overview." *Proceedings of the Second International Conference on Combustor Ash Utilization*, Arlington, VA, November 8-9, 1989.

Chesner, W.H. "The Long Island Ash Utilization Program Preliminary Engineering, Economic and Environmental Findings, and Guidelines for MSW Combustor Ash Utilization." *Proceedings of the Third International Conference on Combustor Ash Utilization*, Arlington, VA, November 13-14, 1990.

Collins, R.J., Miller R.H., and Ciesielski, S.K. (1977). "Guidelines for Use of Incinerator Residue As Highway Construction Material." *FHWA-RD-77-150*, U.S. Department of Transportation, FHWA.

Demars, K.R., Garrick, N.W., Long R.P., Lentz, D., Maddali, R., Stephens, J.E., and Recchia, C. "Municipal Waste Combustor Bottom Ash Road Paving and Structural Fill Demonstration Project." *Proceedings of the Sixth International Conference on Combustor Ash Utilization*, Arlington, VA, November 16-17, 1993.

Forrester, K.E. "Use of Soluble Phosphates for Stabilizing Heavy Metal Bearing Wastes." *Proceedings of the Fourth International Conference on Combustor Ash Utilization*, Arlington, VA, November 12-13,1991.

Franklin, M.A. "Sources of Heavy Metals in Municipal Solid Waste in the United States, 1970 to 2000." *Proceedings of the Third International Conference on Combustor Ash Utilization*, Arlington, VA, November 13-14,1990.

Dunn, I.S., Anderson, L.R., and Kielfer, F.W. (1980). *Fundamentals of Geotechnical Analysis*. John Wiley & Sons, New York.

Gibbs, D.R., and Hepp, M.P. (1990). "Mass-Burn Plant Achieves High Availability, Low Emissions." *Power*, 134(4), S-51-S-54.

Goodwin, R.W. "The Case for Ash Use." Proceedings of the Fifth International Conference on Combustor Ash Utilization, Arlington, VA, November 17-18, 1992.

Grasso, D. (1993). *Hazardous Waste Site Remediation Source Control.* Lewis Publishers, Boca Raton.

"Hazardous Waste Management System; Identification and Listing of Hazardous Waste; Toxicity Characteristic Revisions; Final Rule." *Federal Register*, U. S. Environmental Protection Agency, June 29, 1990.

Hartlen, J., and Fallman, A. "Sorted Bottom Ash from MSW Incineration in Road Embankments." *Proceedings of the Third International Conference on Combustor Ash Utilization*, Arlington, VA, November 13-14, 1990.

Hooper W.F. "Processed Ash Demonstration Project." *Proceedings of the Fourth International Conference on Combustor Ash Utilization*, Arlington, VA, November 12-13, 1991.

Hooper, W.F. "Innovative Ash Use in Florida." *Proceedings of the Sixth International Conference on Combustor Ash Utilization*, Arlington, VA, November 16-17, 1993.

Kalajian, E.H., Johnson, O.O., and Wu, C. "Artificial Reef Structures Constructed of Waste to Energy Ash-Concrete." *Proceedings of the Third International Conference on Combustor Ash Utilization*, Arlington, VA, November 13-14, 1990.

Lambe, W.T., and Whitman, R.V. (1969). *Soil Mechanics*, John Wiley & Sons, New York.

Plumley, A.L., and Boley, G.L. "ABB Ash Treatment Technologies." *Proceedings of the Third International Conference on Combustor Ash Utilization*, Arlington, VA, November 13-14, 1990.

Roethel ,F.J., and Breslin, V.T. "Stony Brook's MSW Combustor Ash Demonstration Programs." *Proceedings of the Third International Conference on Combustor Ash Utilization*, Arlington, VA, November 13-14, 1990.

Roffman, H.K. "Results of Three Year Monitoring of Ashes, Leachates and Soils at the Woodburn Ash-Monofill." *Proceedings of the Third International Conference on Combustor Ash Utilization*, Arlington, VA, November 13-14, 1990.

Roffman, H.K. "Summary of Major Findings of the CORRE/EPA Ash Study." *Proceedings of the Second International Conference on Combustor Ash Utilization*, Arlington, VA, November 8-9, 1989.

Schoenberger, R.J., and Fungaroli, A.A. (1971). "Incinerator-Residue-Fill Site Investigation." *Journal of the Soil Mechanics and Foundations Division*, ASCE, 97(10), 1431-1443.

Shepherd, P.B., Gupta, B.P., and Friedrich, S. "Importance of Ash Research to the Municipal Solid Waste Management Program at the National Renewable Energy Laboratory." *Proceedings of the Sixth International Conference on Combustor Ash Utilization*, Arlington, VA, November 16-17, 1993.

Standard Specifications for Roads, Bridges and Incidental Construction, Form 814. (1988). State of Connecticut Department of Transportation.

"State of Connecticut Adopted Solid Waste Management Plan." (1991). Connecticut Department of Environmental Protection.

Styron, R.W. "Ash Fill in Cell Leachate Treatment." *Proceedings of the Fifth International Conference on Combustor Ash Utilization*, Arlington, VA, November 17-18, 1992.

Sundstrom, D.W., Klei, H.E., Weir, B.A., and Perna, A.J. "Leaching Behavior of Residues from Mass Burn and Refuse Derived Fuel Incinerators." *Second International Conference of Municipal Waste Combustion*, Tampa, FL, April 16-19, 1991.

Taras, M.J., editor. (1971). *Standard Methods for the Examination of Water and Wastewater, 13th Edition*, American Public Health Association, Washington D.C.

Tay, J., and Goh, A.T.C. (1991). "Engineering Properties of Incinerator Residue." *Journal of Environmental Engineering*, ASCE, 115(2), 224-235.

Test Methods for Evaluating Solid Waste Physical/Chemical Methods-Third Edition. United States Environmental Protection Agency, Washington, D.C., 1987.

Theis, T.L., and Gardner, K.H. "Dynamic Evaluation of Municipal Waste Combustion Ash Leachate." *Proceedings of the Fifth International Conference on Combustor Ash Utilization*, Arlington, VA, November 17-18, 1992.

Williams, B.A. "Metal Extraction and Ash Conditioning." *Proceedings of the Second International Conference on Combustor Ash Utilization*, Arlington, VA, November 8-9, 1989.

APPENDICES

APPENDIX A - GRADATION OF FILL MATERIALS SAMPLED DURING EMBANKMENT CONSTRUCTION

SAMPLE NUMBER	% PASSING #4	% PASSING #40	% PASSING #200
A-1	59.1	16.9	6.6
A-2	53.6	16.3	6.2
A-3	56.8	18.1	6.8
A-4.5	51.5	15.8	6.4
A-5.5	53.2	14.2	5.1
A-6	50.1	15.7	6.1
A-7	56.7	15.3	7.4
A-8	45.8	13.7	5.1
A-9	51.4	15	5.3
A-10	53.9	16.3	6.5

Appendix A1 Gradation of bottom ash samples

SAMPLE NUMBER	% PASSING #4	% PASSING #40	% PASSING #200
S-1	62.0	30.3	10.1
S-2	36.1	15.5	7.3
S-3	53.0	24.9	9.3
S-4	54.1	26.4	11.5
S-5	66.2	33.4	10.2
S-6	49.3	20.3	8.0

Appendix A2 Gradation of gravel samples

SAMPLE NUMBER	% PASSING #4	% PASSING #40	% PASSING #200
AS-1	48.6	18.8	6.8
AS-3	54.1	23	7.6
AS-4	49	22.2	8.6
AS-6	52.6	23.9	8.9
AS-7	48	22.7	8.3
AS-8	56.2	23.7	8.5
AS-9	43.9	20.4	7.3

Appendix A3 Gradation of mixed material samples

APPENDIX B - PEAK AND RESIDUAL FRICTION ANGLE RESULTS FOR EMBANKMENT FILL MATERIALS

NORMAL STRESS = 77.8 kPa

	TRIAL 1	TRIAL 2	TRIAL 3	TRIAL 4	TRIAL 5	TRIAL 6
Peak Angle*	64.1	63.5	64.9	63.9	60	57.5
Residual Angle*	54.9	51.3	52.1	53.7	44.9	44.1

NORMAL STRESS = 155.5 kPa

	TRIAL 1	TRIAL 2	TRIAL 3	TRIAL 4	TRIAL 5	TRIAL 6
Peak Angle	59.8	56.1	60.5	57.4	56.1	54.5
Residual Angle	42.8	43.3	45.2	51.9	49.4	45.7

NORMAL STRESS = 311.1 kPa

	TRIAL 1	TRIAL 2	TRIAL 3	TRIAL 4	TRIAL 5	TRIAL 6
Peak Angle	57.4	48.4	55.6	56.3	54.4	52.2
Residual Angle	40.2	44.2	40.4	44.3	42.2	43.4

NORMAL STRESS = 622.1 kPa

	TRIAL 1	TRIAL 2	TRIAL 3	TRIAL 4	TRIAL 5	TRIAL 6
Peak Angle	46.7	49.7	49.1	46.5	44.4	45.7
Residual Angle	40.2	40.3	40.3	40.7	38.6	40.2

* Friction angles in degrees

Appendix B1 Peak and residual friction angle results for bottom ash subjected to varying confining stresses

NORMAL STRESS = 77.8 kPa

	GRAVEL	MIXED MATERIAL
Peak Angle*	54.5	55.5
Residual Angle*	49	44.6

NORMAL STRESS = 155.5 kPa

	GRAVEL	MIXED MATERIAL
Peak Angle	50.4	46.4
Residual Angle	40.9	40.8

NORMAL STRESS = 311.1 kPa

	GRAVEL	MIXED MATERIAL
Peak Angle	47.7	45.1
Residual Angle	41.5	38.7

NORMAL STRESS = 622.1 kPa

	GRAVEL	MIXED MATERIAL
Peak Angle	45.2	43.1
Residual Angle	42.7	38.7

* Friction angles in degrees

Appendix B2 Peak and residual friction angle results for gravel and mixed material subjected to varying confining stresses

APPENDIX C - CONCENTRATION OF CONTAMINANTS IN LEACHATE EXTRACTED FROM LABORATORY LYSIMETER #2

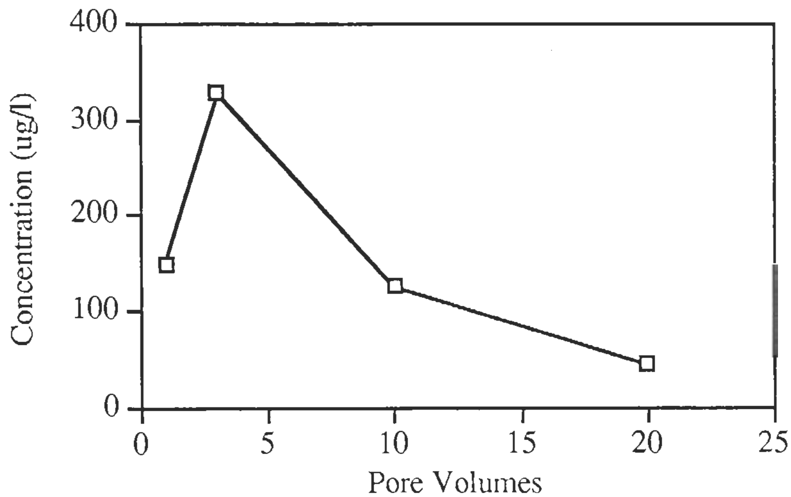

Appendix C1 Arsenic concentration in Lysimeter #2 leachate

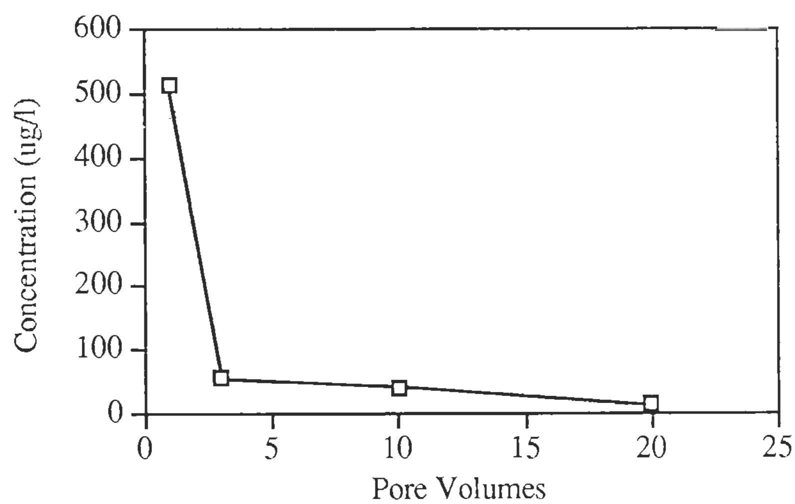

Appendix C2 Barium concentration in Lysimeter #2 leachate

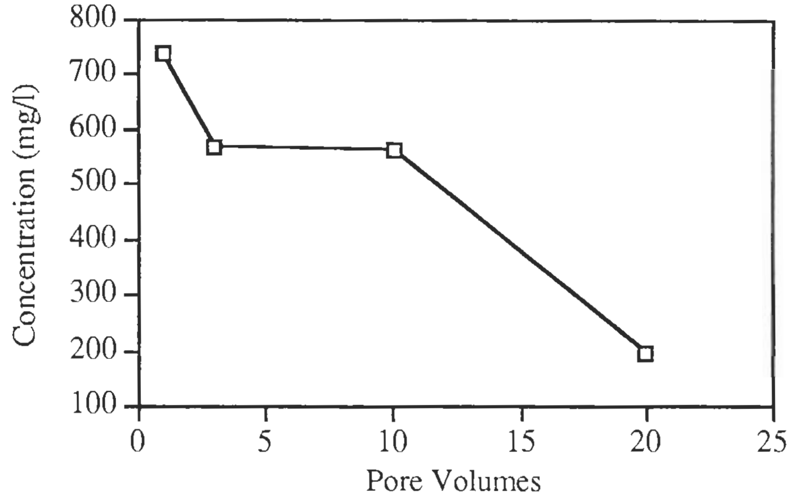

Appendix C3 Calcium concentration in Lysimeter #2 leachate

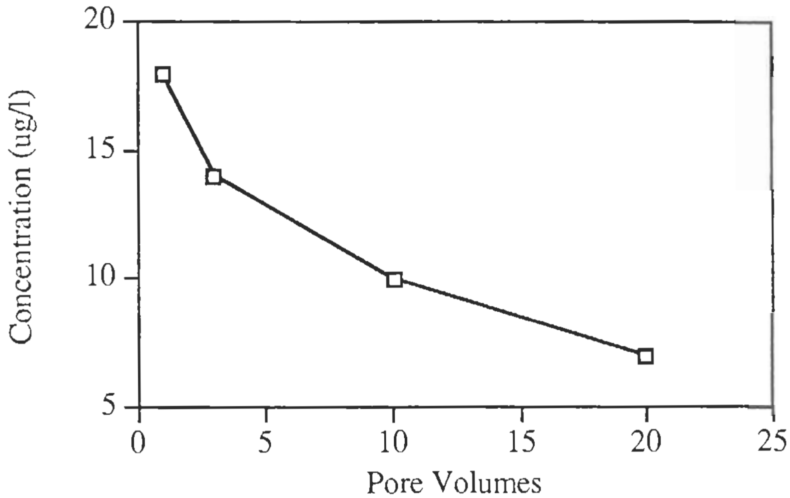

Appendix C4 Cadmium concentration in Lysimeter #2 leachate

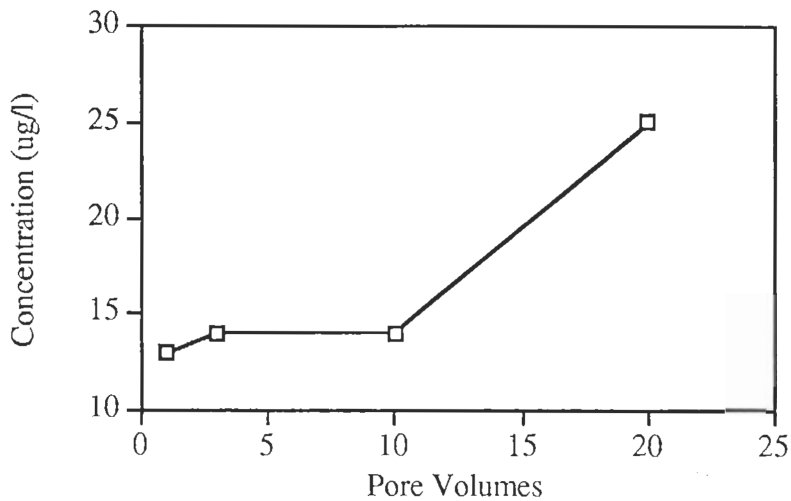

Appendix C5 Chromium concentration in Lysimeter #2 leachate

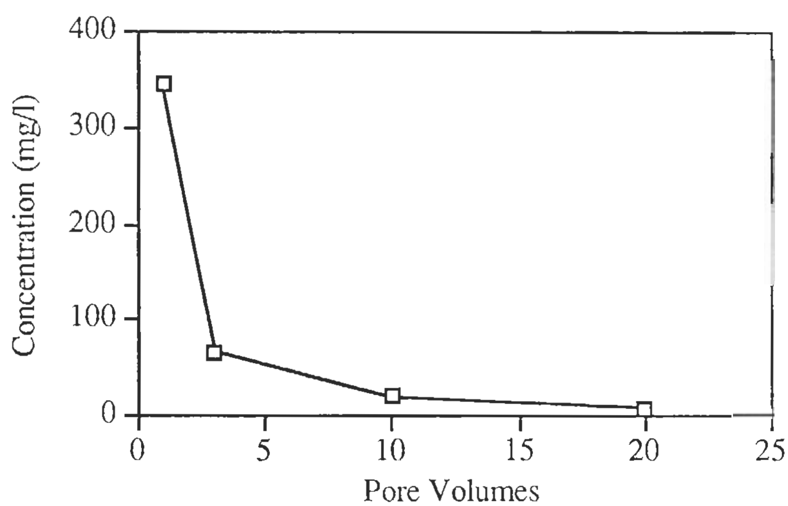

Appendix C6 Potassium concentration in Lysimeter #2 leachate

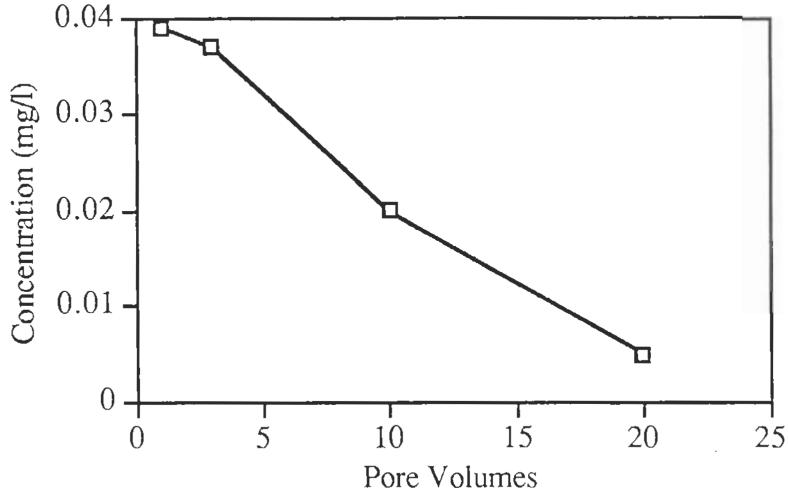

Appendix C7 Manganese concentration in Lysimeter #2 leachate

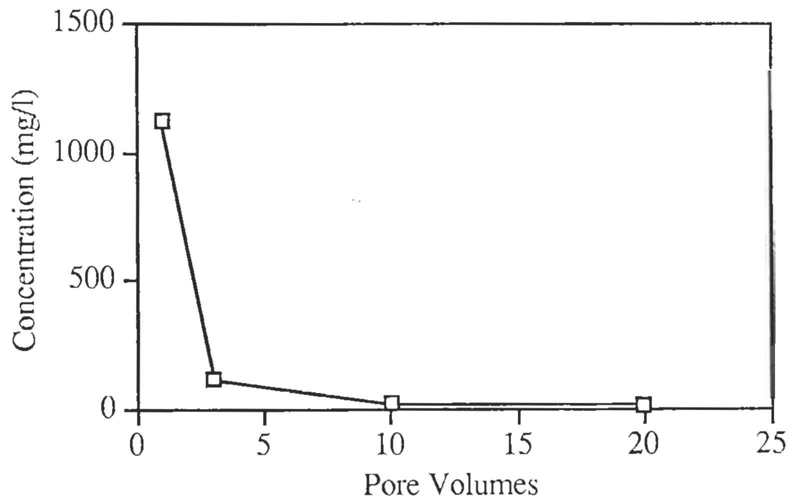

Appendix C8 Sodium concentration in Lysimeter #2 leachate

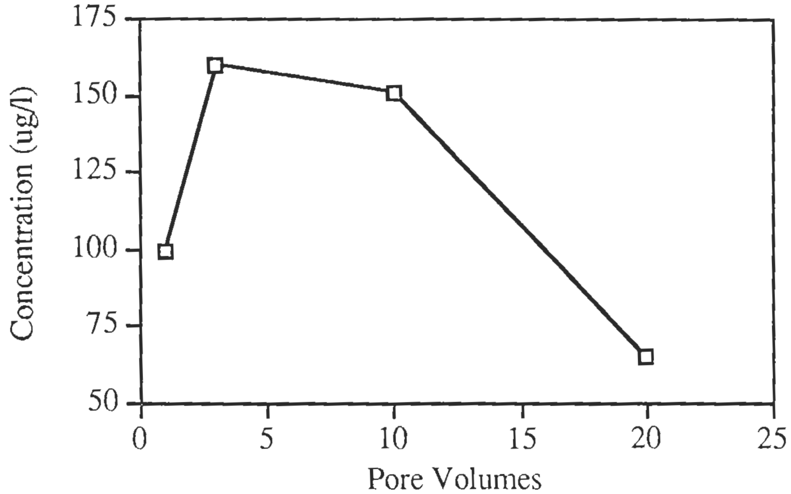

Appendix C9 Lead concentration in Lysimeter #2 leachate

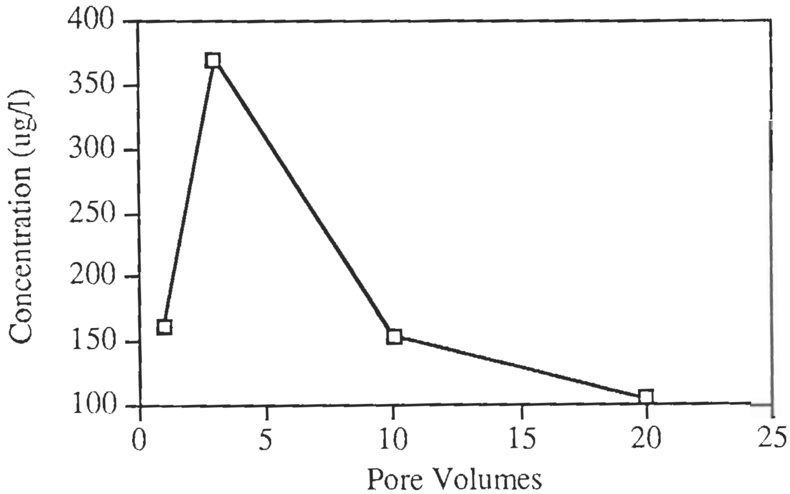

Appendix C10 Selenium concentration in Lysimeter #2 leachate

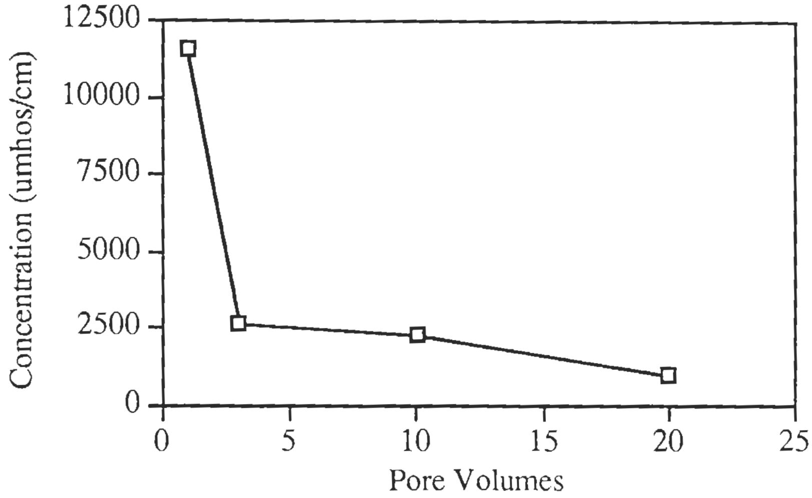

Appendix C11 Leachate conductivity from Lysimeter #2

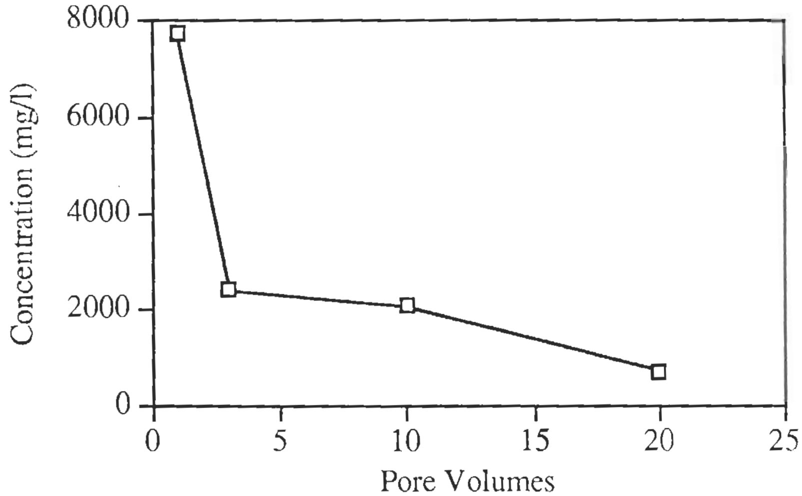

Appendix C12 Total dissolved solids concentration in Lysimeter #2 leachate

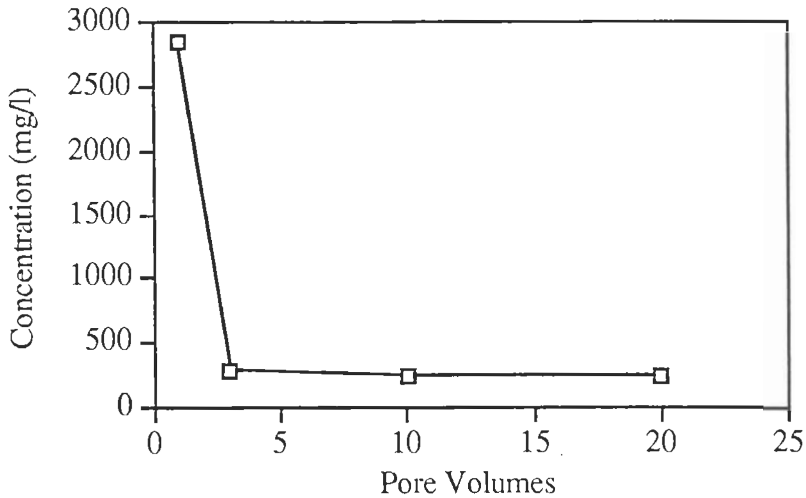

Appendix C13 Chlorides concentration in Lysimeter #2 leachate

APPENDIX D - SETTLEMENT DATA SHOWING COMPRESSION OF TEST EMBANKMENT SUBSECTIONS AND COMPRESSION OF UNDERLYING MSW

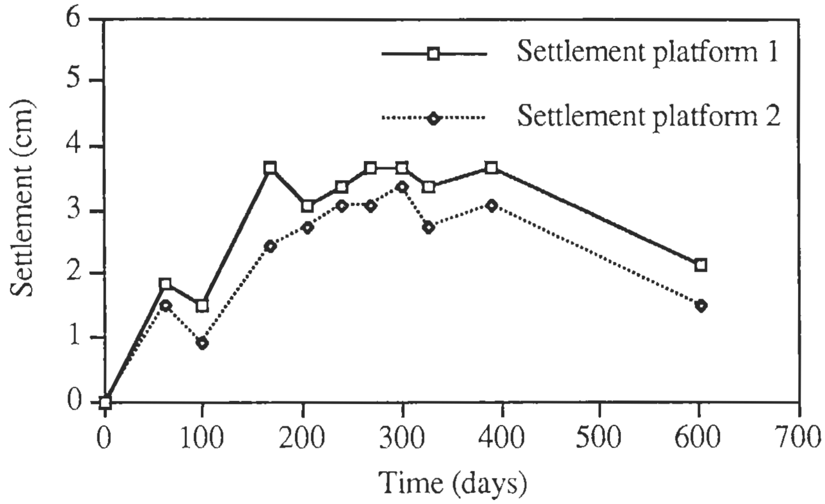

Appendix D1 Compression of bottom ash subsection from end of construction

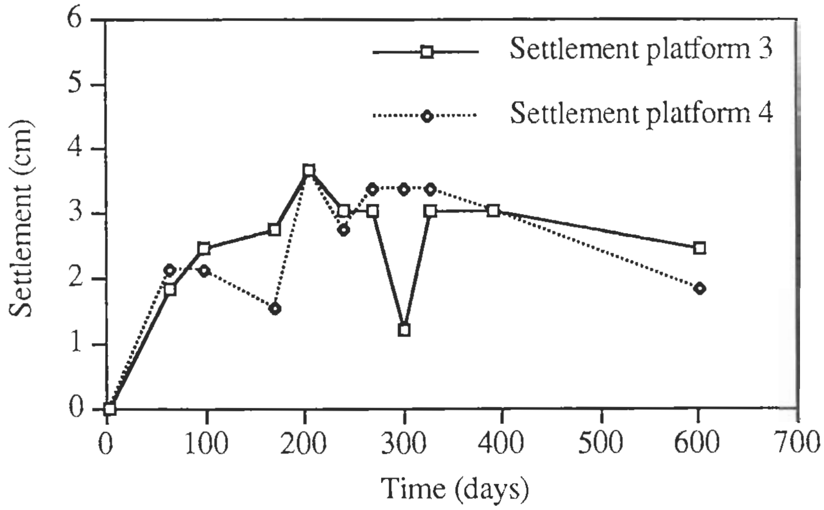

Appendix D2 Compression of mixed material subsection from end of construction

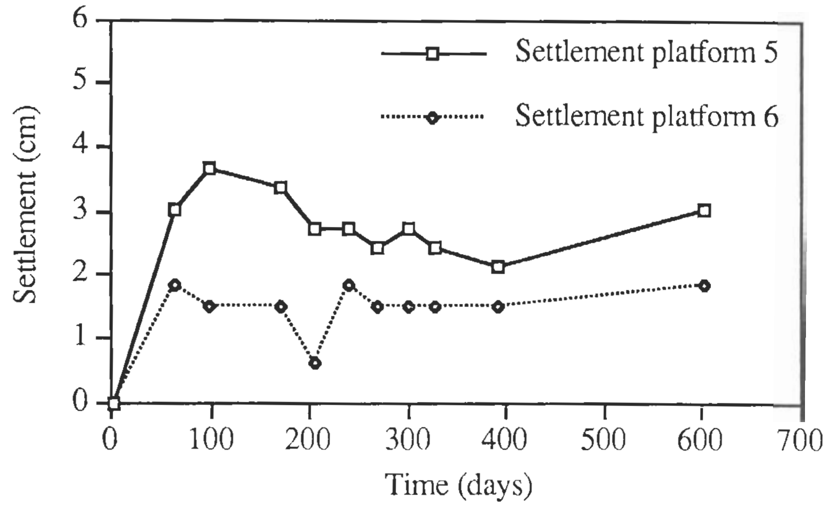

Appendix D3 Compression of gravel subsection from end of construction

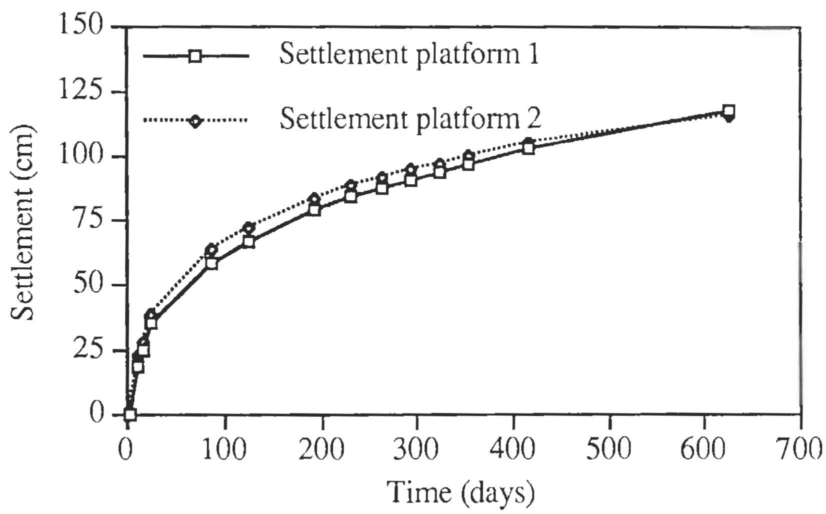

Appendix D4 Compression of MSW underlying bottom ash subsection from beginning of construction

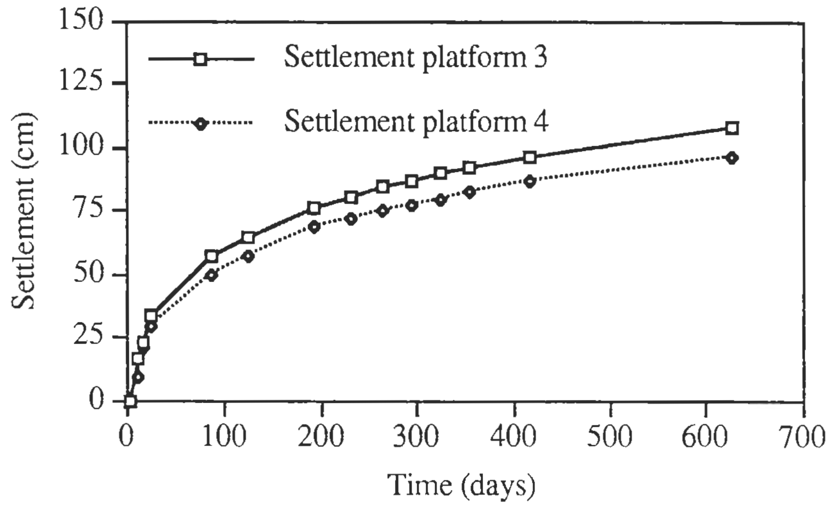

Appendix D5 Compression of MSW underlying mixed material subsection from beginning of construction

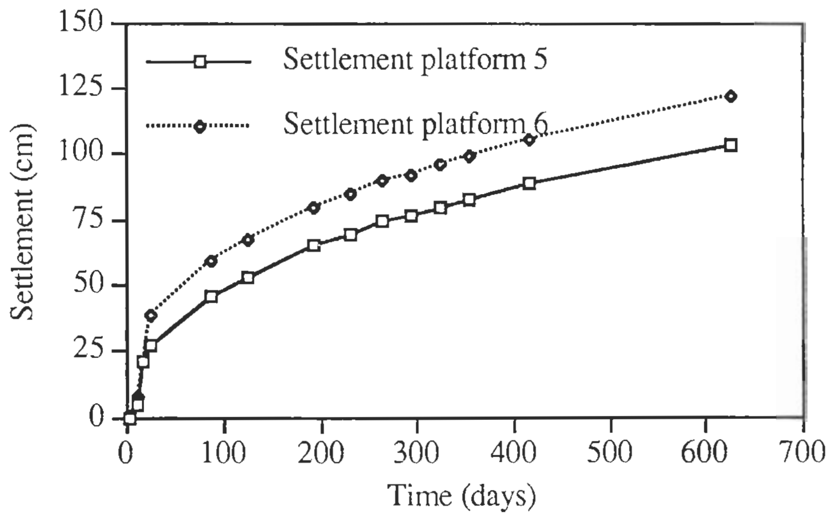

Appendix D6 Compression of MSW underlying gravel subsection from beginning of construction

APPENDIX E - CONTAMINANT CONCENTRATIONS IN LEACHATE EXTRACTED FROM GLOBAL AND LOCAL SUMPS

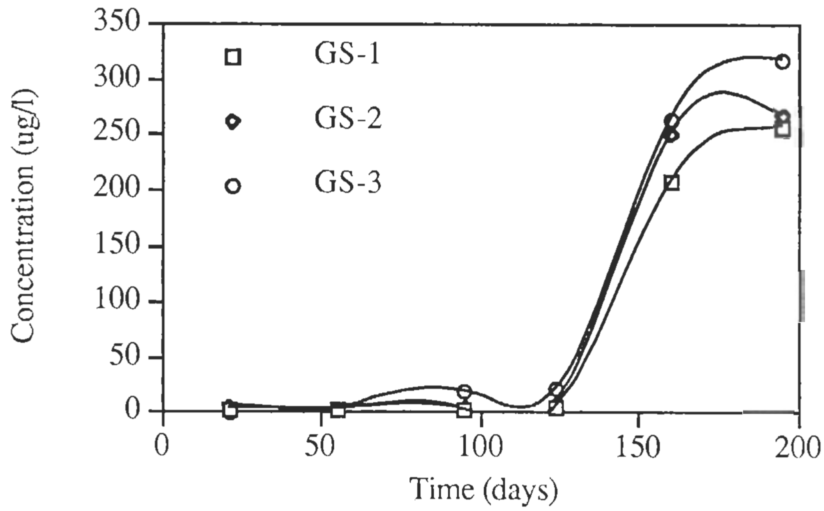

Appendix E1 Concentration of arsenic in global sumps from beginning of constr.

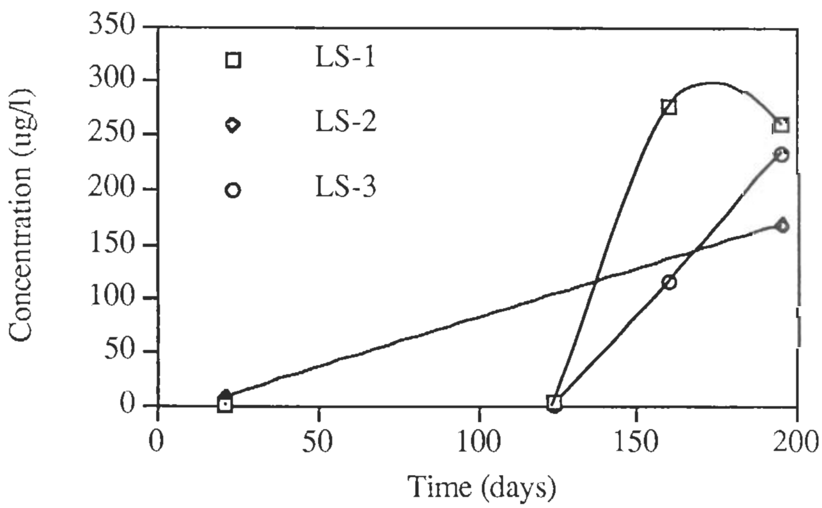

Appendix E2 Concentration of arsenic in local sumps from beginning of constr.

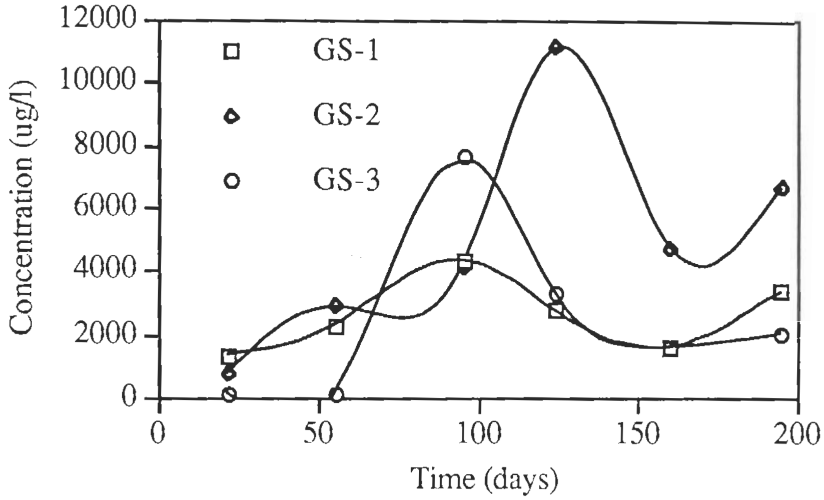

Appendix E3 Concentration of barium in global sumps from beginning of constr.

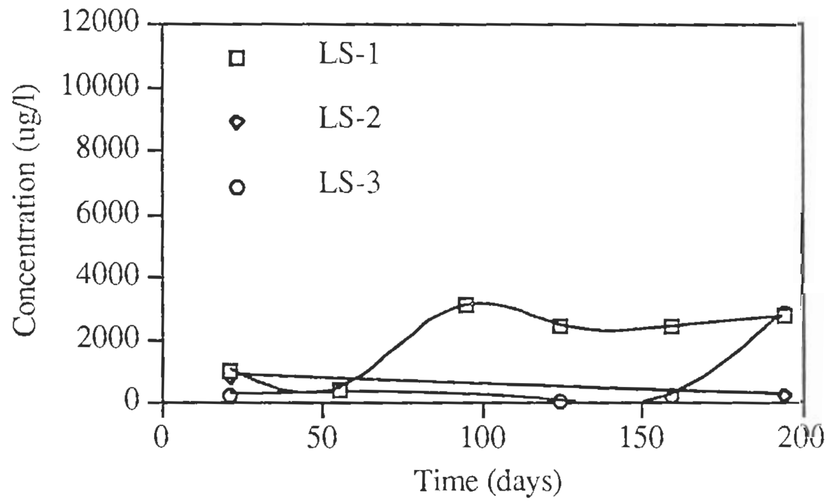

Appendix E4 Concentration of barium in local sumps from beginning of constr.

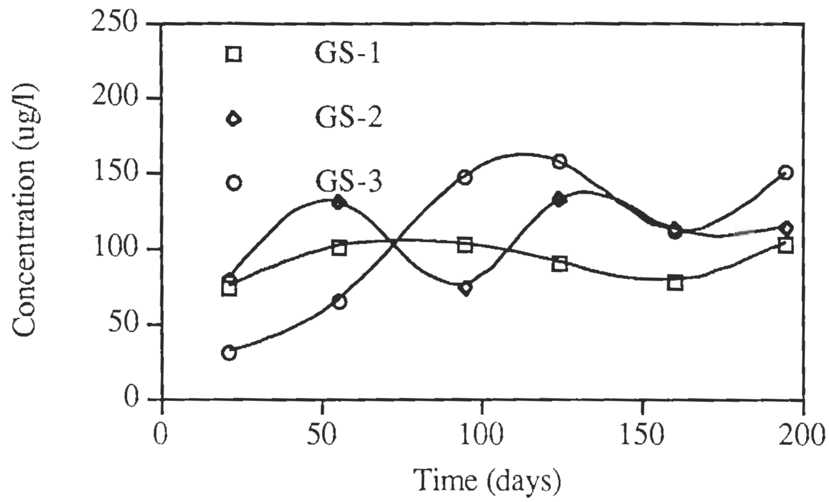

Appendix E5 Concentration of cadmium in global sumps from beginning of constr.

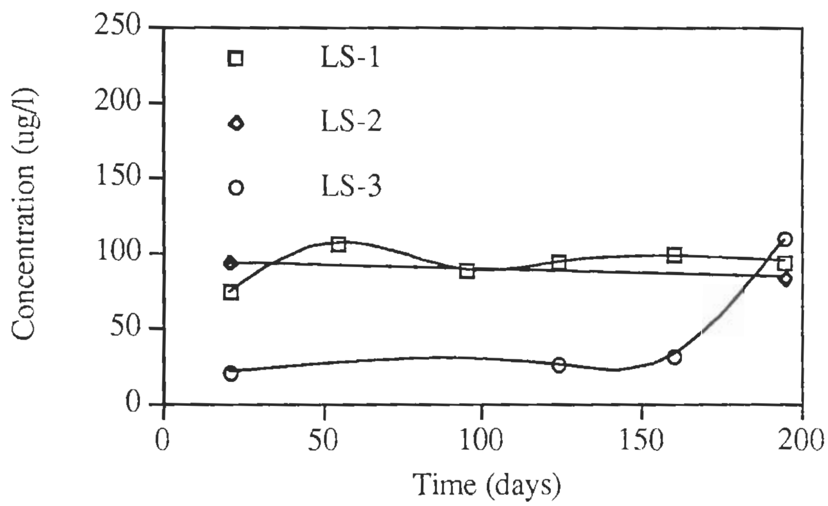

Appendix E6 Concentration of cadmium in local sumps from beginning of constr.

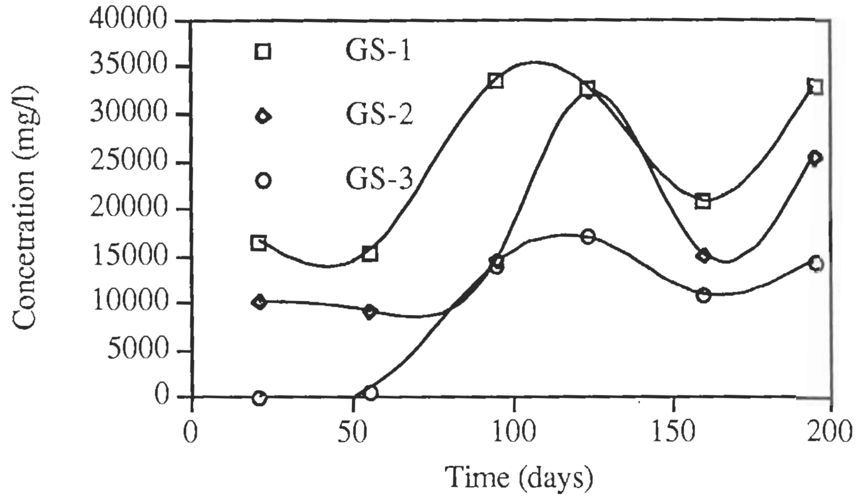

Appendix E7 Concentration of chlorides in global sumps from beginning of constr.

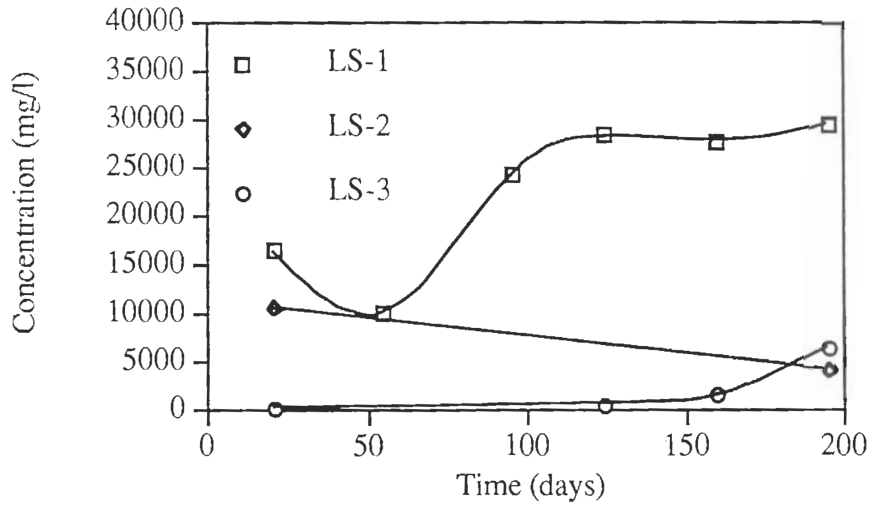

Appendix E8 Concentration of chlorides in local sumps from beginning of constr.

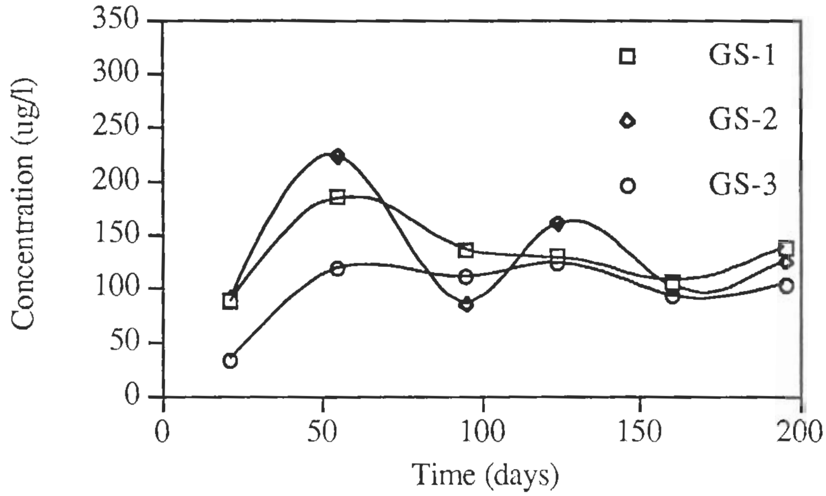

Appendix E9 Concentration chromium in global sumps from beginning of constr.

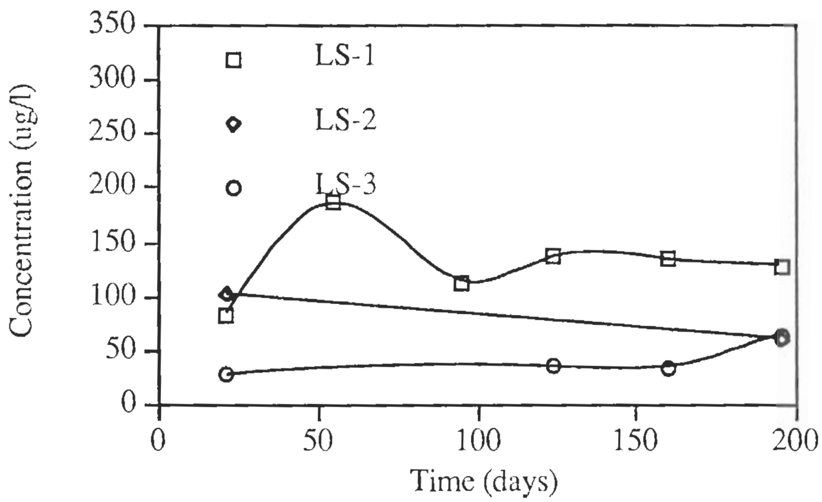

Appendix E10 Concentration of chromium in local sumps from beginning of constr.

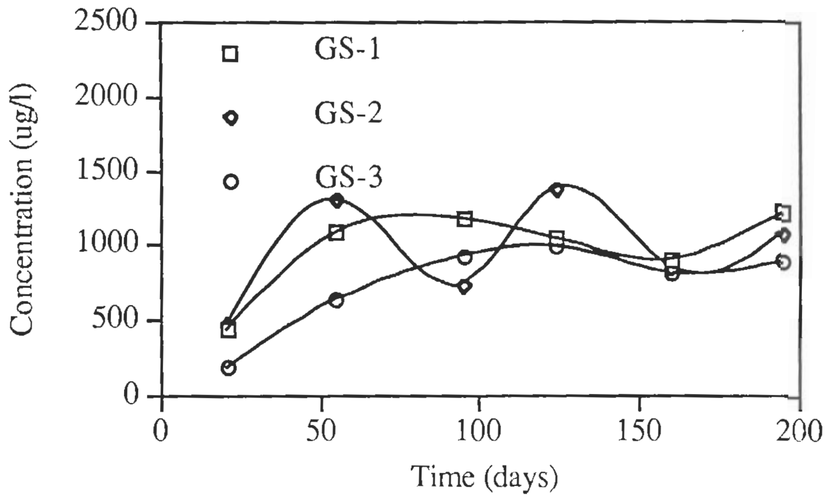

Appendix E11 Concentration of lead in global sumps from beginning of constr.

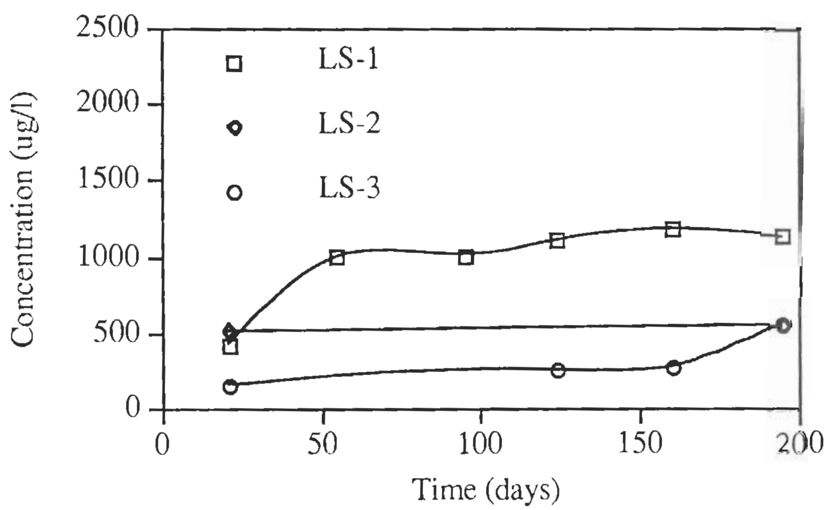

Appendix E12 Concentration of lead in local sumps from beginning of constr.

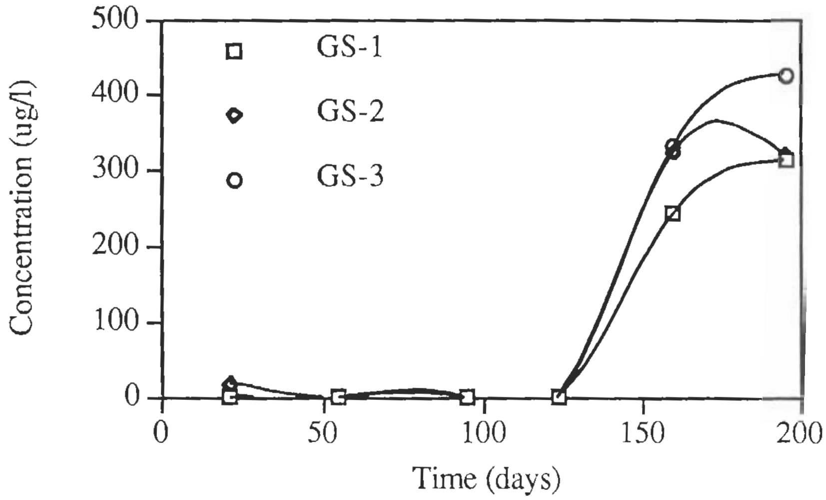

Appendix E13 Concentration of selenium in global sumps from beginning of constr.

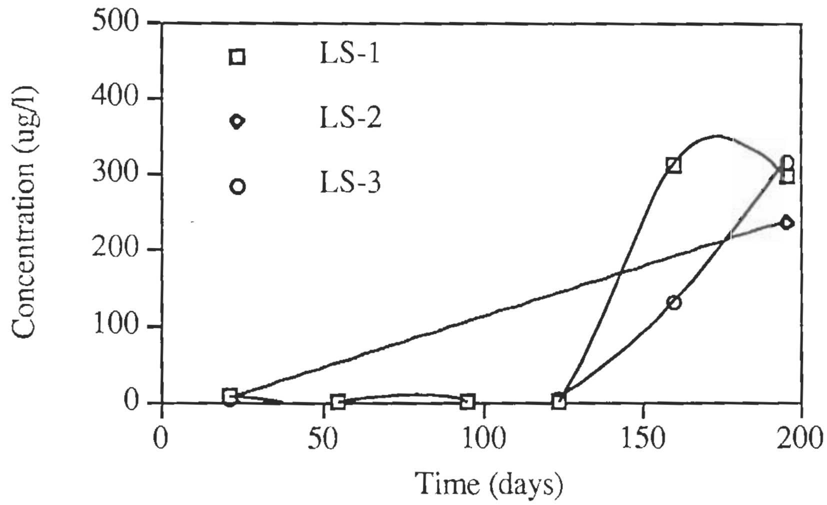

Appendix E14 Concentration of selenium in local sumps from beginning of constr.

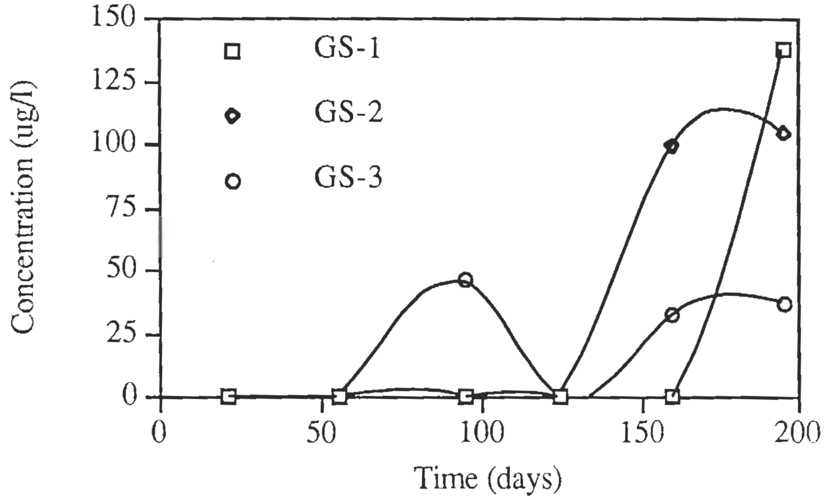

Appendix E15 Concentration of silver in global sumps from beginning of constr.

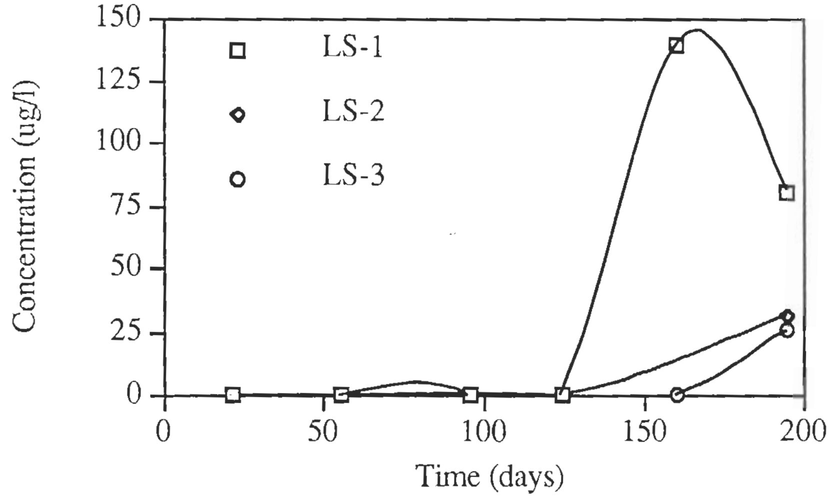

Appendix E16 Concentration of silver in local sumps from beginning of constr.

APPENDIX F - CONTAMINANT CONCENTRATIONS IN LEACHATE EXTRACTED FROM LOCAL SUMPS FOLLOWING MANUAL DOWSING WITH TAP WATER

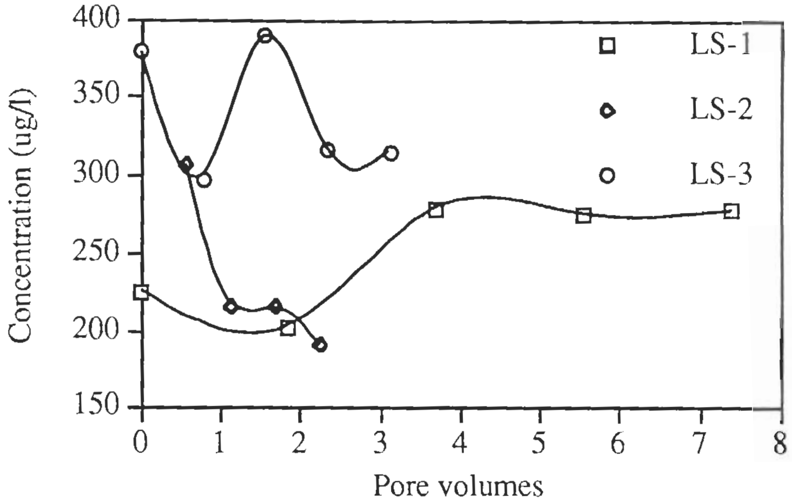

Appendix F1 Arsenic concentration in local sumps resulting from dowsing

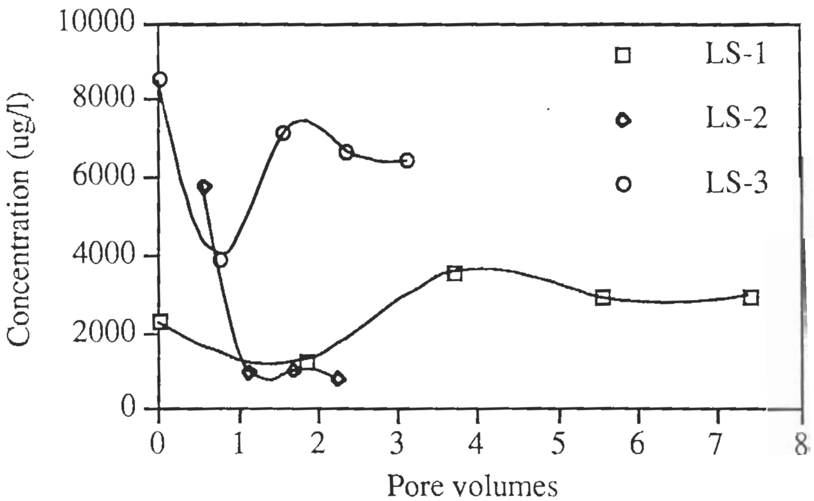

Appendix F2 Barium concentration in local sumps resulting from dowsing

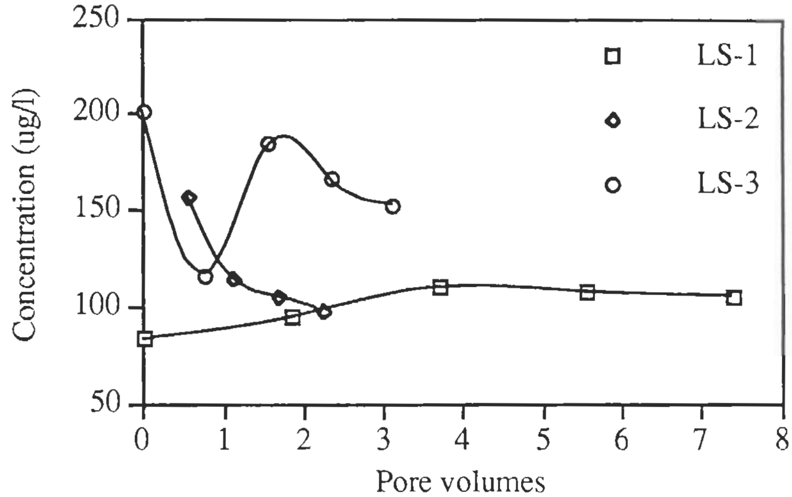

Appendix F3 Cadmium concentration in local sumps resulting from dowsing

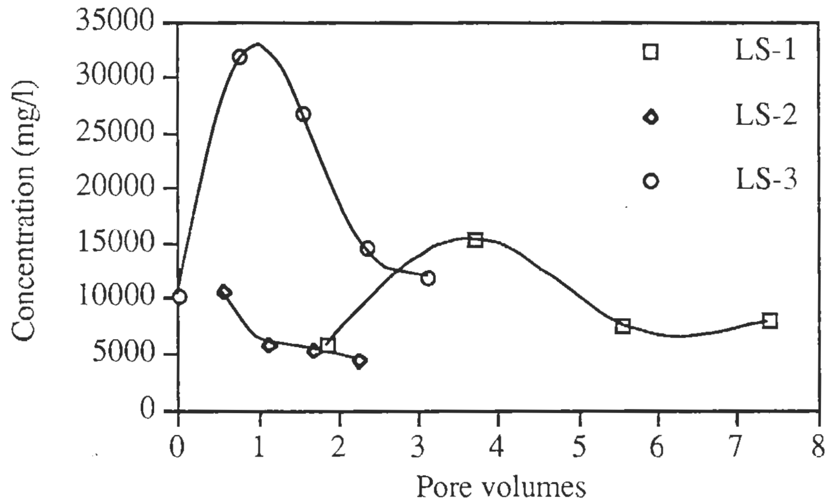

Appendix F4 Chlorides concentration in local sumps resulting from dowsing

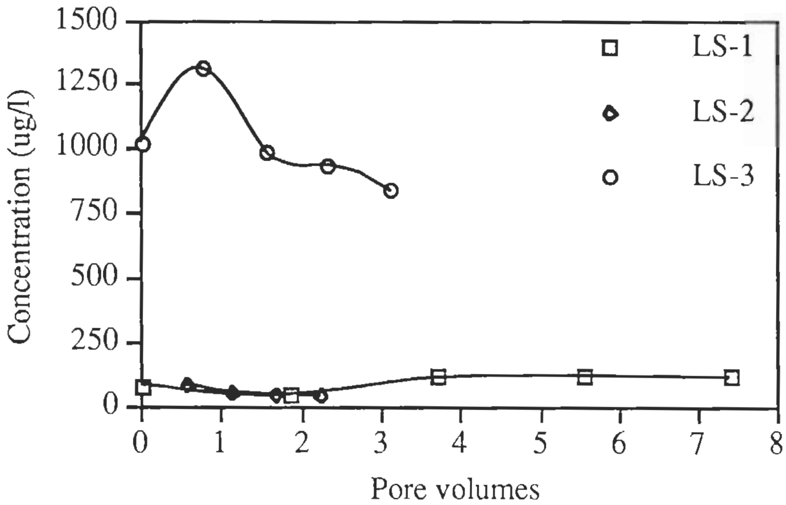

Appendix F5 Chromium concentration in local sumps resulting from dowsing

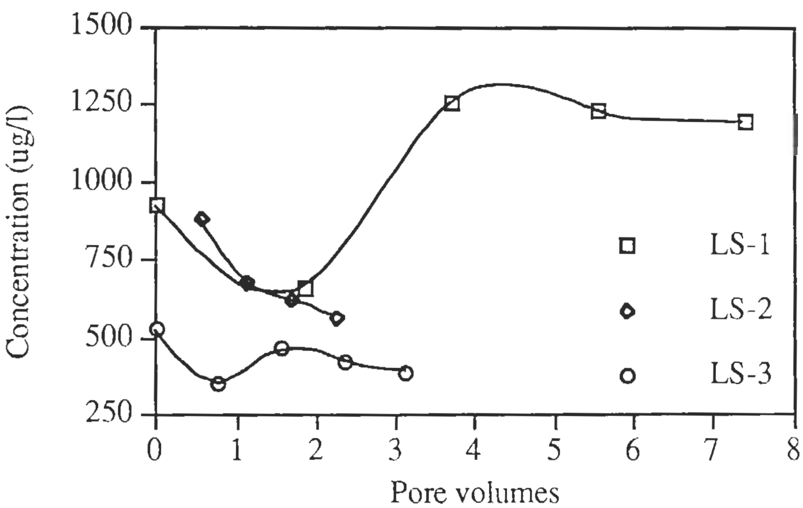

Appendix F6 Lead concentration in local sumps resulting from dowsing

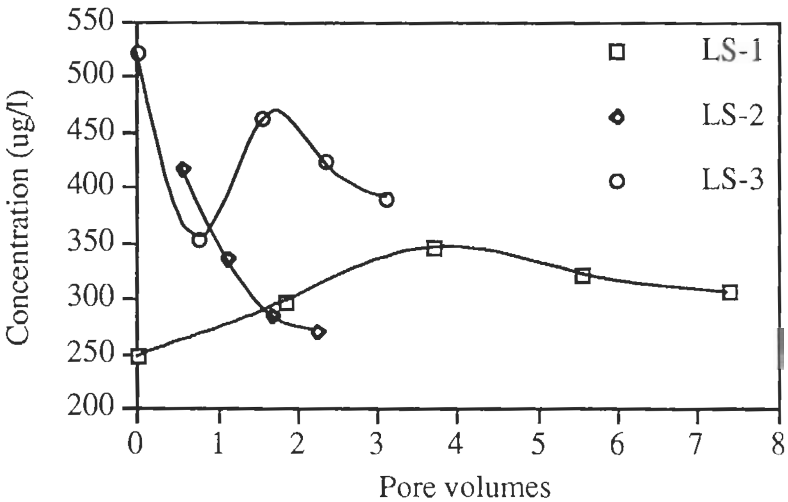

Appendix F7 Selenium concentration in local sumps resulting from dowsing

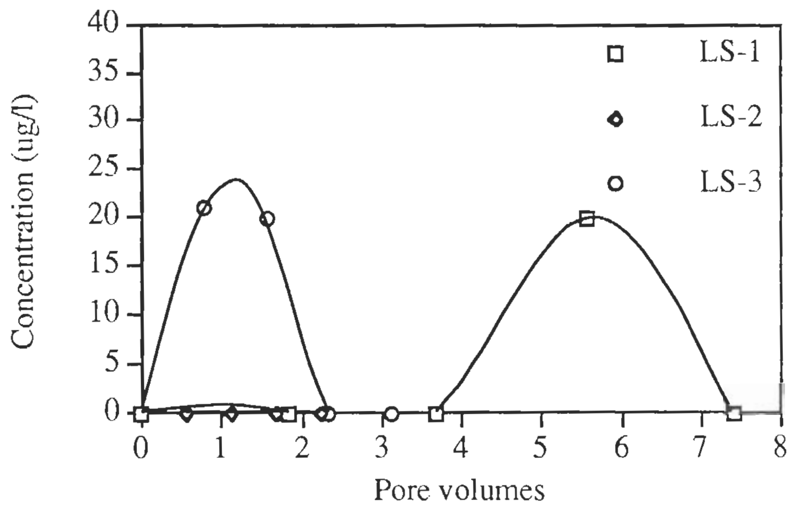

Appendix F8 Silver concentration in local sumps resulting from dowsing